

Rockefeller University

Digital Commons @ RU

Student Theses and Dissertations

1968

The Structure and Replication of a Parainfluenza Virus

Richard W. Compans

Follow this and additional works at: [https://digitalcommons.rockefeller.edu/
student_theses_and_dissertations](https://digitalcommons.rockefeller.edu/student_theses_and_dissertations)

THE STRUCTURE AND REPLICATION OF
A PARAINFLUENZA VIRUS

A thesis submitted to the Faculty of The Rockefeller University
in partial fulfillment of the requirements
for the degree of Doctor of Philosophy

by
Richard W. Compans, B. A.

Accepted For Publication
Purnell M. Choppin
Associate Professor, The Rockefeller University

25 January 1968

The Rockefeller University

New York, New York

ACKNOWLEDGMENTS

I am particularly indebted to Dr. Purnell W. Choppin, my research advisor, for the guidance and encouragement he has provided throughout these studies. His suggestions and efforts have been invaluable to me, both in carrying out this research and preparing this manuscript. I also wish to express my deep gratitude to Dr. Igor Tamm, in whose laboratory this work was done, for his hospitality and for many valuable discussions.

The electron microscopic studies of SV5 replication were carried out in collaboration with Dr. Samuel Dales, whom I sincerely thank for his interest and assistance, and for introducing me to many of the techniques of electron microscopy. I also thank Mrs. Kathryn V. Holmes and Dr. Donald H. Harter for collaboration in portions of the work described here. I am grateful to Dr. George E. Palade for his helpful and encouraging comments, and for extending to me the use of the electron microscopic facilities. I wish to thank Dr. Walter Doerfler for instruction in the use of the analytical ultracentrifuge, and for many helpful discussions. I thank Dr. Peter Elsbach for carrying out the gravimetric determination of lipids, and Dr. Daniel H. Levin for assistance with the electrophoretic separation of nucleotides. Miss Cathleen O'Connell and Miss Linda Ferrer provided excellent technical assistance during portions of this work.

SUMMARY

The simian parainfluenza virus SV5 is a member of myxovirus subgroup II, which includes parainfluenza, mumps, and Newcastle disease viruses. These viruses are 120-500 m μ in diameter, and consist of an envelope covered with surface projections and an internal ribonucleoprotein component which is a single-stranded helix, 150-180 A in diameter. A high yield of infective SV5 is produced by primary cultures of rhesus monkey kidney (MK) cells, and the virus-cell interaction is moderate: infected cells divide normally, exhibit little cytopathic effect, and cellular macromolecular synthesis is not inhibited.

An electron microscopic study of SV5 replication in MK cells was undertaken. Virus adsorbs to the cell surface and is then taken into cells by phagocytosis. Virus-induced morphological changes appear only in the cytoplasm of infected cells. The helical nucleocapsid of the virus appears to form in the cytoplasmic matrix and align under regions of the cell membrane which acquire viral surface projections. Assembly and release of virus particles at the cell surface occurs by a budding process involving incorporation into the viral envelope of a unit membrane, which is continuous with and morphologically identical to that of the host cell. Both spherical and filamentous virus particles are formed. Filaments frequently contain nucleocapsid in a regular spiral which extends throughout their length. SV5 causes minimal cytopathic changes in MK cells, and there appears to be a balance between the rate of synthesis of nucleocapsid and its continuous release within mature virus particles.

Under certain conditions, a gradual accumulation of nucleocapsid is seen in the cytoplasm of infected cells. This observation suggested an approach to the isolation of SV5 nucleocapsid. Equilibrium sedimentation in cesium chloride gradients was used to purify nucleocapsid released from cells by osmotic shock. The length distribution of the released nucleocapsid shows a sharp peak with a mean of 1.02 μ , and it is probable that this length contains one SV5 genome. Chemical determinations indicate that the nucleocapsid is a ribonucleoprotein with an RNA content of 4.1%. The length distribution of the nucleocapsid of Newcastle disease virus closely resembles that obtained for SV5. On the basis of these and other results,

it seems likely that $\sim 1 \mu$ is the unit length of the nucleocapsid of all subgroup II myxoviruses.

SV5 RNA was isolated from purified nucleocapsid or from virus purified by equilibrium zonal centrifugation in a potassium tartrate gradient, in which the virus bands at a density of 1.22-1.23. The RNA was dissociated from protein by treatment with sodium dodecyl sulfate, and purified by sedimentation in a sucrose density gradient. RNA's isolated from virions and from purified nucleocapsid are indistinguishable in sedimentation behavior. The sedimentation coefficient of SV5 RNA was estimated to be 50 S in sucrose gradients containing 0.05 M NaCl. On the basis of its ribonuclease sensitivity, base composition, and sedimentation behavior, SV5 RNA appears to be single-stranded.

The methods used in the studies of SV5 were applied to pneumonia virus of mice (PVM), an unclassified virus whose structure had not been previously determined. PVM virions are spheres 80-120 m μ in diameter, or filaments of similar diameter with lengths up to 3 μ . The particles possess an outer, spike-covered envelope and helical internal component 120-150 A in diameter. Virus particles acquire their envelope by a budding process at the cell membrane; mature particles are seen only extracellularly. Dense inclusions are prominent in the cytoplasm of PVM-infected BHK21 cells, and appear to consist of aggregates of the PVM internal component. The helical component was isolated in a cesium chloride gradient from extracts of osmotically shocked cells. Murine erythrocytes, which are agglutinated by PVM, adsorb to the surfaces of infected cells and to budding and extracellular PVM particles. On the basis of its structure and morphogenesis, PVM appears to be a myxovirus; however, the details of its structure and replication differ from either of the two established subgroups of myxoviruses, and suggests that a third subgroup of these viruses exists.

TABLE OF CONTENTS

ACKNOWLEDGMENTS	ii
SUMMARY	iii
LIST OF TABLES	vii
LIST OF FIGURES	viii
I. INTRODUCTION	1
Principal Features of Virus Structure	2
Major Groups of Animal Viruses	3
A Brief Description of the Myxovirus Group	6
The Replication and Assembly of Myxovirus Particles	10
Isolation and Properties of the Parainfluenza Virus SV5	13
II. AN ELECTRON MICROSCOPIC STUDY OF THE REPLICATION OF SV5 IN MONKEY KIDNEY CELLS	17
Materials and Methods	20
Results	20
Uninfected MK cells	20
Morphology of SV5 virions	21
Adsorption and penetration	21
Morphogenesis of virus particles	24
Virus-induced alterations in infected MK cells	30
Discussion	33
III. ISOLATION AND PROPERTIES OF SV5 NUCLEOCAPSID	36
Materials and Methods	37
Results	39
Release of nucleocapsid from osmotically shocked cells	39
Purification of nucleocapsid	42
Properties of SV5 nucleocapsid	46
a. Chemical composition	46
b. Density in cesium chloride	50
c. Sedimentation in sucrose gradients	50

Effects of enzymes on SV5 nucleocapsid	53
Length of the nucleocapsid of Newcastle disease virus. . . .	53
Discussion.	56
IV. ISOLATION AND PROPERTIES OF SV5 RNA.	59
Materials and Methods	60
Results	61
Purification of SV5 virions.	61
Isolation of SV5 RNA	61
Sedimentation coefficient of SV5 RNA	64
Ribonuclease sensitivity of SV5 RNA.	64
Comparison of RNA's from virions and purified nucleocapsid .	64
Base composition of SV5 RNA.	70
Discussion.	70
V. GENERAL DISCUSSION AND CONCLUSIONS	72
The Structure of Myxoviruses.	73
The Replication of SV5.	76
APPENDIX. THE STRUCTURE AND MORPHOGENESIS OF PNEUMONIA VIRUS OF MICE. .	81
Materials and Methods	82
Results	83
Structure of PVM virions: negative stain	83
Structure of PVM virions: thin sections.	83
Release of a helical component from cells infected with PVM. .	84
Formation of virus particles	85
Interaction of PVM and infected cells with murine erythrocytes	89
Discussion.	94
BIBLIOGRAPHY.	97

LIST OF TABLES

<u>Table</u>	<u>Table Heading</u>	<u>Page</u>
1.	Characteristics of major groups of animal viruses	5
2.	Chemical composition of some myxoviruses	8
3.	Segregation of myxoviruses into two subgroups	11
4.	Failure of SV5 nucleocapsid to elicit hemagglutination-inhibiting or neutralizing antibodies	47
5.	Chemical composition of SV5 nucleocapsid	48
6.	Base composition of SV5 RNA	69
7.	Helical nucleocapsids of animal viruses	77
 Appendix		
1.	Comparison of properties of pneumonia virus of mice with the two subgroups of myxoviruses	96

LIST OF FIGURES

<u>Figure No.</u>		<u>Page</u>
1.	Nomenclature for viral components	4
2.	Structure of the parainfluenza virus SV5	15
3.	Growth curve of SV5 in MK cells	19
4-5.	SV5 in thin section	22
6.	SV5 in phagocytic vacuoles	23
7-13.	Maturation of SV5	25-29
14.	MK cells 3 days after infection	31
15.	Large intracellular aggregate of nucleocapsid 6 days after infection	32
16.	SV5 nucleocapsid released by osmotic shock	40
17.	Length distribution of SV5 nucleocapsid	41
18.	SV5 nucleocapsid band in a cesium chloride density gradient	43
19-20.	Gradient-purified SV5 nucleocapsid	43
21.	Purification procedure for SV5 nucleocapsid	44
22.	Absence of cellular RNA in purified nucleocapsid	45
23.	Ultraviolet absorption spectrum of SV5 nucleocapsid	49
24.	Analytical equilibrium centrifugation of SV5 nucleocapsid	51
25.	Sedimentation of SV5 nucleocapsid in sucrose gradients	52
26-29.	NDV nucleocapsid released by osmotic shock	54
30.	Length distribution of NDV nucleocapsid	55
31.	Purification of SV5 in potassium tartrate gradient	62
32.	Sedimentation of SDS-treated SV5	63
33.	Ultraviolet absorption spectrum of SV5 RNA	65
34.	Sedimentation coefficient of SV5 RNA	66
35.	Ribonuclease sensitivity of SV5 RNA	67
36.	Comparison of RNA's from SV5 virions and nucleocapsid	68
37.	Schematic diagram of a parainfluenza virus	74

LIST OF FIGURES (continued)

<u>Figure No.</u>		<u>Page</u>
Appendix		
1-2.	PVM virions negatively stained with sodium phosphotungstate	86
3-4.	PVM virions in thin section	86
5.	Helical nucleocapsid from PVM-infected cells	87
6.	Helical nucleocapsid of SV5	87
7.	PVM nucleocapsid at higher magnification	87
8.	Low magnification view of a PVM inclusion	90
9.	Higher magnification of a cytoplasmic inclusion	90
10-14.	Maturation of PVM	91-92
15-17.	Interaction of PVM and infected cells with murine erythrocytes	93

I. INTRODUCTION

Principal Features of Virus Structure

Current ideas about the structure of viruses have emerged from a variety of experimental approaches, including chemical analysis, electron microscopy, and X-ray diffraction. The earliest structural information, the estimation of the sizes of virus particles, was obtained by ultrafiltration with graded collodion membranes (Elford, 1931). The crystallization of tobacco mosaic virus by Stanley (1935) stimulated studies of the chemistry of viruses. Many viruses, including tobacco mosaic, were found to consist only of protein and nucleic acid, with protein generally comprising the major portion of the mass of the particle (Knight, 1963). The high ratio of protein to nucleic acid, and the insensitivity of viral nucleic acids to nucleases, suggested that the protein formed a coat around the nucleic acid. Since nucleic acid appeared to function as genetic material (Avery et al., 1944; Hershey and Chase, 1952), and viral nucleic acid appeared to determine the structure of viral proteins (Harris and Knight, 1952; 1955; Fraenkel-Conrat, 1956), a problem in coding arose because the total number of amino acids always greatly exceeded the number of nucleotides in the viral nucleic acid. The suggestion was therefore made (Crick and Watson, 1956; 1957) that the viral protein coat consists of a large number of chemically identical subunits.

The construction of a protein coat from identical subunits seemed likely to occur in such a manner that each subunit would be in an equivalent environment, with the same kinds of inter-subunit bonds serving to hold each subunit in place. The predicted result (Crick and Watson, 1957) was a symmetrical structure, which was demonstrated by X-ray diffraction studies (Franklin et al., 1957; Caspar, 1956) and electron microscopy (Williams and Smith, 1958). Two types of symmetry have been described for viral protein shells: helical and icosahedral. A large number of plant viruses are nucleoproteins with helical symmetry. Icosahedral viruses include many animal viruses, plant viruses, and some bacteriophages.

Although a large number of viruses are constructed as simple, symmetrical nucleoproteins, others possess a much greater degree of structural complexity. These include many bacteriophages with specialized tail structures to facilitate penetration of their nucleic acid into a host cell, and also a number of animal viruses with complex structures with lipid as an essential component. The nucleic acid, in many of the lipid-containing viruses, is

contained in a symmetrical protein coat similar to that of the simpler viruses. This nucleoprotein internal component is then further enclosed, by a lipid-containing covering, to form the infective virus particle.

A system of nomenclature has been applied to virus particles and their structural components (Caspar et al., 1962). Figure 1 illustrates the application of this terminology to schematic sections of virus particles. The symmetrical protein shell which surrounds the nucleic acid is called the capsid. It is composed of identical subunits, called structure units. These are normally arranged in clusters which are visible with the electron microscope, and are called morphological units or capsomeres. The capsid, together with its enclosed nucleic acid, is termed the nucleocapsid. Nucleocapsids may possess either helical or icosahedral symmetry. The outer, lipoprotein covering which encloses the nucleocapsids of some animal viruses is termed the envelope. The complete, infectious virus particle is the virion. This terminology will be employed in this dissertation.

Segregation of Animal Viruses into Major Groups

The large and increasing number of known animal viruses make it desirable to have a system of virus classification. Early systems grouped viruses according to certain biological properties, such as tissue specificity. Recent advances in our knowledge of the structure and chemistry of virus particles have made it possible to devise a classification system for viruses based on their fundamental structural features (Lwoff et al., 1962; Green, 1965). Viruses grouped together because of a similar structure frequently possess many biological properties in common.

The properties which are used to define the major groups of animal viruses include type of nucleic acid, particle size, presence of an envelope, symmetry, and number of capsomeres (when known). When viruses are classified according to these properties, the vast majority fall into one of eight major groups, which are listed in Table 1. In addition to the eight well-established groups, two other groups have been suggested: small (~ 20 m μ) icosahedral DNA-containing viruses, and bullet-shaped (65 x 150 m μ) RNA viruses which appear to have a helical internal structure. A number of other animal viruses have not yet been classified because of lack of detailed information about their structure.

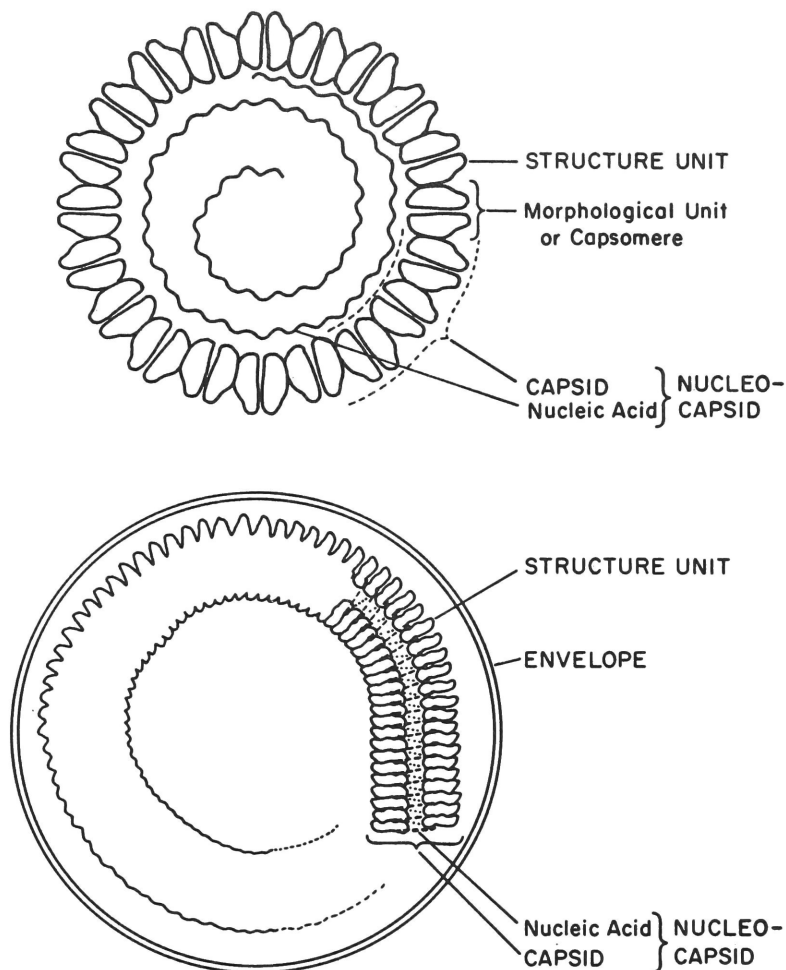


Figure 1. Schematic sections through virus particles, illustrating the current terminology for viral components: above, naked nucleocapsid indicating the general structure of an icosahedral virus; below, enveloped helical nucleocapsid (modified from Caspar et al., 1962).

TABLE 1

Characteristics of Major Groups of Animal Viruses

	Particle Size (m μ)	Presence of Envelope	Capsid Symmetry	Number of Capsomeres
<u>RNA Viruses:</u>				
Picornavirus	17-30	-	icosahedral	32 (?)
Reovirus	70-75	-	icosahedral	92 or 180
Arbovirus	20-100	+	?	
Myxovirus				
Subgroup I	80-120	+	helical, 9 m μ	
Subgroup II	120-450	+	helical, 18 m μ	
<u>DNA Viruses:</u>				
Papovavirus	40-55	-	icosahedral	72
Adenovirus	70-85	-	icosahedral	252
Herpesvirus	120-180	+	icosahedral	162
Poxvirus	225-290	+(complex)	?	

A Brief Description of the Myxovirus Group

The term myxovirus was proposed by Andrewes, Bang, and Burnet (1955) for a group of viruses which then included influenza, mumps, fowl plague, and Newcastle disease. The name was suggested because of the affinity of these viruses for certain mucoid substances. Since this original proposal, a number of viruses have been added to the myxovirus group. The most numerous are the parainfluenza viruses, which possess both the structural and biological properties of the original myxoviruses (Andrewes et al., 1959). Other viruses which have been proposed as myxoviruses largely on the basis of structural similarity include measles, canine distemper, rinderpest, and respiratory syncytial virus. A variety of diseases may result from myxovirus infection, although most myxoviruses infect the respiratory tract.

Early electron microscopic studies of influenza virus (Taylor et al., 1943) showed particles which were roughly spherical, with a mean diameter of approximately 80 m μ . The exact size and shape of the particles were variable, and depended to some extent on the preparative procedures used. Later, it was pointed out (Mosley and Wyckoff, 1946) that filamentous forms, with the same diameter as the spheres, were characteristic of many influenza virus preparations. The filamentous particles were found in greatest number in newly isolated influenza strains (Chu, Dawson, and Elford, 1949). In early studies of Newcastle disease virus (Bang, 1946a; b) the observed particles varied in size and shape, and the preparative procedure used could markedly affect virus morphology. All of these results therefore indicated mainly the general particle size and an apparent pleomorphism, and did not serve as a basis for classifying these agents together as a virus group.

The property of myxoviruses which did distinguish them from other viruses was the nature of their interaction with receptors on susceptible host cells and on red blood cells. The agglutination of red blood cells by a virus was first described for influenza (Hirst, 1941; McClelland and Hare, 1941), and thereafter, hemagglutination was also shown to be a property of Newcastle disease (Burnet, 1942), fowl plague (Lush, 1943), and mumps (Levens and Enders, 1945). Hemagglutination can be used as a

means of quantitating virus suspensions, and is inhibited by specific antibody to the virus. It was recognized by Hirst (1942) that the virus gradually destroys the receptors for hemagglutination on the red cell surface, presumably by an enzymatic process. Identification of the split product of this reaction (Klenk, 1955), and studies of the splitting of oligosaccharides by the viral enzyme (Gottschalk, 1957) demonstrated that the enzyme is a neuraminidase, which splits neuraminic acid residues on mucoproteins. The receptors for myxovirus attachment, either to red blood cells or susceptible host cells, appear to be mucoproteins, and hemagglutination or infection can be prevented by pretreatment of cell surfaces with neuraminidase (receptor-destroying enzyme) (Gottschalk, 1966). The neuraminidase of myxoviruses was the first example of an enzyme as an integral part of a virus particle. Recent studies of influenza virus (Mayron et al., 1961; Laver, 1964) indicate that the viral hemagglutinating component (hemagglutinin) and neuraminidase are two distinct proteins.

Chemical determinations on myxoviruses indicate a low content of RNA, with protein and lipid comprising the major portion of the mass of the particle. In addition, those viruses which have been analyzed for carbohydrate have contained more than could be accounted for by their nucleic acid content. Table 2 summarizes the chemical composition of several representative myxoviruses. Since in many cases the viruses were purified only by differential centrifugation, it is uncertain whether these values are correct. Intact RNA was not isolated in early studies of myxoviruses, but attempts were made to estimate the average RNA content per virus particle. Such estimation yielded values of 2×10^6 daltons for influenza A and B (Ada, 1957), and 3×10^6 for Newcastle disease (Rott, 1962). As described later, the latter value is now considered to be too low. The base ratios which have been determined indicate that myxovirus RNA's are single-stranded (Schaffer and Schwerdt, 1965).

When myxoviruses are treated with ether, virus particles are disrupted and two separate antigenic components can be isolated (Hoyle, 1952; Schäfer, 1957; Schäfer and Rott, 1959). One antigen is the viral hemagglutinin, which is presumed to be the surface component of the intact particle, and is devoid of RNA. The other antigen, called soluble (s) or gebunden (g), is usually measured by complement fixation, and is a nucleoprotein

TABLE 2
Chemical Composition of Some Myxoviruses*

Virus	% RNA	% Protein	% Lipid	% Non-nucleic acid carbohydrate	Reference
Influenza A and B	0.8-1	60-75	18-37	6	Ada and Perry, 1954; Fromm- hagen et al., 1959
Fowl plague	1.8-4	60-70	25	+	Schäfer, 1959
Newcastle disease	3.5	65	27	7	Schäfer, 1959; Cunha et al., 1947

* Adapted from Schaffer and Schwerdt (1965).

containing all of the virion's RNA. It is released from virus particles in fragments of variable length.

After the development of the negative staining technique for high resolution microscopy of viruses (Hall, 1955; Brenner and Horne, 1959), it was observed that the various members of the myxovirus group possess some strikingly similar structural features. The envelopes of myxovirus particles are composed of a membrane covered with closely-spaced projections, or spikes, 80-100 A in length (Horne et al., 1960). In this study, such surface projections were reported to be absent on influenza virus filaments. However, in subsequent studies of a large number of influenza virus strains (Choppin et al., 1961), every strain was found to possess filaments with surface projections indistinguishable from those seen on spherical virus particles. In the interior of virus particles, elongated structures are visible with a regular periodicity suggesting a helical arrangement within the strands (Horne and Waterson, 1960; Horne and Wildy, 1961). These structures are identical to the nucleoprotein antigen obtained by disrupting virus particles with ether, whereas the hemagglutinin possesses the spikes characteristic of the viral envelope (Hoyle et al., 1961; Choppin and Stoeckenius, 1964a).

Although all myxoviruses appear to possess a helical internal component the detailed structure of this component differs in the various members of the group, and two subgroups of myxoviruses can thus be clearly recognized (Waterson, 1962). Influenza and fowl plague viruses possess an internal component approximately 90 A in diameter, the substructure of which is difficult to resolve, and it is released from particles in short segments after ether treatment (Hoyle et al., 1961). The internal component of Newcastle disease, mumps, and parainfluenza viruses is about 180 A in diameter, has a periodicity of about 45 A along its length, and is sometimes released as relatively long pieces (Horne and Waterson, 1960). Although it was first proposed (Horne and Waterson, 1960) that the internal components of myxoviruses were constructed as double helices of two intertwining strands, recent studies of the 180 A nucleoproteins have clearly demonstrated that they are single helices (Choppin and Stoeckenius, 1964b). The detailed structure of the influenza virus internal component has not been elucidated. A number of other structural and biological differences

have been recognized between the influenza viruses (subgroup I myxoviruses) and the Newcastle disease-mumps-parainfluenza viruses (subgroup II myxoviruses), which are summarized in Table 3. In view of recent studies, some of the differences between the two subgroups must be reexamined, and the possibility of at least one additional subgroup must be considered (Compans et al., 1967).

The Replication and Assembly of Myxovirus Particles

The most detailed information about the biochemistry of RNA virus multiplication has come from studies of picornaviruses, the small, icosahedral RNA viruses (Darnell, 1965). Although some significant differences probably exist between the replication processes of myxoviruses and picornaviruses, and even between myxovirus subgroups I and II, it is likely that some of the information concerning the picornavirus "model" system applies also to macromolecular synthesis in myxovirus-infected cells. According to this model, single-stranded viral RNA serves as messenger RNA, complexing with host cell ribosomes to form virus-specific polyribosomes. These polysomes function in the synthesis of viral proteins, including structural proteins. Among the new proteins to appear in infected cells is a virus-induced RNA polymerase, capable of synthesizing viral RNA in the cytoplasm of infected cells. Double-stranded RNA is presumed to be an intermediate in viral RNA synthesis. When a pool of newly-synthesized viral RNA and protein has been built up, formation of viral progeny is thought to occur by a self-assembly process.

Because of their structural complexity, the replication of myxoviruses must differ from the multiplication of picornaviruses in some respects, since the assembly of virus progeny cannot occur by a one-step crystallization of proteins around nucleic acid. In studies of the development of the antigens of subgroup I myxoviruses by immunofluorescence, two discrete sites of antigen formation were recognized (Liu, 1955; Breitenfeld and Schäfer, 1957). First, the "g" or nucleoprotein antigen was detected in the nuclei of infected cells. At later times, this antigen was found in the cytoplasm, and the hemagglutinin antigen of the viral envelope was then also observed in the cytoplasm. With the subgroup II myxoviruses, however,

TABLE 3
Segregation of Myxoviruses into Two Subgroups*

	Subgroup I	Subgroup II
Members	Influenza A, B, and C	Parainfluenza 1, 2, 3, and 4; Newcastle disease virus, mumps, and SV5
Particle size	80-120 mμ	120-500 mμ
Diameter of helical nucleocapsid	9 mμ	18 mμ
Filamentous forms	+	+ †
Easily disrupted	-	+
Apparent site of synthesis of nucleocapsid antigen	nucleus	cytoplasm
Cytoplasmic inclusions	usually absent	+
Hemolytic and cell-fusing activities	-	+
Cooperative genetic reactions: genetic recombination, multiplicity and cross reactivation, incomplete virus formation	+	-

* Modified from Waterson, 1962, and Hirst, 1965.

† It was thought that filaments were rare among subgroup II myxoviruses; however, many filaments have recently been observed in fixed, sectioned preparations of parainfluenza viruses (Prose et al., 1965; Compans et al., 1966; Howe et al., 1967b).

antigens have been detected only in the cytoplasm in most host cell systems, although some instances of nuclear antigens have been reported (Chanock and Parrott, 1965).

Early electron microscopic studies of myxovirus-infected cells primarily served to indicate the process by which virus is released from cells. It was observed by Murphy and Bang in 1952 that influenza virus filaments and spheres projected from the cell surface into the extracellular space. No virus particles were observed in the interior of cells at times when infective virus was being synthesized, and it therefore appeared that the particles matured at the cell surface. This was the first demonstration of virus release occurring by a process other than lysis. With the addition of ferritin-conjugated antibody (Morgan et al., 1961a) it was observed that cell surfaces contained viral antigen in areas where virus was differentiating, and it was then suggested that virus was coated with this material upon emerging. The relationship of the normal cellular unit membrane (Robertson, 1961) to the envelope of the emerging virus was not determined. Ferritin-conjugated antibody also was used to identify influenza antigen in dense aggregates in cell nuclei, and dispersed antigen in the cytoplasm (Morgan et al., 1961b). The structure of these antigenic components was not resolved.

Early electron microscopic studies of mumps and Newcastle disease-infected cells also suggested that mature virus particles were elaborated at the surfaces of infected cells (Bang and Isaacs, 1957). More recently, Berkaloﬀ (1963) demonstrated that portions of the plasma membrane of cells infected with parainfluenza virus became morphologically altered to resemble the structure of the viral envelope. The nucleocapsid of the virus could be visualized in sections immediately beneath the altered membrane. Myxoviruses of both subgroups therefore appear to be elaborated at the surface of cells by a budding process, similar to the shedding of membrane fragments which occurs continuously in uninfected cell cultures (Hoyle, 1954).

Because the maturation of myxoviruses was observed to be intimately associated with the cell membrane, the question arose as to whether myxovirus particles acquired some normal material of the host cell during budding. Evidence from radioactive labelling experiments (Wecker, 1957) indicated that preexisting host cell lipids are incorporated into fowl

plague virus. More recently, analysis of the lipid composition of purified influenza virus grown in two different cell types indicated that the lipid of the virus reflected the lipid pattern of the host cell (Kates et al., 1962). Although it is now generally agreed that myxoviruses derive their lipid components from preexisting cell material, a controversy continues to exist concerning the presence of host cell antigens within myxovirus particles. A number of reports have described host cell antigens in purified myxovirus preparations (Knight, 1946; Smith et al., 1953; Isacson and Koch, 1965; Haukenes et al., 1965; Drzeniek et al., 1966; Laver and Webster, 1966; Howe et al., 1967a), but their absence has also been claimed (Ananthanarayan, 1954; Kroeger, 1962). The difficulty in deciding this question is largely due to use of virus preparations of an unknown degree of purity. In addition, failure to demonstrate host antigen may be explained because virus particles were not disrupted, since it is possible that such antigens would be in the interior of virus particles.

Isolation and Properties of the Parainfluenza Virus SV5

This dissertation describes the results of investigations on the structure and replication of simian virus 5, a parainfluenza virus (Compans et al., 1966; Compans and Choppin, 1967a). SV5 is one of many simian viruses, all designated by the initials SV, which have one common property, i.e., they were originally isolated from primary cultures of rhesus monkey kidney cells. A large number of these agents were detected as contaminants in these cultures during the preparation of poliovirus vaccines. Another commonly studied simian virus is a papovavirus, the small DNA-containing tumorigenic virus, SV40.

SV5 was first isolated in 1956 by Hull and co-workers, and is one of the most common contaminants of monkey kidney cell cultures. However, viruses which are antigenically related to SV5 have also been isolated from man or the hamster (Schultz and Habel, 1959), from human blood and throat swabs (Hsiung, 1959; Hsiung et al., 1962; von Euler et al., 1963), from a line of human conjunctival cells (Krim et al., 1961), from patients with infectious hepatitis (Liebhaber et al., 1965), and from a cell culture from a human atheromatous lesion (Behbehani et al., 1965). The role of the virus in human or simian disease has not been established. SV5 has

failed to cause detectable disease in laboratory animals, although virus multiplication has been demonstrated (Chang and Hsiung, 1965). Studies of SV5 have been stimulated by several interesting biological properties of the virus. Its contrasting behavior in various cell types has suggested that the response of the host cell membrane determines the virulence of the virus (Holmes and Choppin, 1966), and the failure of SV5 to interfere with superinfection by other viruses (Choppin, 1964) has permitted investigation of the effect of one virus on the RNA and protein synthesis of another (Choppin and Holmes, 1967).

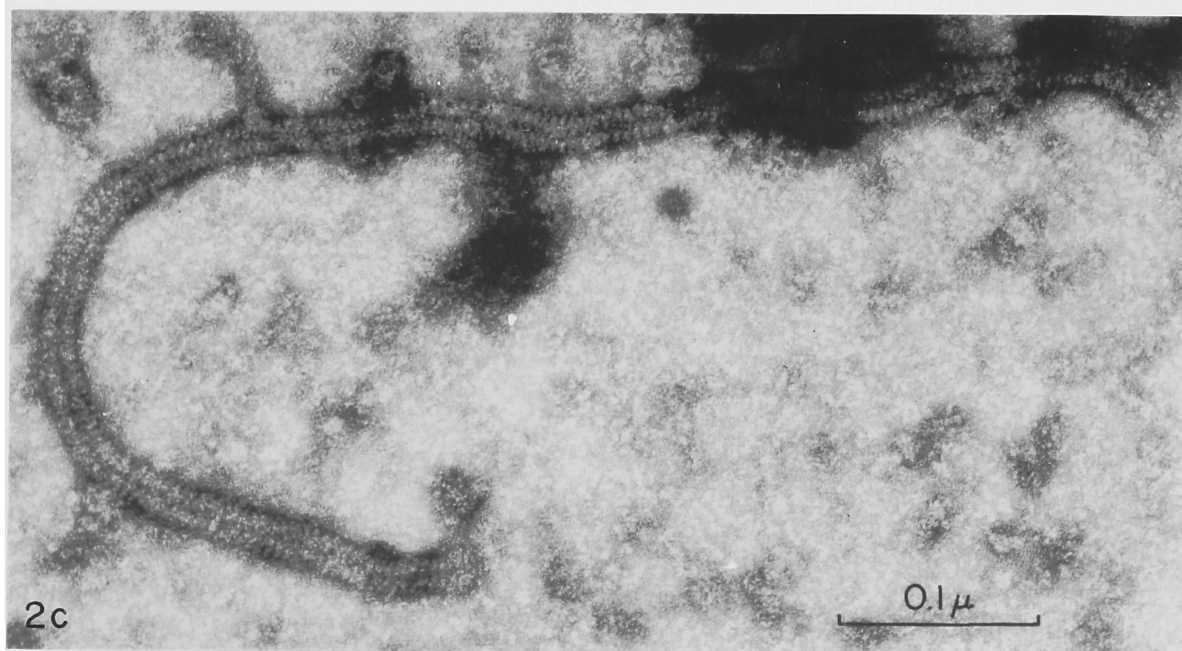
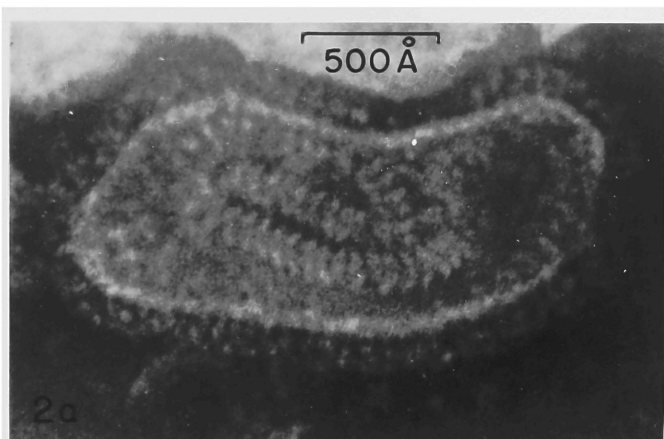
The biological and structural properties of SV5 indicate that it belongs to the parainfluenza-mumps-Newcastle disease subgroup of myxoviruses. SV5-infected cells exhibit hemadsorption, i.e., adsorption of erythrocytes (Chanock et al., 1961), a known property of myxoviruses (Vogel and Shelokov, 1957). The virus is antigenically related and similar in hemagglutination behavior to subgroup II myxoviruses (Hsiung et al., 1962). SV5 does not undergo the cooperative genetic interactions characteristic of influenza virus, i.e., incomplete virus formation at high multiplicity (Choppin, 1964), and the synthesis of SV5 RNA is not inhibited by actinomycin D (Choppin, 1965). The classification of SV5 as a subgroup II myxovirus was clearly established by electron microscopic studies (Choppin and Stoeckenius, 1964b) which indicated that the virus particle is very similar in structure to the other members of the parainfluenza-mumps-Newcastle disease subgroup (Horne et al., 1960; Waterson et al., 1961; Waterson and Hurrell, 1962).

SV5 virions (Figure 2) have an envelope covered with projections approximately 100 Å in length. The internal component, or nucleocapsid of SV5 is a single helix 160-180 Å in diameter, with a central hollow core 40-55 Å in diameter. It is constructed from ellipsoidal subunits with a long axis of 55-70 Å and a short axis of ~ 25 Å. The dimensions of SV5 nucleocapsid, as well as its subunit, appear to correspond closely to those of tobacco mosaic virus (Klug and Caspar, 1960).

Chemical studies of myxoviruses have been hampered by the lability of the virion and the difficulties involved in obtaining purified virus. Although many of the major structural features of SV5 and other myxoviruses have now been established, the exact sizes of their nucleic acids have not been determined, nor have the length and composition of their helical

Figure 2. The structure of the parainfluenza virus SV5, as shown by negative staining (from Choppin and Stoeckenius, 1964b).

- a. SV5 virion showing the helical nucleocapsid coiled inside, and the envelope covered with a layer of closely spaced projections or spikes 100 A in length.
- b. Segments of the nucleocapsid released from disrupted virus particles with the helical structure extended and the individual turns of the single helix clearly resolved (arrows).
- c. A long, tightly coiled piece of nucleocapsid that was released from virus by treatment with phospholipase C.



nucleocapsids. The chemical architecture of the viral envelope is also unknown. SV5 is a particularly suitable myxovirus for chemical studies because large amounts can be grown in tissue culture (Choppin, 1964). Further studies of the structure and chemistry of SV5, its helical nucleocapsid, and its RNA genome are described in the succeeding portions of this dissertation.

II. AN ELECTRON MICROSCOPIC STUDY OF THE REPLICATION
OF SV5 IN MONKEY KIDNEY CELLS

In previous studies of the multiplication of SV5 in monkey kidney (MK) cells (Choppin, 1964), it was demonstrated that the virus multiplies to high titer with minimal cytopathic effects. A growth curve of the virus is shown in Figure 3. The latent period was approximately 6 hours, and the doubling time during the exponential rise was approximately 50 minutes. After 12 hours, there was a gradual increase in virus which continued throughout the experiment. SV5-infected MK monolayers could be maintained for periods up to 30 days with minimal cell damage, which consisted of slight granularity, some giant cell formation, scattered rounded cells and floating debris. Such monolayers continued to produce high titers of infective virus if the culture medium was changed daily. In a representative experiment, 1500 plaque-forming units (PFU) per cell were produced on the first day, and even on the thirtieth day, 175 PFU/cell were produced. SV5-infected MK cells can divide at a normal rate, and cellular macromolecular synthesis is not inhibited by infection (Holmes and Choppin, 1966). The type of steady state multiplication of virus of which SV5 infection in MK cells is an example has been termed moderate virus-cell interaction (Dulbecco, 1965).

SV5 does not interfere with infection and plaque formation by a wide variety of superinfecting viruses, including some which are extremely sensitive to interferon (Choppin, 1964). The yield of a superinfecting virus from an SV5-infected MK monolayer is usually similar to the yield from control monolayers. The normal yields of superinfecting viruses on SV5-infected MK monolayers provide an additional demonstration that SV5 replication causes minimal deleterious effects on the cells.

The present electron microscopic study describes the morphological stages which are recognizable in the replication of SV5 virus in MK cells. The observations confirm the results of earlier studies describing the multiplication of SV5 with little cell damage, and support the previous evidence which suggested that the virulence and yield of SV5 may depend on the response of the cell membrane to the virus (Holmes and Choppin, 1966).

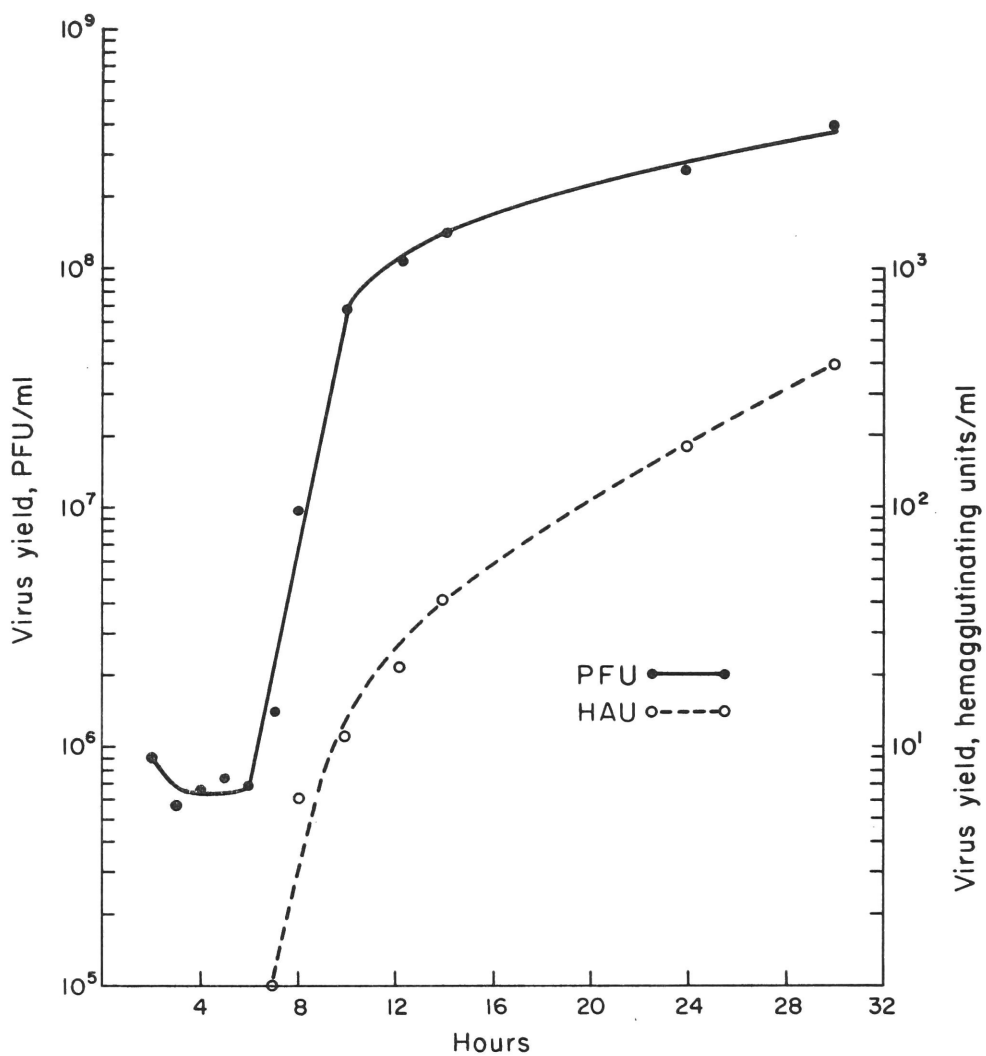


Figure 3. Growth curve of SV5 in primary rhesus monkey kidney cells (from Choppin, 1964).

Materials and Methods

Virus. The W3 strain of SV5 was grown in primary cultures of rhesus monkey kidney cells in lactalbumin hydrolyzate medium with 2% calf serum (Choppin, 1964).

Preparation and inoculation of cell cultures. Primary cultures of rhesus monkey kidney cells were prepared in 60 mm plastic petri dishes in lactalbumin hydrolyzate medium with 2% calf serum (Choppin and Philipson, 1961).

Monolayers of approximately 2×10^6 cells were washed with a phosphate-buffered salt solution (PBS) (Dulbecco and Vogt, 1954) and inoculated with 0.5 ml of SV5 suspension. After an adsorption period of 1 or 2 hours at 37°C, the inoculum was replaced with growth medium.

Electron microscopy. Cells were scraped from petri dishes, centrifuged for 4 minutes at 200 g, and the pellets fixed for 4 minutes in 1% glutaraldehyde in PBS (Sabatini et al., 1962) and postfixed 20-30 minutes with 1% osmium tetroxide (Palade, 1952) in isotonic phosphate-buffered saline, pH 7.2 (BS). The pellets were dehydrated in a series of alcohols and embedded in epoxy resin (Luft, 1961). Thin sections were stained by a 1 minute application of a saturated solution of uranyl acetate diluted 1:1 with ethanol, followed by a 1-2 minute application of 0.4% lead citrate in 0.1 N NaOH (Reynolds, 1963). Specimens were examined in a Hitachi HS-7S or Siemens Elmiskop I electron microscope.

Results

Uninfected MK cells. Rhesus monkey kidney cells in primary culture are generally epithelioid with highly lobated nuclei. In addition to other cytoplasmic organelles of usual appearance, they contain extensive rough-surfaced endoplasmic reticulum and few smooth-surfaced cisternae. The plasma membrane of the MK cell can easily be resolved into two distinct electron-dense layers separated by a less dense layer; this structure is referred to as a unit membrane (Robertson, 1961). Adjacent MK cells are frequently in contact, have interdigitating borders, and possess the tight junctions and desmosomes characteristic of cells in kidney tissue (Farquhar and Palade, 1963). Other specializations of kidney tissue cells, such as brush border, are not seen in cell cultures.

Morphology of SV5 virions. In thin sections, SV5 virions are either circular profiles 1200-1500 A in diameter or long, rigid-appearing filaments with a uniform diameter of about 1200 A (Figures 4 and 5). The latter are frequently over 1 μ in length. Such filamentous particles had not been observed in negatively stained, unfixed preparations (Choppin and Stoeckenius, 1964b). The viral envelope consists of a unit membrane similar to that of the host cell, but with dense outer surface projections, or spikes, added. In longitudinal or oblique sections, the helical internal component or nucleocapsid appears as a dense tubular structure 150-180 A in diameter, and in cross section, as an electron dense circular outline of the same diameter with a less dense center (Figures 4 and 5).

In filaments, the helical nucleocapsid is frequently further coiled into a regular spiral which extends throughout the length of the particle (Figures 5 and 12). This permits an estimate of the length of the nucleocapsid in such regularly packed filaments, e.g., approximately 8 μ in the filament on the right in Figure 12. It is possible that long filaments contain more than one piece of nucleocapsid. The length of nucleocapsid in sectioned spherical particles cannot be directly estimated because it is not packed in a regular arrangement; however, when the volume of the smaller spheres, which are 120-180 m μ in diameter, is compared to that of filaments, a length of $\sim 1 \mu$ would appear to be reasonable for their nucleocapsid.

Adsorption and penetration. The early stages of SV5 infection were examined after inoculating MK cells at a multiplicity of 5000 PFU/cell. Cells sampled 10-30 minutes after inoculation show virus particles on or near their outer membranes. Within 20 minutes, virus particles are frequently seen in cytoplasmic vacuoles or deep invaginations of the cell membrane (Figure 6). Within such vacuoles, alterations of virus morphology such as swelling, disruption, or condensation of particles are seen, suggesting destructive processes. Neither fusion of the viral envelope with the cell membrane, nor disintegration of the virus at the cell surface with entry of viral material has been observed. Intact virus particles seen in the interior of the cells are invariably surrounded by cell membranes and never free in the cytoplasmic matrix. It was not possible to detect SV5 nucleocapsid free within the cytoplasmic matrix of MK cells at times when virus penetration was occurring.

Figure 4. A circular profile of a sectioned SV5 virion located adjacent to the surface of a MK cell. Note the clearly resolved unit membrane in the envelope of the virion, which is identical in appearance to the unit membrane of the host cell surface. The outer leaflet of the viral membrane is covered with a layer of projections corresponding to the spikes seen with negative staining. Such projections are absent on normal cellular plasma membrane.

Figure 5. A filamentous SV5 particle $\sim 1.5 \mu$ in length, with nucleocapsid traversing the central portion. On the right, cross sections of nucleocapsid are seen as electron opaque circular profiles with less dense central regions. The unit membrane is apparent in the viral envelope.

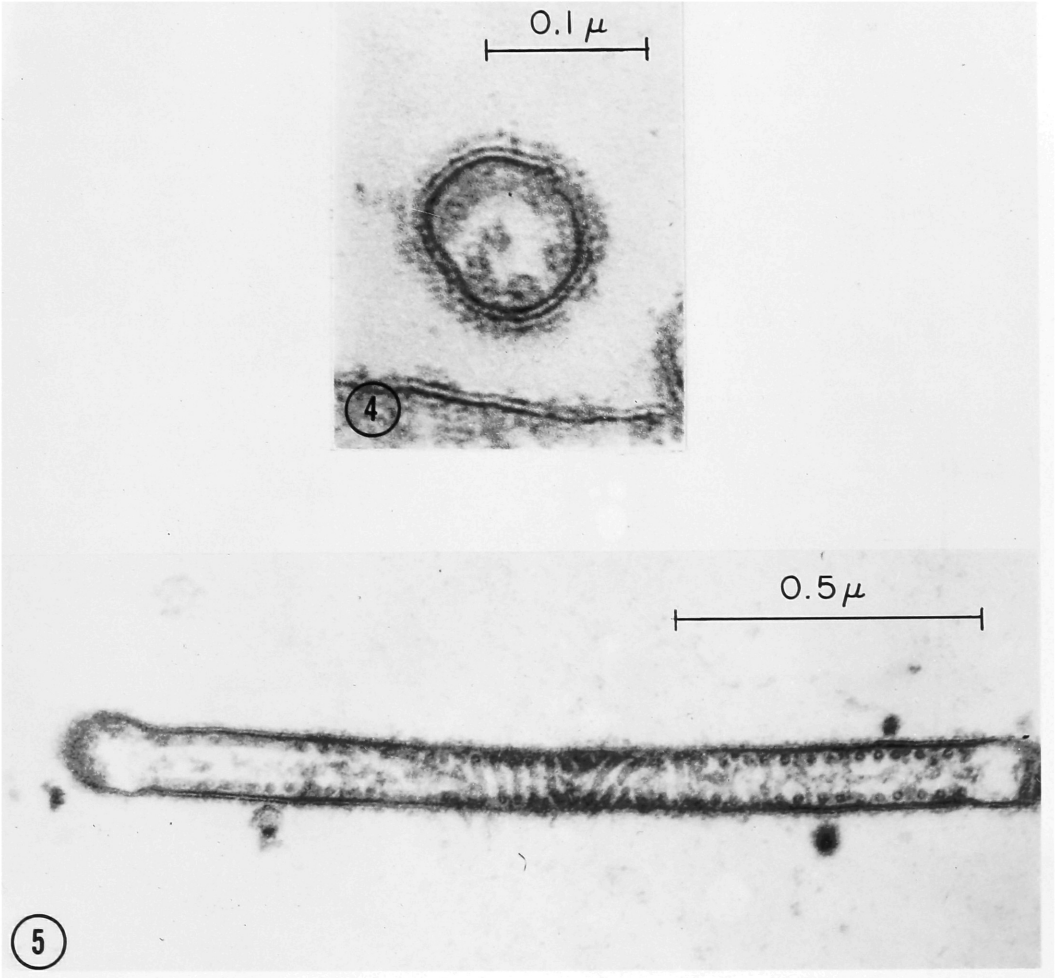
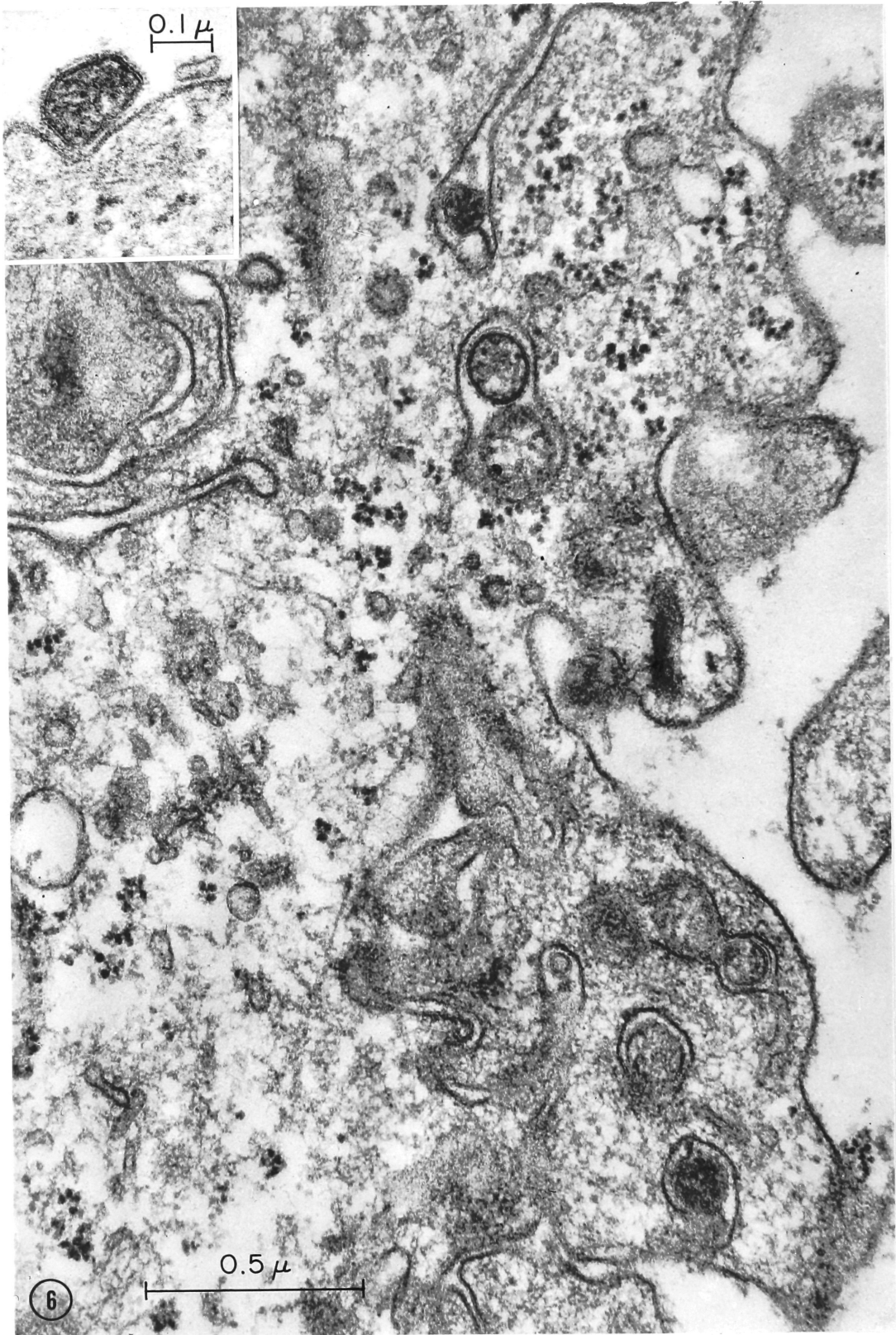


Figure 6. A portion of the surface of a monkey kidney cell 20 minutes after inoculation with SV5, showing virus particles within vacuoles or deep invaginations of the cell membrane. Some particles, possibly viral, within vacuoles have a dense, amorphous appearance. Insert: SV5 virion which appears to be adsorbed to the cell surface, with the viral spikes in contact with the plasma membrane.



Morphogenesis of virus particles. The replication of SV5 was examined in samples taken 8-144 hours after inoculation of MK cells at a multiplicity of 40 PFU/cell. Under these conditions, essentially all cells are infected (Holmes and Choppin, 1966). Extensive scanning is required to observe any viral components in MK cells sampled 8 hours after infection; by 12 hours or later, all stages in virus formation are seen. Figures 7-13 illustrate MK cells at 22 hours, when all stages in virus formation are frequently observed.

Segments of the viral nucleocapsid are seen free in the cytoplasmic matrix of infected cells, usually in the vicinity of the cell surface (Figure 7). They are not associated with any cellular membranes, but are commonly found near aggregates of ribosomes. Despite the high yield of virus at 22 hours, only small numbers of nucleocapsid strands are seen in the cytoplasm. Apart from this, no virus-specific alterations were detected in the interior of infected cells. Cell nuclei appeared normal, changes in distribution of free vs. membrane-associated ribosomes were not noticeable, and "factories" of dense material seen in other virus infections (Dales, 1965a) were absent.

As has been found with other myxoviruses, SV5 particles mature by budding from the cell surface. The viral nucleocapsid is seen aligned under some regions of the outer cell membrane (Figures 8, 12). In these regions, the cell membrane is covered with the surface projections characteristic of the virus particles. Such projections are particularly distinct on surfaces of BHK21-F cells infected with SV5 (Holmes, 1968; Compans et al., 1966). Areas such as these comprise a relatively small proportion of the total cell surface, and regions of modified membrane as long as in Figure 8 are extremely rare. Nucleocapsid aligned under the cell membrane and surface projections on the outer leaflet are invariably associated; neither has been observed to occur alone. The nucleocapsid lies in a single layer beneath the membrane; the regular spiral arrangement of nucleocapsid observed in filamentous virions has not been seen beneath the cell membrane, but appears to arise during the budding process.

Figures 7-13. Monkey kidney cells 22 hours after inoculation with SV5.

Figure 7. Strands of nucleocapsid (arrows) free in the cytoplasmic matrix near the surface of a cell. Few nucleocapsids are seen, although the rate of virus production is close to maximal.

Figure 8. Nucleocapsids, many in cross section, closely aligned under a long region of the cell membrane. A layer of dense material (arrows) resembling the viral surface projections is present on the outer surface of the membrane (micrograph courtesy of Dr. Samuel Dales).

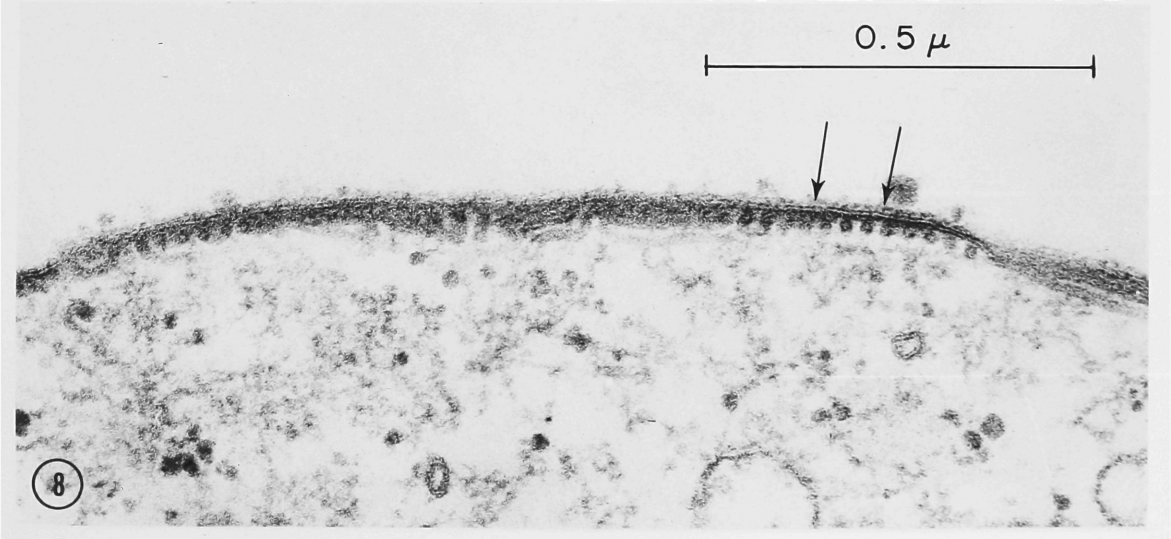
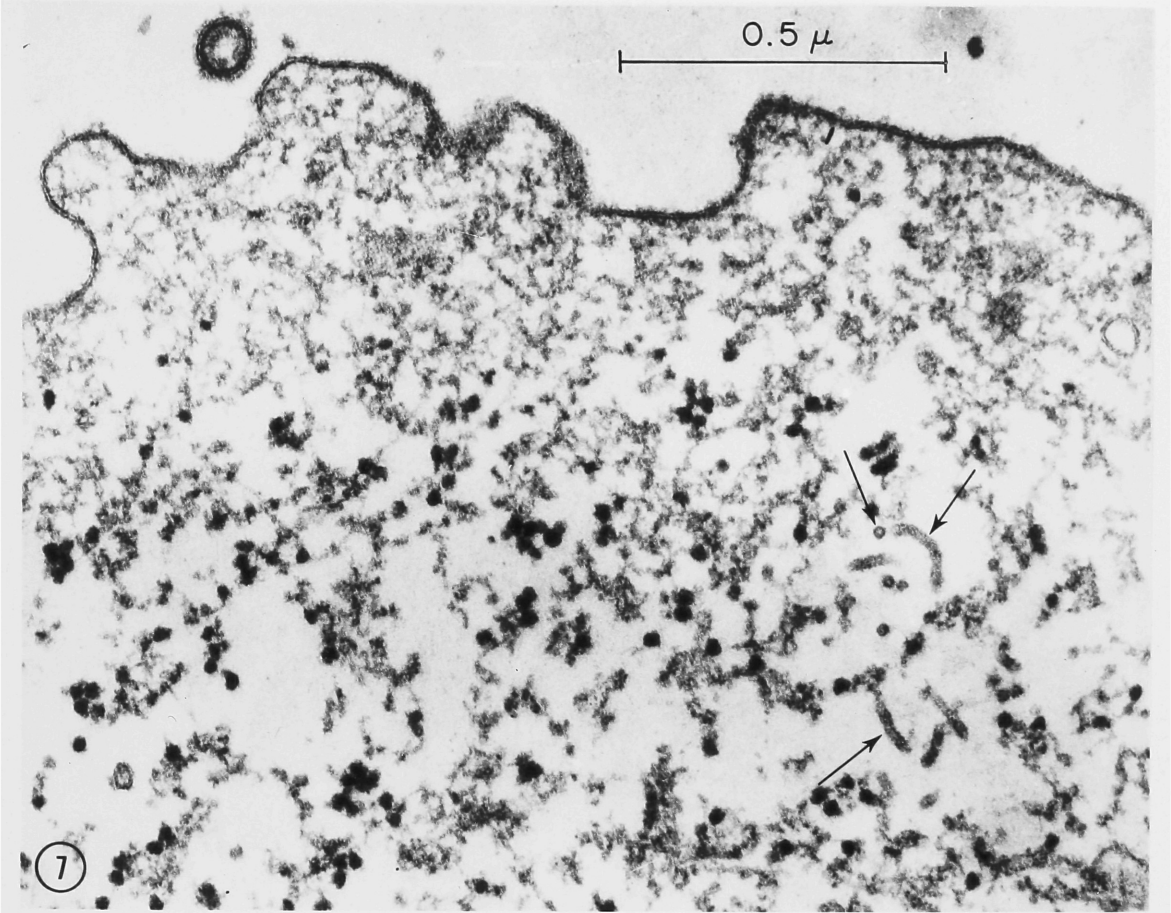


Figure 9. Two outfoldings of the cell membrane (arrows) with nucleocapsid under the membrane and viral projections on the outer surface. The unit membrane on apparently normal cell surfaces appears continuous with that in the modified budding region on the right.

Figure 10. A row of eight closely adjacent budding particles, and a single particle which appears to have been released. Many cross sections of nucleocapsid are apparent in the interior of budding particles.

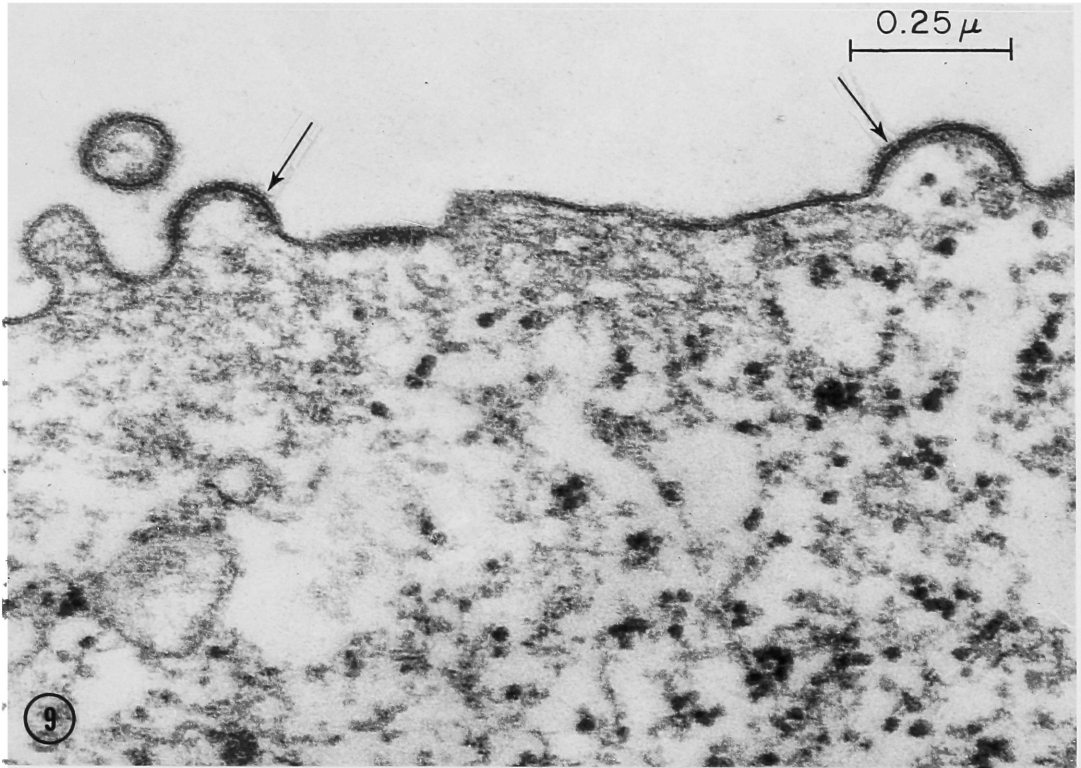


Figure 11. Portion of the cell surface with SV5 filaments in the process of budding and circular profiles which appear to be released spherical particles. Viral surface projections and nucleocapsid are present along the entire length of filaments but are absent on the adjacent cell membrane. At the base of the filament (arrow) the layers of the cell membrane are continuous with those of the unit membrane in the viral envelope. Near the bottom of the photograph, a region of the cell membrane is modified by underlying nucleocapsid and surface projections (double arrow).

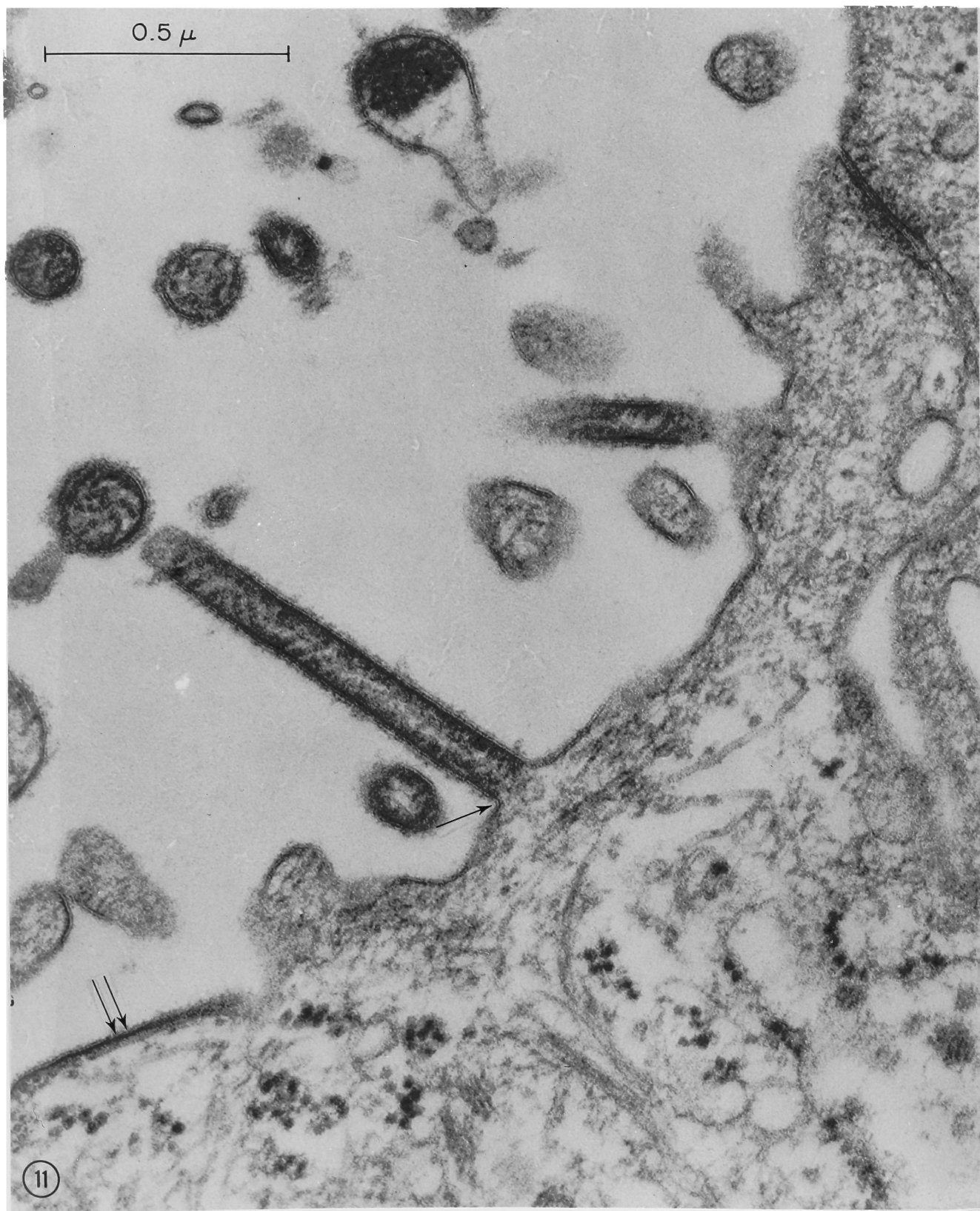
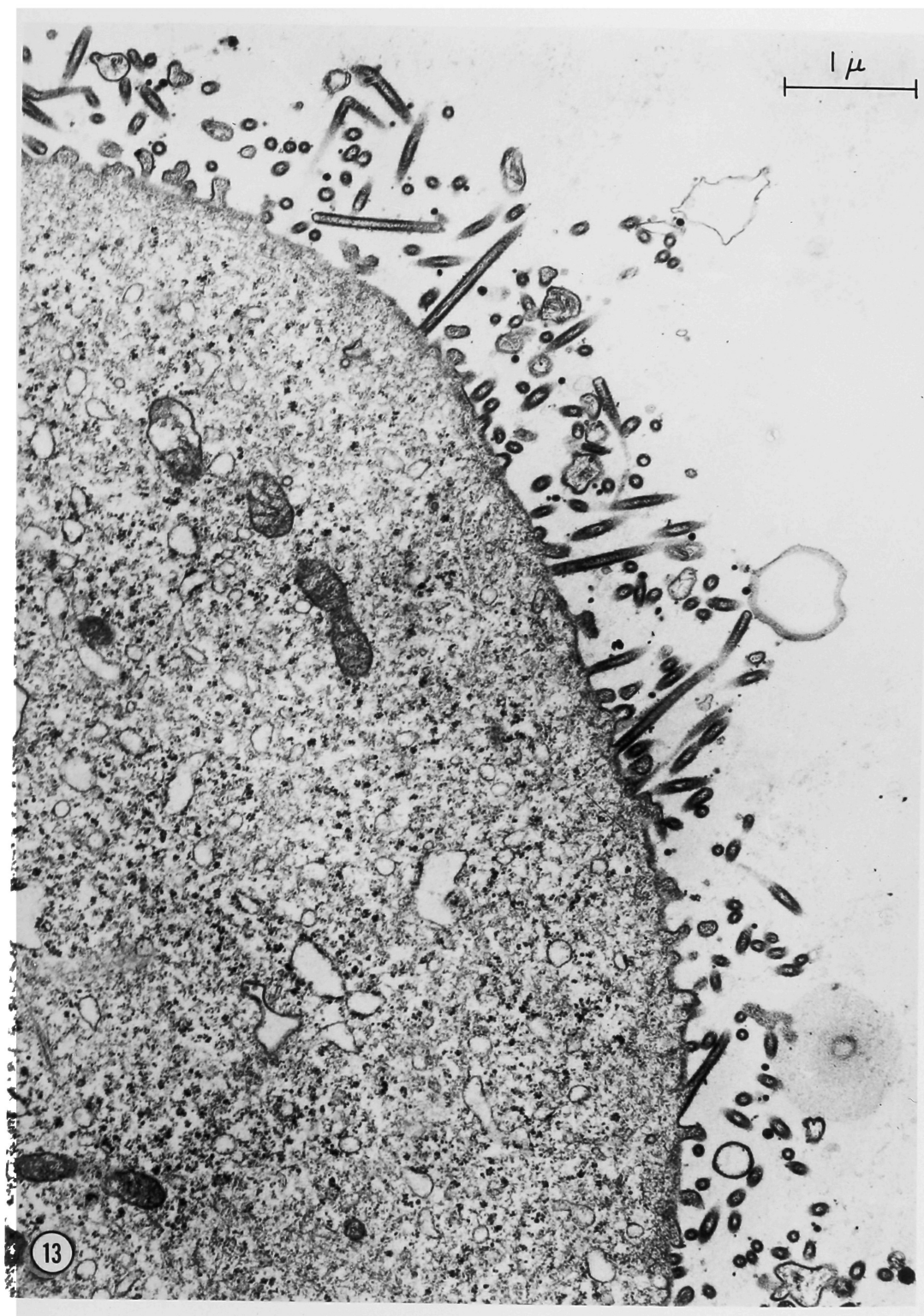


Figure 12. A portion of the cell surface showing nucleocapsid aligned under several regions of the cell membrane. Two long filaments contain nucleocapsid arranged in a regular spiral extending the length of the particles.



Figure 13. Low magnification view of an area of the cell showing many particles in the process of budding, and some possibly released. The cytoplasm of the cell appears essentially normal.



Beginning outfolding of the modified membrane is shown in Figure 9, and a row of eight budding particles is illustrated in Figure 10. Filamentous particles, typically oriented perpendicular to the cell surface, are shown in Figures 11-13. The filaments contain nucleocapsid and surface projections along their entire length, but neither are seen along the cell surface immediately adjacent to the filament. The layers of the unit membrane in the envelopes of budding virus particles are indistinguishable from and clearly continuous with those of the outer cell membrane (Figure 11).

Virus-induced alterations in infected MK cells. As described above, at 22 hours after inoculation, although high titers of SV5 have been produced by MK cells, only scattered small groups of nucleoprotein strands can be detected in the interior of infected cells. In striking contrast, in the BHK21-F cell line derived from hamster kidney, SV5 causes rapid and extensive cell fusion and little SV5 is produced. By 18 hours after infection, all cells have fused into a single multinucleate syncytium (Holmes and Choppin, 1966). In BHK21-F cells, there appears to be a block in virus maturation at the cell surface, and large cytoplasmic masses of SV5 nucleocapsid are observed (Holmes, 1968; Compans et al., 1966). Although MK cells can produce virus for many days with little cytopathic effects if the culture medium is replaced daily (Choppin, 1964), prolonged incubation of infected cells without change of the medium produces gradual cell fusion and accumulation of nucleocapsid.

Figure 14 shows cells sampled 3 days after inoculation. By this time, little fusion has taken place, and virus formation at the cell surface is still frequently observed. However, much greater amounts of nucleocapsid are seen, filling large areas of the cytoplasm. Cytopathic effects are not marked although some mitochondria appear swollen and segregated in clusters. By 6 days after inoculation, many giant cells are formed, containing 10-20 nuclei per cell. Cytopathic effects are clearly noticeable in some cells, consisting of vacuolized cytoplasm and myelin figure formation. The most striking change is the presence of large aggregates of SV5 nucleocapsid in the cytoplasmic matrix of these cells (Figure 15). Some of the strands show periodic striations indicating the helical structure. These aggregates, which are seen in MK cells only after prolonged incubation, are similar to the large inclusions of nucleocapsid which appear rapidly in BHK21-F cells infected with SV5 (Holmes, 1968).

Figure 14. Low magnification view of MK cells 3 days after inoculation with SV5. Virus production at the cell surface is still frequently observed at this time. Although no marked cytopathic effects are present, large areas of the cytoplasmic matrix are filled with SV5 nucleocapsid (arrows).

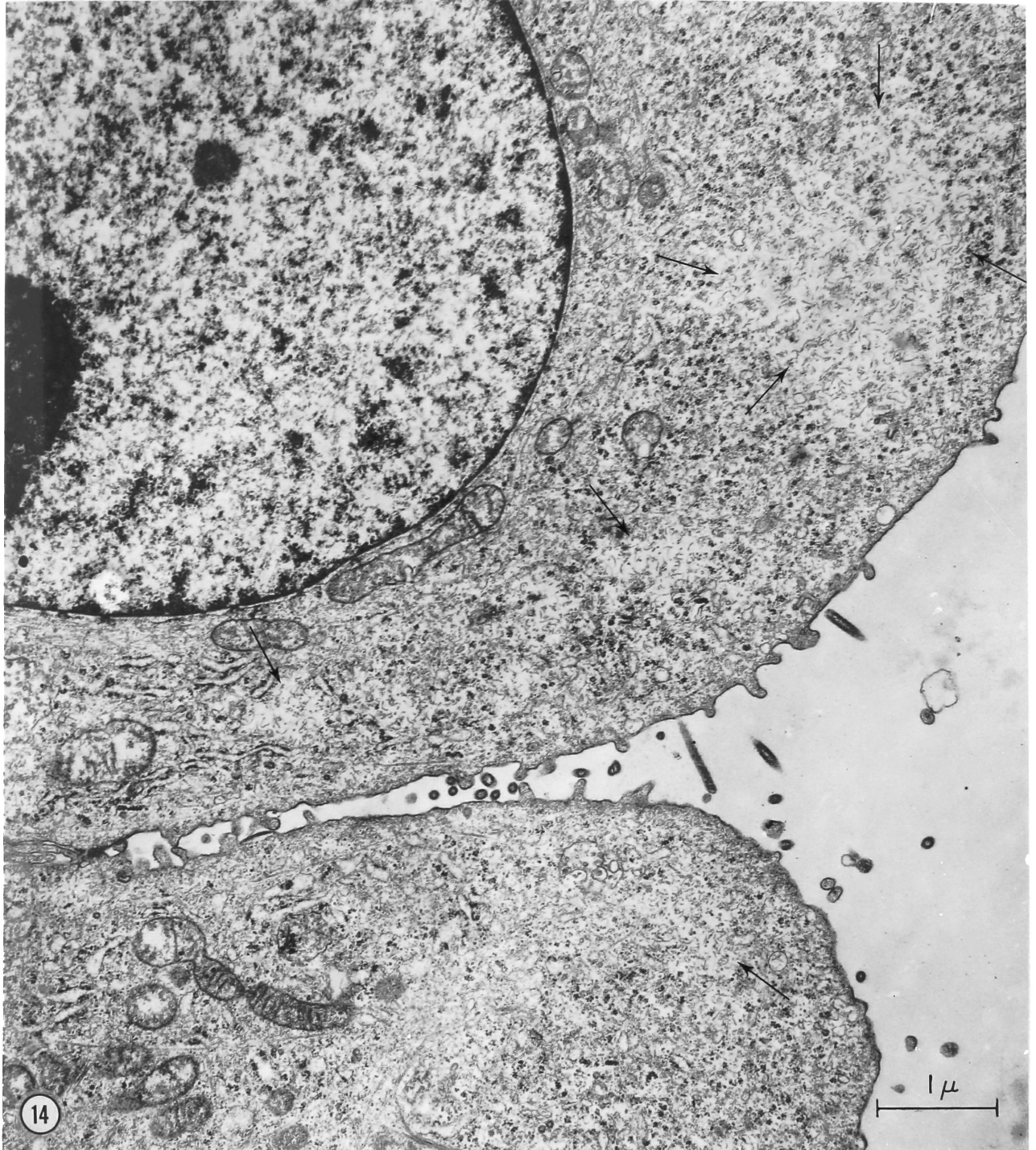
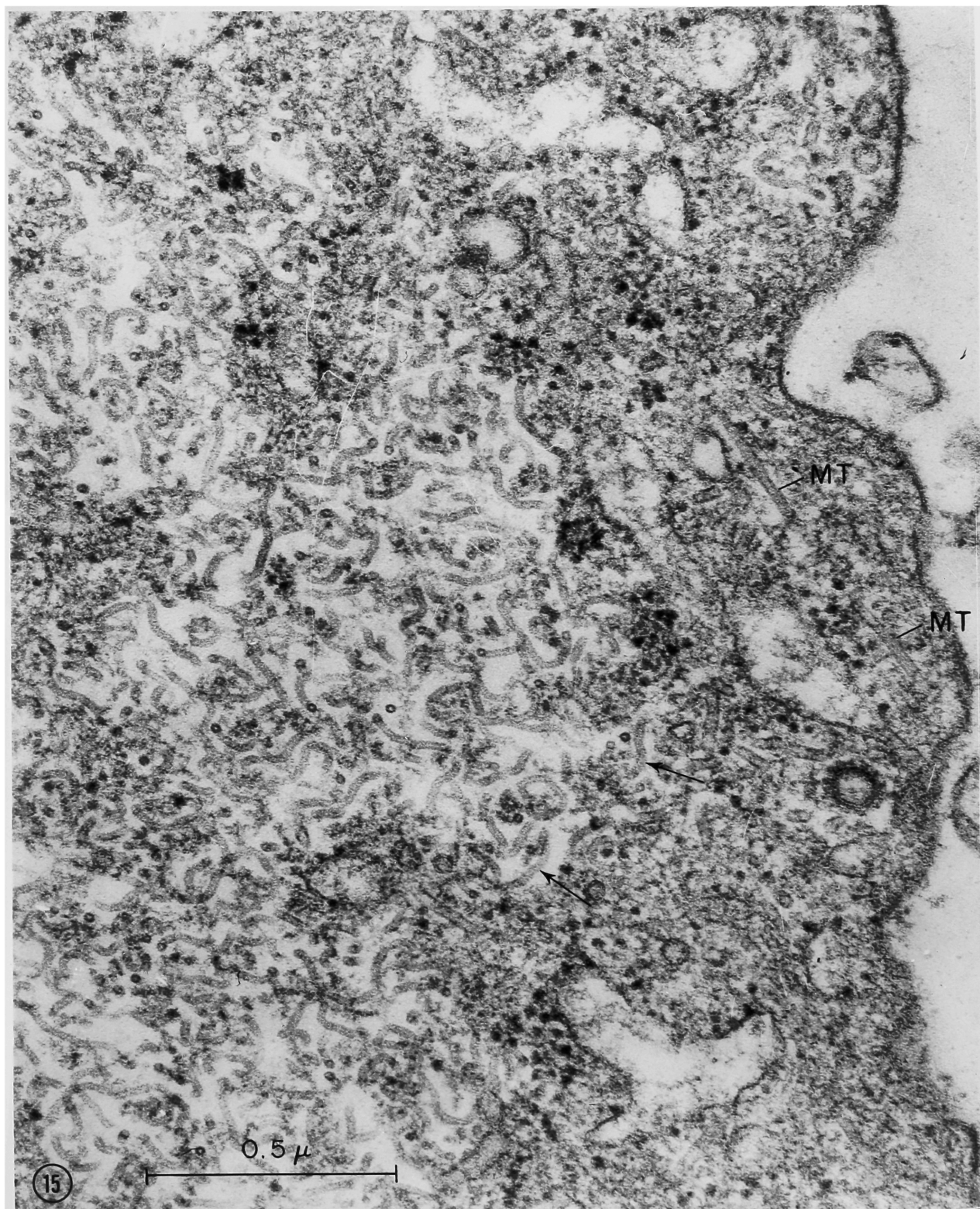


Figure 15. Portion of a MK cell 6 days after inoculation with SV5, with no intervening change of the culture medium. A large collection of SV5 nucleocapsid is shown at high magnification. Some of the strands (arrows) show periodicity indicative of the helical structure. The nucleocapsid is easily distinguished from the cellular microtubules (MT) which have a larger diameter and are rigid.



Discussion

These electron microscopic studies extend previous studies of the replication of SV5 (Choppin, 1964; Holmes and Choppin, 1966), and suggest a sequence of steps in the maturation of virus particles. SV5 appears to adsorb to host cells and enter by a process resembling phagocytosis, as previously found with several other animal viruses (Dales, 1965b). It is not clear whether nucleocapsid or free nucleic acid is released from phagocytic vacuoles to the cytoplasmic matrix. In agreement with previous studies employing immunofluorescence (Holmes and Choppin, 1966), the present observations indicate that the replication of SV5 occurs in the cytoplasm, although the nuclear synthesis of precursor molecules cannot be completely excluded. The helical nucleocapsid appears to be formed in the cytoplasmic matrix and becomes aligned under regions of the cell membrane. In such regions, the cell membrane acquires viral surface projections or spikes by a mechanism which is not clear. Identifiable spikes have not been detected on intracellular membranes nor have they been seen in the process of penetrating the plasma membrane, though this may occur. Since spikes on the outer leaflet and nucleocapsid beneath the cell membrane are always associated, it is not unlikely that they appear simultaneously at the cell surface. This could occur by incorporation of precursors of the spike into regions of the membrane, resulting in specific sites with an affinity for nucleocapsid. The presence of virus-specific components in cell surfaces prior to any morphological change is also suggested by the specific adsorption of erythrocytes to regions of cell membrane which are of normal appearance (Hotchin et al., 1958; Compans et al., 1967). As nucleocapsid aligns under such regions, spikes might appear by a polymerization or rearrangement. Virus maturation is then completed by an outfolding of the modified membrane, enclosing the underlying nucleocapsid.

The surface changes seen with SV5 in the present study are similar to those described by Berkaloﬀ (1963) in a study of KB cells infected with parainfluenza 1 virus. The presence of nucleocapsid in the cytoplasm of cells infected with WB virus, another parainfluenza virus, was described by Prose and co-workers (1965), while the present study was in progress. Subsequent to the present investigation (Compans et al., 1966), other electron microscopic studies of subgroup II myxovirus replication showed

morphological stages in virus formation similar to those reported here (Howe et al., 1967b; Duc-*Nguyen* and Rosenblum, 1967; Ane, 1967).

It is now well established that myxoviruses acquire their envelope during the budding process. As discussed previously, it has been shown that the lipids of the virus are derived from the host cell, but a controversy continues to exist concerning the presence of host cell antigens in the virion. The present results indicate that the cellular unit membrane is incorporated into the virion and, with the added virus-specific surface projections, makes up the viral envelope. The unit membrane of the cell has been clearly resolved, and is morphologically indistinguishable from that in the virus particle; during budding, the leaflets of the unit membrane of the cell are continuous with those of the virion. It therefore seems likely that host antigen in the form of a component(s) of the unit membrane could form a part of the viral envelope, although the possibility that all cellular macromolecules are replaced by virus-specific proteins cannot be ruled out. The presence of host cell antigen in the unit membrane of the viral envelope is not incompatible with the recent finding by Duc-*Nguyen* and co-workers (1966) that ferritin-labelled anti-host cell antibody did not attach to the surface of influenza virus particles, because such an antigen would probably not be accessible to such antibody, being protected by the overlying layer of closely packed surface projections.

SV5 filaments typically arise perpendicular to the cell surface, rather than forming tangentially as described by Prose and co-workers (1965) with WB virus. Although filament formation is frequent, long areas (such as in Figure 8) of cell membrane which have surface projections and underlying nucleocapsid, are rare and do not appear to be necessary intermediates for filament formation. Spikes are not seen on the cell surface immediately adjacent to filaments, as would be expected if filaments gradually developed from such long areas. It is possible that filaments are formed by the continued elongation of small buds, and that spikes and nucleocapsid are incorporated at the base.

It has been generally thought that filamentous virions are infrequent in the parainfluenza-mumps-Newcastle disease subgroup of myxoviruses (Waterson, 1962), and in unfixed, negatively stained preparations of SV5

typical filaments were not seen (Choppin and Stoeckenius, 1964b). However, numerous filaments are found in sections of fixed SV5-infected cells. The absence of filaments in negatively stained preparations of this subgroup of myxoviruses could result from removal by low speed centrifugation or disruption during purification, concentration, or staining. In addition, some of the large pleomorphic forms filled with nucleocapsid, that are commonly seen, might result from distortion of filaments, and the large amounts of free nucleocapsid found in negatively stained preparations could result in part from disruption of filaments.

Evidence has been presented (Holmes and Choppin, 1966) which suggests that the behavior of SV5 either as a moderate virus (in MK cells) or a cytotoxic virus (in BHK21-F cells) depends on the response of the cell membrane. The MK cell membrane is relatively resistant to fusion by SV5, and infected, virus-producing cells survive for days. The BHK21-F membrane is extremely sensitive to fusion, and inhibition of macromolecular synthesis and cell death occur after extensive fusion. The present electron microscopic studies demonstrate that SV5 causes minimal cell damage to MK cells while large quantities of virus are being produced, and there is only a gradual accumulation of nucleocapsid by the cells. There appears to be a balance between the synthesis of nucleocapsid and its extrusion from the cell in virus particles. In marked contrast, BHK21-F cells are unable to incorporate nucleocapsid into mature virus at the rate at which it is synthesized, and large quantities of nucleocapsid accumulate in the cytoplasm (Holmes, 1968; Compans et al., 1966). The moderate interaction of SV5 with MK cells therefore appears correlated with extrusion of viral components by an efficient budding mechanism, and a cell membrane which is resistant to the cell-fusing activity of the virus.

III. ISOLATION AND PROPERTIES OF SV5 NUCLEOCAPSID

The nucleocapsid of subgroup II myxoviruses, as already described, is a single-stranded helix with a diameter of 150-180 A. Estimates have been made of the total length of nucleocapsid within negatively stained subgroup II myxoviruses (Cruickshank, 1964; Hosaka et al., 1966) but this is difficult because the nucleocapsid is usually seen in an irregular, tangled arrangement, and also because virions are often not penetrated by the stain. In addition, some large virus particles contain much more nucleocapsid than others. A precise determination of the length of nucleocapsid released from disrupted virus particles is also difficult because the nucleocapsid is often fragmented, or at times stretched into a loose coil. Due to this inability to obtain a significant number of intact nucleocapsids, it has not been possible to establish the length which contains one genome in this group of viruses.

An approach to the isolation of myxovirus nucleocapsids was suggested by the observation that large amounts of SV5 nucleocapsid can accumulate within the cytoplasm of infected cells. A procedure for obtaining apparently intact nucleocapsid from infected cells is described here. The nucleocapsid was purified by gradient centrifugation, and its length and RNA and protein content were determined.

Materials and Methods

Virus and cells: The W3 strain of SV5 and rhesus monkey kidney cell cultures have been described in part II. Newcastle disease virus (Hickman strain) was grown by allantoic inoculation of 10-day-old chick embryos with approximately 10^5 PFU, and harvesting allantoic fluid after 2 days. The BHK21-F cell line, a heteroploid variant of the BHK21 cell line derived from baby hamster kidney (Macpherson and Stoker, 1962), was grown in reinforced Eagle's medium (Bablanian et al., 1965) with 10% calf serum and 10% tryptose phosphate broth, as described by Holmes and Choppin (1966).

Plaque assay: For plaque assay of SV5 (Choppin, 1964) virus dilutions were made in Eagle's medium with 1% bovine serum albumin at 4° C. Confluent MK monolayers in 60 mm Petri dishes were washed with PBS and inoculated with 0.5 ml of the dilutions to be assayed. Plates were incubated at 37° C for 2 hours with agitation at 20-minute intervals, after which

the inoculum was removed and an overlay of reinforced Eagle's medium with 4% calf serum and 0.95% agar (Noble) was applied. Plates were stained with 2 ml of 0.01% neutral red in the above overlay medium (without serum) after 3 days, and plaques read on the 4th and 5th days.

BHK21 plates were inoculated for plaque assay as described above, and overlayed with Eagle's medium containing 4% calf serum, 2% tryptose phosphate broth, and 0.95% agar. Plates were stained and plaques read as above.

Electron microscopy: A drop of sample was applied to a formvar-coated grid with a heavy carbon film, excess liquid was removed, and a drop of 2% sodium phosphotungstate, pH 6.2, was applied for negative staining. A Hitachi HS-7S electron microscope was used.

Analytical procedures: Protein was determined by the Lowry procedure (Lowry et al., 1951), using bovine serum albumin as a standard. RNA was determined by the orcinol reaction (Mejbaum, 1939) with a yeast RNA standard. DNA was determined by the diphenylamine reaction (Burton, 1956) with calf thymus DNA as a standard. The anthrone reaction (Scott and Melvin, 1953) was used to determine total hexoses. Total lipid was determined on an aliquot of washed lipid extract (Folch et al., 1957) by a microgravimetric technique.

Sucrose gradients: Linear 4.8 ml gradients of 5-20% sucrose in TEN buffer (0.005 M Tris HCl, 0.05 M NaCl, 0.001 M EDTA, pH 7.2) were routinely prepared in 1/2" x 2" cellulose nitrate tubes.

Radioactivity determinations: Samples were dissolved in 10 ml Liquiflor (Pilot Chemicals, Inc.) in toluene-methanol (1:1) unless indicated otherwise in legends.

Immune serum: Purified nucleocapsid was diluted with phosphate-buffered saline to a concentration of 25 µg/ml, and 100 µg was injected intravenously into rabbits weighing 2-3 kg; 10 days later 100 µg was injected intraperitoneally. Rabbits were bled 18 days after the second injection.

Chemicals and isotopes: Cesium chloride and sucrose (30% w/w) optical grade were obtained from Harshaw Chemical Co., Cleveland, O.; ribonuclease and calf thymus DNA from Worthington Biochemical Corp., Freehold, N.J.; yeast RNA, purified type X1, from Sigma Chemical Co., St. Louis, Mo.; crystallized bovine plasma albumin, from Armour Pharmaceutical Co.,

Kankakee, Ill.; and pronase, from Calbiochem, Los Angeles, Calif. Sodium dodecyl sulfate (SDS) obtained from Amend Drug and Chemical Co., New York, N.Y., was recrystallized from 90% ethanol. ^{14}C -linoleic acid and uridine-5- ^3H were obtained from Nuclear Chicago, Des Plaines, Ill.; and ^{14}C -algal protein hydrolysate, from New England Nuclear Corp., Boston, Mass.

Results

Release of nucleocapsid from osmotically shocked cells. The rapid accumulation of nucleocapsid in the cytoplasm of SV5-infected BHK21-F cells and its gradual accumulation in MK cells have been already described. For isolation of SV5 nucleocapsid, BHK21-F cells were disrupted 18-24 hours after inoculation at a multiplicity of 5-20 PFU/cell, and MK cells, 6 to 8 days after inoculation at a similar multiplicity.

Cells were suspended with 0.25% trypsin and 0.05% EDTA in PBS, pelleted at 250 g for five minutes, and resuspended in distilled water at a concentration of 4×10^6 MK cells or 1.5×10^7 BHK21-F cells/ml, based on cell numbers at time of inoculation. The large syncytia and many smaller cells were disrupted by this treatment. Electron microscopic examination of these distilled water extracts showed that SV5 nucleocapsid had been released from the cells. The majority of the nucleocapsids were long and tightly wound; examples are shown in Figure 16. Loosely coiled segments of the helix were rare.

The distribution of lengths of nucleocapsid was determined by photographing and measuring all tightly coiled pieces within a randomly selected region of the grid; the infrequent pieces of nucleocapsid with stretched-out segments were not measured. The cumulative result of two experiments is shown in Figure 17. A sharp peak is evident around 1μ ; of 254 pieces measured, 72% had a length falling in the interval between 0.9μ and 1.1μ . Fifteen pieces had lengths ranging from 1.8μ to 2.4μ , but pieces with lengths between 1.2μ and 1.8μ were strikingly rare. Although pieces $>2.4 \mu$ in length were not encountered in these determinations, scanning of grids with large numbers of nucleocapsids revealed rare pieces up to 4μ in length. The mean length, and the standard deviation, of the pieces between 0.9μ and 1.1μ were calculated for each of the two experiments, and the values obtained were $1.01 \pm 0.04 \mu$ and $1.03 \pm 0.03 \mu$.

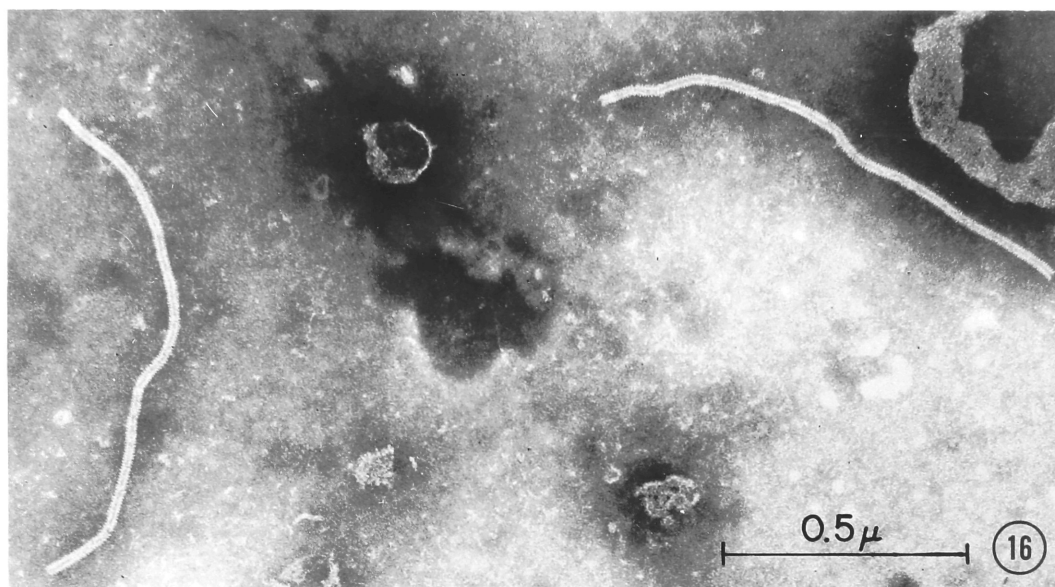


Figure 16. SV5 nucleocapsids released from MK cells by osmotic shock and fixed with glutaraldehyde prior to negative staining.

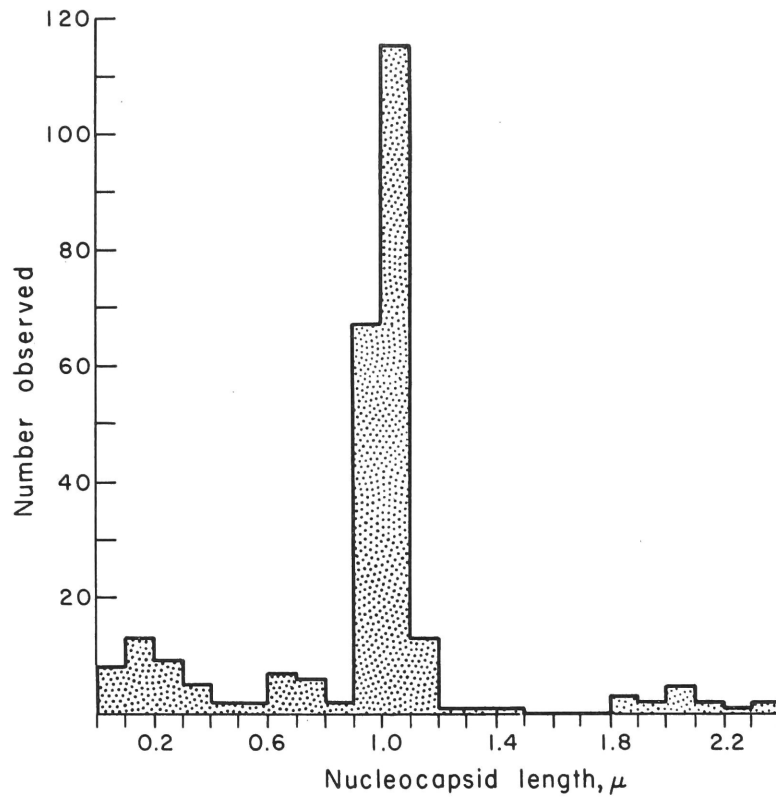


Figure 17. Distribution of lengths of nucleocapsid released from MK cells. Electron micrographs were taken and all tightly coiled pieces were measured.

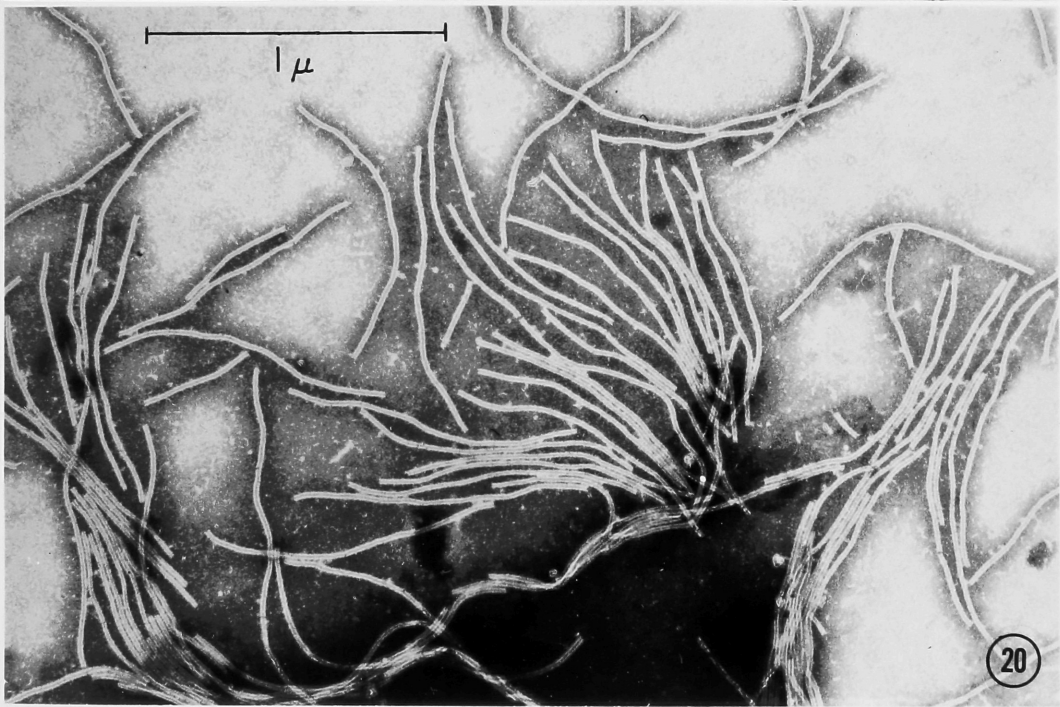
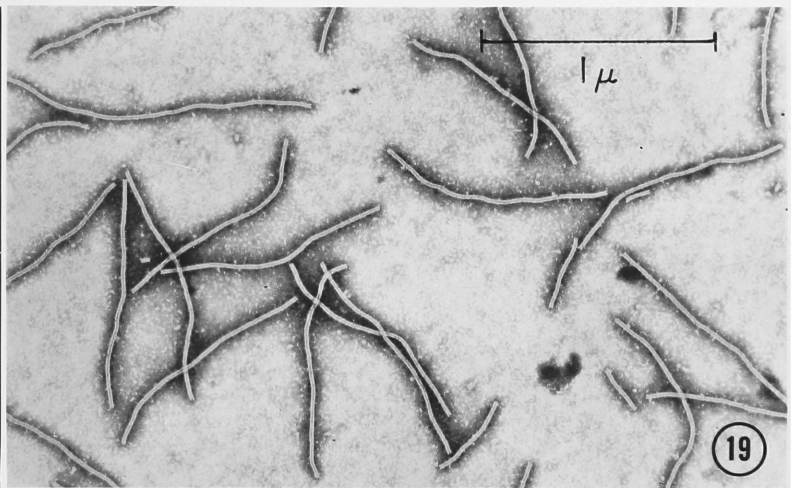
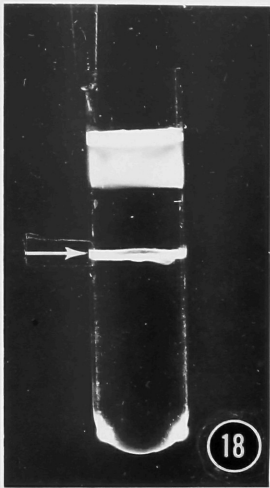
Purification of nucleocapsid. Equilibrium centrifugation in cesium chloride has greatly facilitated the concentration and purification of SV5 nucleocapsid. Figure 18 shows a membrane-like band obtained by centrifugation of a distilled water extract of infected MK cells. Electron microscopic examination indicated that the band consisted of nucleocapsid with well-preserved structure; typical fields are shown in Figures 19 and 20. No contaminating cellular material or intact virions were found. Nucleocapsid banded once in cesium chloride showed a length distribution similar to that observed immediately after release from cells, as in Figure 17.

The complete procedure employed for purification of nucleocapsid was as follows (Figure 21). Distilled water extracts of infected cells, prepared as described above, were cleared of cellular debris by centrifugation at 6500 g for 15 minutes at 4° C. Centrifugation was then carried out in a CsCl gradient which was preformed by successive layers of 2.5 ml of 40% (w/w) CsCl, 5 ml of 30% CsCl, and 4 ml of 25% CsCl in deionized distilled water. Cell extract (20 ml) was layered over this gradient to fill the tube, and it was spun for 3 hours at 24,000 rpm in a Spinco SW 25.1 rotor. A band of nucleocapsid formed in the 30% CsCl region, whereas most of the contaminating material did not sediment through the 25% CsCl layer. The nucleocapsid band was collected, diluted to 5 ml with 30% CsCl, and recentrifuged to equilibrium as described in Figure 18. The resulting band was collected and again diluted with 30% CsCl and centrifuged a third time by the same procedure.

To demonstrate that the purified nucleocapsid was free of contamination by cellular RNA and protein, distilled water extracts from infected cells were mixed with extracts from uninfected cells grown in the presence of ^{14}C -algal protein hydrolysate or ^3H -uridine, and carried through the purification procedure. Radioactivity in the nucleocapsid preparation thus served as an index of contamination. The optical density and radioactivity of fractions from a gradient are shown in Figure 22; in this experiment, ^3H -labelled cellular RNA was no longer present after the second CsCl centrifugation. Experiments were carried out with both MK and BHK21-F cells, and in each case the purification procedure involving three bandings in CsCl was found sufficient to remove the labelled cellular RNA and protein from the nucleocapsid, indicating that the contamination of nucleocapsid with cellular RNA and protein was < 0.02% and < 0.15% respectively.

Figure 18. A single, membrane-like band of nucleocapsid (arrow), observed after equilibrium centrifugation in CsCl. The band is sharp but with wavy contours, which give the appearance of separate lines in some parts of the photograph. Distilled water extracts were clarified at 1500 g for 10 minutes. Cesium chloride (2.0 gm) was added to the supernatant (4.5 ml), and the solution centrifuged at 36,000 rpm for 12 hours in a Spinco SW 39 rotor. Residual cellular debris is seen at the top of the tube.

Figure 19-20. Negatively stained, unfixed nucleocapsids obtained from a CsCl gradient. A drop from the gradient fraction which contained the band was diluted about tenfold with water, applied to a grid, and stained with sodium phosphotungstate. The nucleocapsids are tightly coiled, and most measure about 1 μ in length.



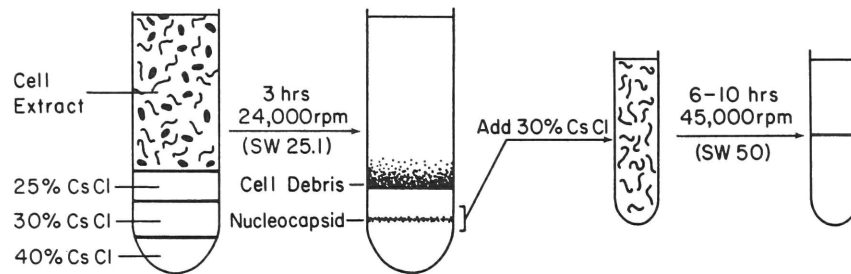


Figure 21. Diagram of the procedure used to purify SV5 nucleocapsid.

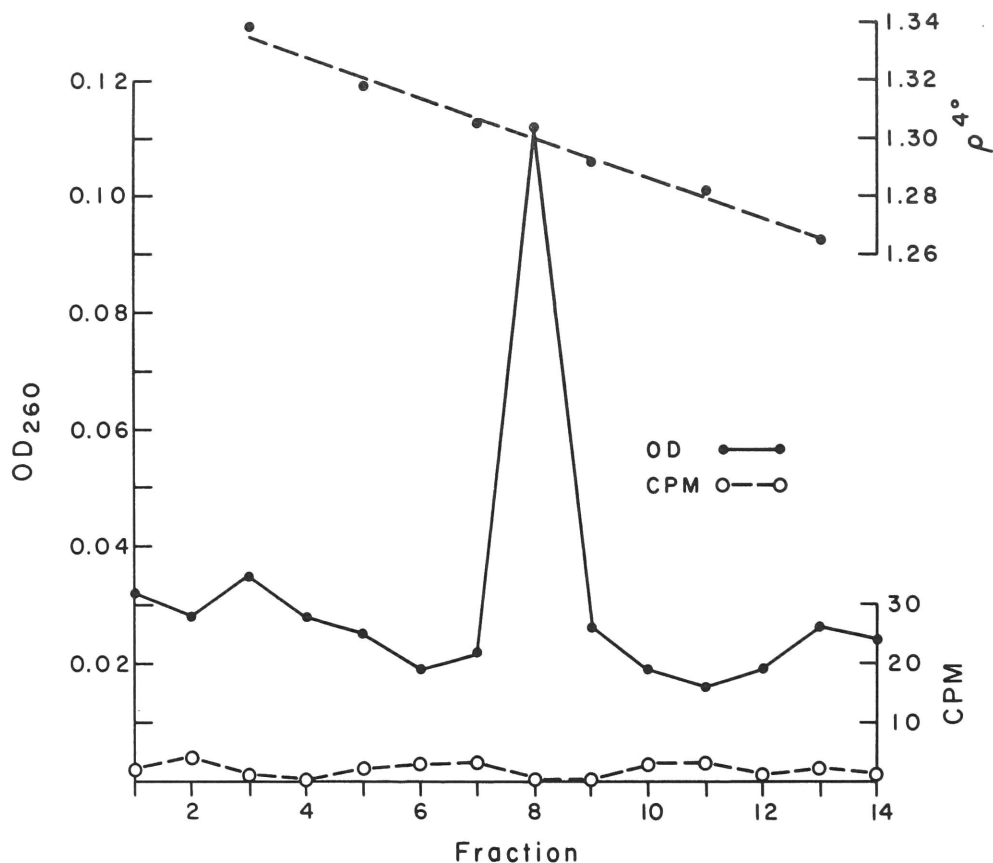


Figure 22. Absence of cellular RNA in nucleocapsid purified from BHK21 cells by CsCl gradient centrifugation. Prior to purification, an extract of uninfected, ^3H -uridine-labelled BHK21-F cells, containing 630 μg of RNA with a specific activity of 2500 cpm/ μg , was mixed with infected cell extract, and carried through the first two CsCl gradients of the purification procedure described in the text. Fractions were collected from below, and radioactivity was determined on 20 μl dissolved in 10 ml of Liquifluor scintillation fluid (Pilot Chemicals, Inc.) in toluene-methanol (1:1). Optical density was measured on 300 μl diluted to 1 ml with water. Density was calculated from refractive index measurements.

A similar technique was used to rule out contamination by lipids. ^{14}C -linoleic acid bound to albumin was added to BHK21-F cells at the time of infection, and the cells were disrupted after 19 hours. The crude extract contained 12,500 μg lipid with a specific activity of 58 cpm/ μg . Thin-layer chromatography confirmed that ^{14}C had been incorporated into phospholipid and neutral fat, and indicated that $< 5\%$ of the label remained in free fatty acid. The purification of nucleocapsid removed all the radioactivity, indicating not only the absence of contamination with cellular lipids, but also that lipid is not an integral part of the nucleocapsid.

These results demonstrate the purity of the nucleocapsid with regard to contamination by cellular materials. In addition, immune serum prepared against nucleocapsid had no neutralizing or hemagglutination-inhibiting activity when tested against intact SV5 virions (Table 4), indicating the absence of SV5 envelope antigens in the purified nucleocapsid preparations. The above procedure was therefore employed to prepare purified nucleocapsid for the analyses described below. Yields of 1-2 mg of purified nucleocapsid were obtained from approximately 10^9 BHK21-F cells or 4×10^8 MK cells.

Properties of SV5 nucleocapsid:

(a) Chemical composition. Purified nucleocapsid preparations, consisting of 1-2 mg, were dialyzed against 0.02 M Tris-HCl, pH 7.2, and analyzed for RNA, DNA, protein, and hexose-containing carbohydrate. Only RNA and protein were present in detectable amounts, and the analyses of six different preparations are listed in Table 5. The mean per cent RNA was found to be 4.1, with a range of 3.7-4.4.

The ultraviolet absorption spectrum of a sample of purified nucleocapsid (Figure 23) shows a minimum at approximately 250 $\text{m}\mu$ and a broad maximum around 265 $\text{m}\mu$. This resembles the absorption spectrum of tobacco mosaic virus (TMV) (Bonhoeffer and Schachman, 1960). The content of nucleic acid and protein was also estimated spectrophotometrically (Warburg and Christian, 1941). To dissociate the material and minimize light scattering, samples were treated with 0.5% sodium dodecyl sulfate (SDS) prior to measuring the optical density (Bonhoeffer and Schachman, 1960). The average 280/260 ratio obtained from three preparations was 0.90,

TABLE 4

Failure of SV5 Nucleocapsid to Elicit Hemagglutination-Inhibiting
or Neutralizing Antibodies

Serum	Hemagglutination- inhibition titer*	Neutralization [†]	
		serum dilution	PFU/plate
Rabbit 1072, normal	< 24	1:20	99 , 90
Rabbit 1072, immunized with SV5 nucleocapsid	< 24	1:20	109 , 92
Rabbit 1073, normal	< 24	1:20	85 , 91
Rabbit 1073, immunized with SV5 nucleocapsid	< 24	1:20	86 , 85
Rabbit 959, immunized with SV5 virions	6144	1:12,800	0 , 0 , 0

* Two-fold serial dilutions of potassium periodate-treated sera were made in BS to give 0.3 ml final volume, after which 0.3 ml SV5 (4 HAU) and 0.6 ml of 0.36% chicken erythrocytes were added. Results were recorded after 90 minutes at 4° C.

† SV5 virus, diluted sufficiently to produce approximately 100 plaques per plate, was incubated for 15 minutes at 25° C in the serum concentration indicated prior to inoculation for plaque assay.

TABLE 5
Chemical Composition of SV5 Nucleocapsid

Preparation	Source, cells	RNA* (μ g/ml of sample)	Protein* (μ g/ml of sample)	% RNA
1	BHK21-F	36	952	3.7
2	BHK21-F	19	474	3.9
3	BHK21-F	41	912	4.3
4	MK	29	708	3.9
5	MK	28	652	4.1
6	MK	27	592	4.4
Mean				4.1

* Mean value of two separate determinations on each preparation of nucleocapsid.

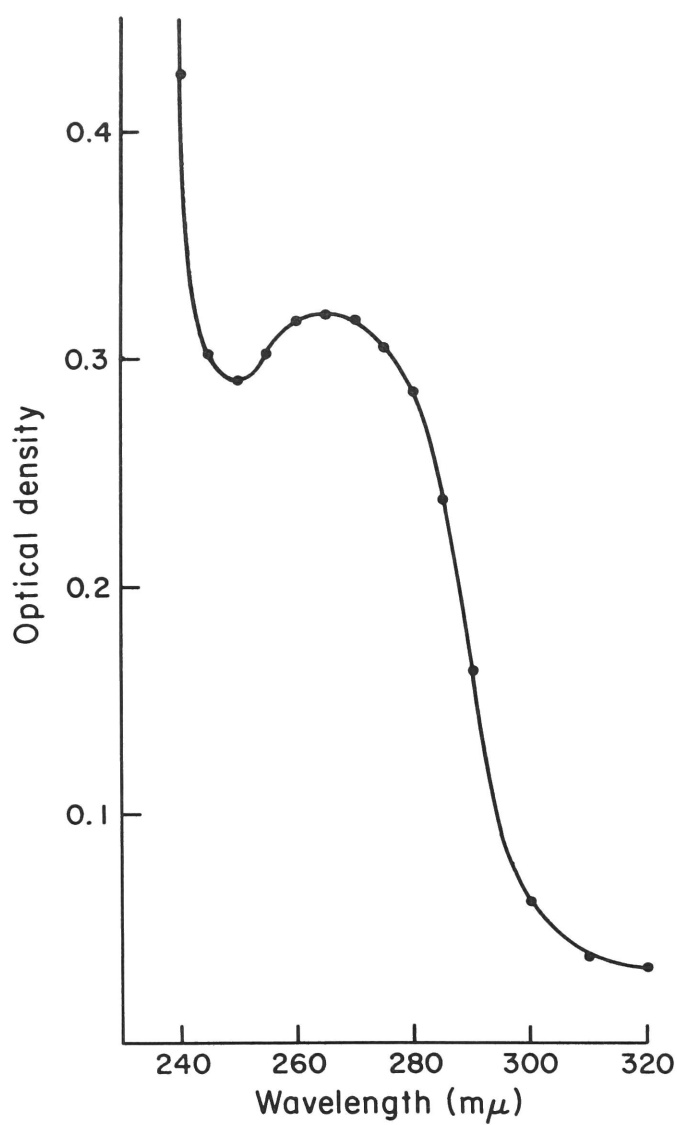


Figure 23. Ultraviolet absorption spectrum of purified SV5 nucleocapsid, determined in a Zeiss PMQ II spectrophotometer.

corresponding to a nucleic acid content of 4.6%, which is similar to the chemically determined value. Without SDS treatment, light scattering caused 280/260 ratios as low as 0.79, which would erroneously suggest an RNA content of 6.8%.

(b) Density in cesium chloride. The buoyant density of SV5 nucleocapsid was determined by equilibrium centrifugation in CsCl in the Spinco model E analytical ultracentrifuge. A single peak was obtained (Figure 24). A value of 1.297 ± 0.002 was calculated for the buoyant density, based on the results of four experiments.

During the purification in CsCl gradients, two closely adjacent bands were observed in some experiments, particularly when large amounts of nucleocapsid were present. These consisted of a lower, membrane-like band and an upper, more diffuse band. The relative sizes of these bands varied, and usually the membrane-like band disappeared by the final gradient. Both bands consisted of SV5 nucleocapsid, and no morphological differences were detected in the electron microscope. The lower band, after collection, contained macroscopic clumps, and the spectrum of this material indicated a high degree of light scattering, as shown by the optical density at 300 m μ . The upper band contained no visible clumps and showed much less light scattering. After treatment with 0.5% SDS, the two bands had similar ultraviolet absorption spectra. These results suggest that the nucleocapsid in the two bands is similar in composition and differs only in extent of aggregation.

(c) Sedimentation in sucrose gradients. The sedimentation coefficient of SV5 nucleocapsid was estimated by sedimentation of ^3H -uridine labelled nucleocapsid on sucrose density gradients. In some preparations, sedimented immediately after removal of CsCl by dialysis, a single broad band was observed (Figure 25A). The radioactivity in this peak was completely resistant to digestion by pancreatic ribonuclease, in agreement with the lack of effect of this enzyme on nucleocapsid morphology described below. The sedimentation coefficient of the nucleocapsid in this band, estimated by comparison with poliovirus, was approximately 300 S.

Many preparations of nucleocapsid sedimented heterogeneously and much more rapidly than the illustrated 300 S peak, with most of the radioactivity at the bottom of the tube. It seems likely, in view of the tendency of

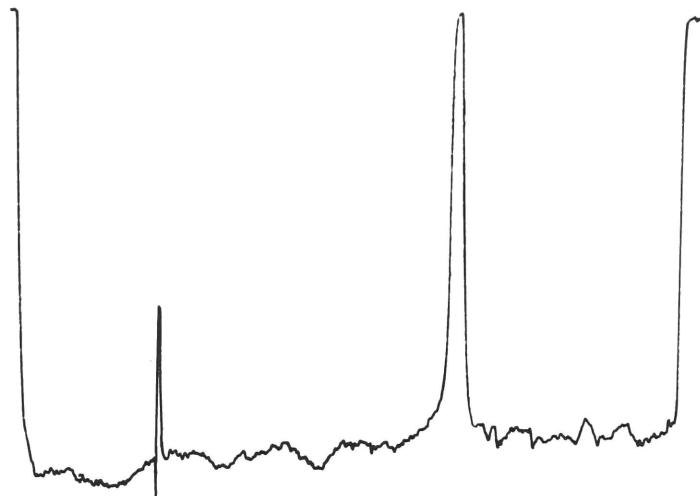


Figure 24. A Joyce-Loebl densitometer trace showing a single peak in the ultraviolet absorption profile after equilibrium sedimentation of SV5 nucleocapsid in the Spinco model E ultracentrifuge. A solution of CsCl (density = 1.2871) in 0.01 M Tris-HCl, 0.001 M EDTA, 0.05 M NaCl, pH 7.4, containing approximately 50 $\mu\text{g/ml}$ of purified nucleocapsid, was centrifuged at 44,000 rpm. Photographs were taken after 18 hours.

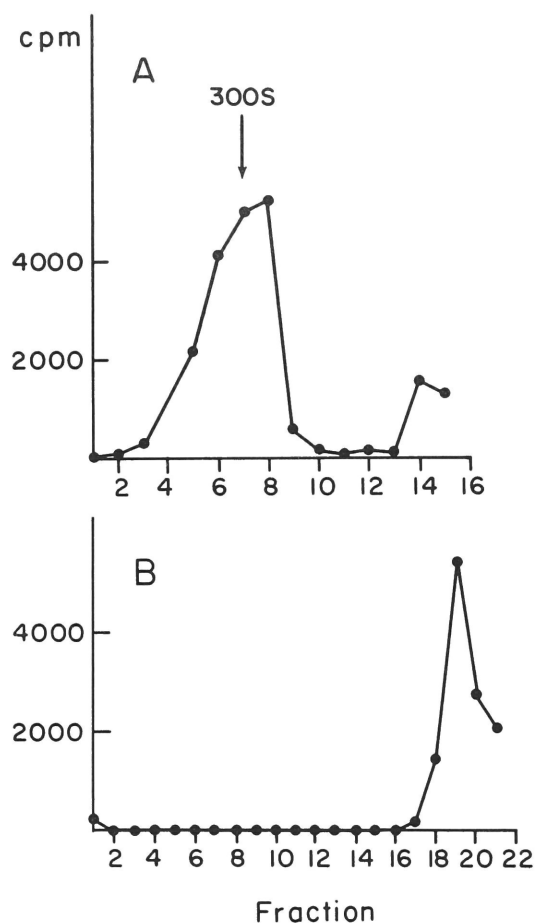


Figure 25. Sedimentation of SV5 nucleocapsid on sucrose density gradients. ^3H -uridine-labelled nucleocapsid was grown in BHK21 cells, purified in CsCl gradients, and dialyzed vs. 0.02 M Tris HCl, pH 7.4. A. 100 μ l was layered over a gradient of 5-20% sucrose in TEN. B. 100 μ l of nucleocapsid was mixed with 10 μ l of 10% SDS and layered over a 5-20% gradient of sucrose in TEN and 0.5% SDS. Gradients were centrifuged for 30 minutes at 30,000 rpm, 4°C , in a Spinco SW39 rotor. Fractions were collected, 10 μ g bovine serum albumin was added as carrier, and 2 ml 10% trichloroacetic acid added for precipitation. The precipitates were collected on millipore filters (0.45 μ), dried, and counted in 10 ml Liquifluor scintillation fluid in toluene.

the nucleocapsid to aggregate in visible clumps, that such rapidly sedimenting material represents aggregates. Aggregation of Newcastle disease virus nucleocapsid has also been observed in sucrose gradients (D. W. Kingsbury, personal communication).

The addition of 1% SDS to the sucrose gradient caused a striking reduction in the sedimentation velocity of incorporated ^3H -uridine (Figure 25B). As described in the following section, SDS treatment appears to dissociate SV5 RNA from nucleocapsid protein, and it is possible to isolate RNA by prolonged centrifugation in a similar gradient.

Effect of enzymes on SV5 nucleocapsid. Incubation of SV5 nucleocapsid with ribonuclease (500 $\mu\text{g}/\text{ml}$ in PBS) for 30 minutes caused no detectable structural change. Trypsin, chymotrypsin, and deoxyribonuclease also caused no detectable change. Pronase (*Streptomyces griseus* protease) produced marked uncoiling within 30 minutes, and complete disintegration of much of the recognizable structure by 60 minutes.

Length of the nucleocapsid of Newcastle disease virus. The success in isolating well-preserved SV5 nucleocapsid by subjecting infected cells to osmotic shock suggested that this method might be generally applicable to nucleocapsids of myxoviruses. The nucleocapsid of Newcastle disease virus (NDV) was examined (Compans and Choppin, 1967b) in order to determine whether other subgroup II myxovirus nucleocapsids have a unit length similar to that observed with SV5. The length of NDV nucleocapsid was of particular interest because an estimate had been made of the size of the viral genome (Duesberg and Robinson, 1965). MK cells were infected with NDV at a multiplicity of 75 PFU/cell, and after 2-3 days cells were harvested and suspended in distilled water as described above. The resulting extracts were fixed with 1% glutaraldehyde, and examined in the electron microscope after negative staining.

The cell extracts contained long, tightly coiled pieces of nucleocapsid (Figures 26-29). The majority were distributed over the grid surface singly or in small groups. Occasionally, however, large masses of intertwining strands were encountered (Figure 27). Such extracellular masses probably result from the release by osmotic shock of the large cytoplasmic aggregates of nucleocapsid seen in sections of cells, which represent the eosinophilic inclusions typical of this subgroup of myxoviruses. A small number ($< 1\%$)

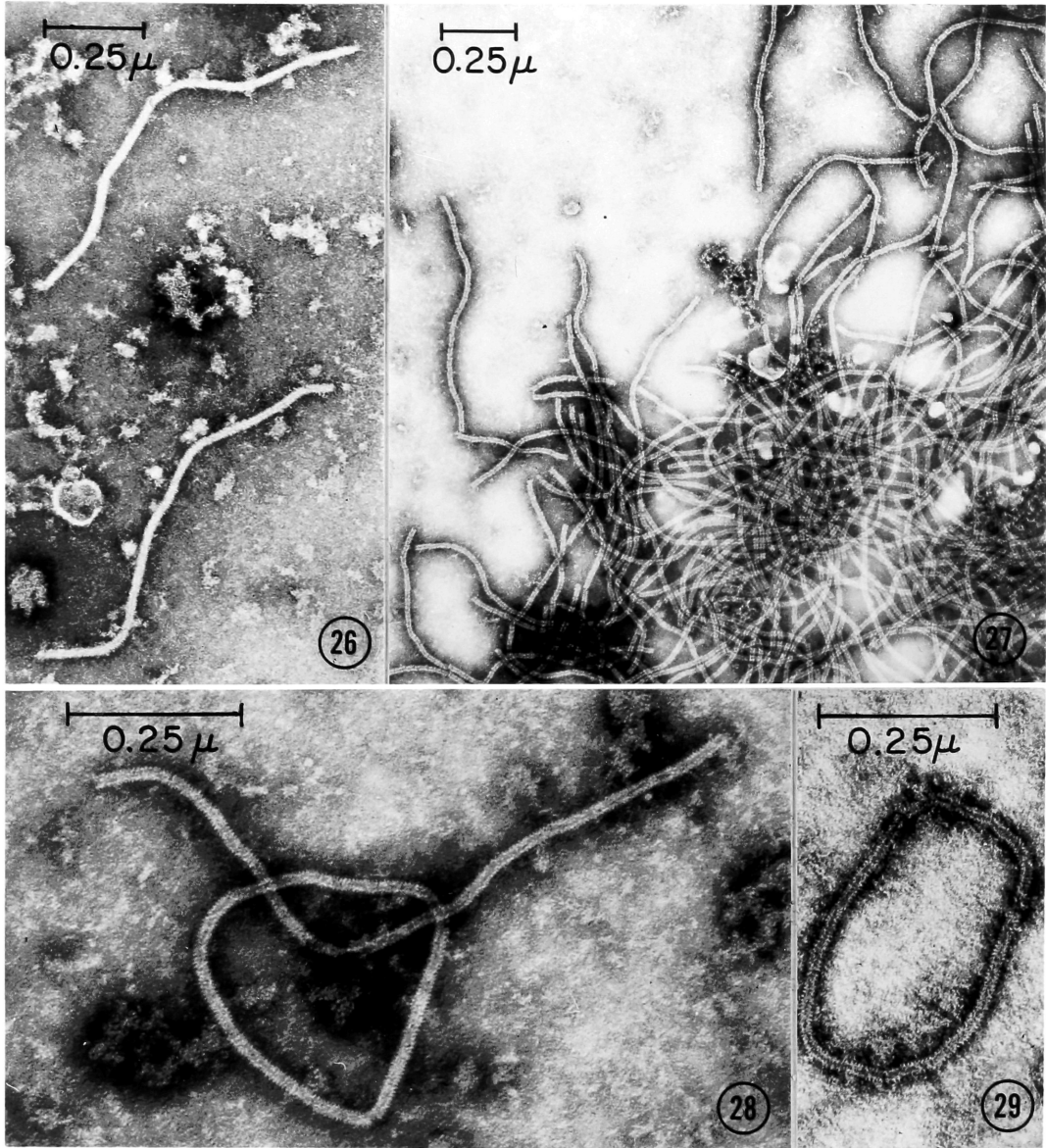
Figures 26-29. NDV nucleocapsids released from infected MK cells by osmotic shock.

Figure 26. Tightly coiled pieces of nucleocapsid typical of those used to determine the distribution of lengths.

Figure 27. Portion of a large aggregate of nucleocapsid which probably represents an inclusion after release from cells.

Figure 28. Circular and linear forms of nucleocapsid, both measuring approximately $1\ \mu$ in length.

Figure 29. An apparent closed circle with a contour length of $1.07\ \mu$. Circular forms are thought to arise from end-to-end aggregation of linear nucleocapsid.



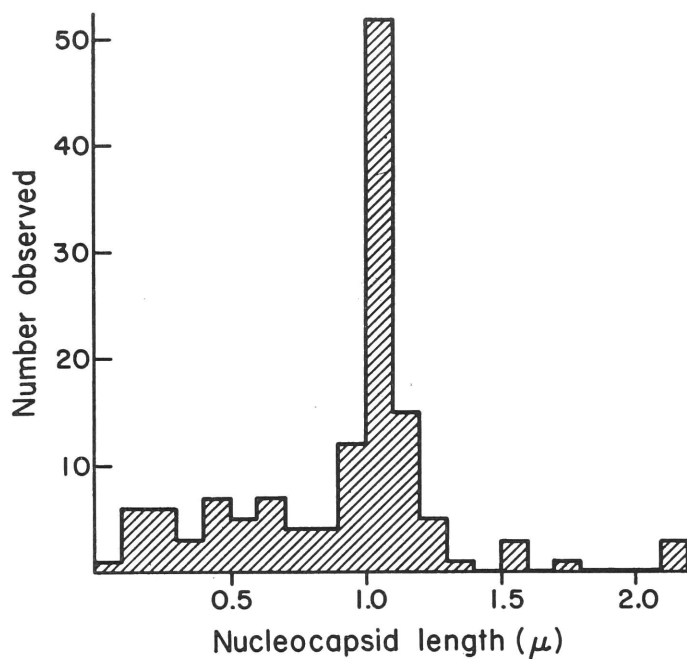


Figure 30. Length distribution of NDV nucleocapsid.

of the nucleocapsids appear to have a closed, circular conformation (Figures 28 and 29). It is noteworthy that of six apparent circles, five consisted of approximately the same length of nucleocapsid, 1.0-1.1 μ .

The length distribution of NDV nucleocapsid was determined by photographing regions of the grid at random, and measuring the lengths of all tightly coiled pieces of nucleocapsid. The cumulative result obtained from three different samples of infected cells shows a single, sharp peak centered between 1.0 and 1.1 μ (Figure 30), which is very similar to the result with SV5. The mean length of the nucleocapsids falling within this interval was 1.06 μ . Of the remaining nucleocapsids a large majority were short, presumably broken, pieces. A few longer pieces were present, and several had lengths of approximately 2 μ .

Discussion

These results demonstrate that it is possible to obtain purified nucleocapsids in milligram quantities from cells infected with a myxovirus. This has enabled determination of its length and RNA and protein content, and should facilitate further studies on the structure and chemistry of SV5 RNA and nucleocapsid protein.

The observed length distributions of SV5 and NDV nucleocapsid suggest that a 1.0-1.1 μ length of nucleocapsid contains one viral genome. Because of the size and sharpness of the peaks around 1 μ , the relatively few pieces with lengths around 2 μ , and the striking paucity of pieces between 1 and 2 μ , it appears unlikely that the true length is 2 μ and the 1 μ pieces are due to a single break in the center of almost all the pieces. In addition, there is no peak around 0.5 μ , which might be expected if breaking into halves and quarters were occurring. It therefore seems likely that the occasional 2 μ , and the rare 3- or 4 μ pieces, result from end-to-end aggregation, as has been observed with TMV (Francki, 1966). Other data are also compatible with a length of ~ 1 μ . Filamentous SV5 virions often contain nucleocapsid packed in a regular spiral, so that its length can be estimated, e.g., about 8 μ of nucleocapsid in a filament ~ 1.3 μ long. Since the smaller SV5 virions are commonly 120-180 m μ in longest dimension, a 1 μ length of nucleocapsid seems reasonable for these particles. In addition, Hosaka and co-workers (1966) estimated the amount of nucleocapsid

within negatively stained HVJ, a parainfluenza 1 virus, and concluded that smaller virions contained a total length of nucleocapsid of $1.0\ \mu$, and larger virions contained multiples of this up to $20\ \mu$. Measurements have also been made on isolated HVJ nucleocapsid, and a length of about $1\ \mu$ has been observed (Hosaka et al., 1966; A. J. Gibbs, personal communication). On the basis of measurements on 3 different members of the NDV-mumps-parainfluenza subgroup of myxoviruses, it now seems likely that a $\sim 1\ \mu$ unit length may apply to all members of this subgroup. The larger virions of this subgroup probably contain multiples of the $1\ \mu$ unit length, and therefore more than one genome.

Since $>99\%$ of the observed NDV nucleocapsids were linear, it appears that this is the usual form, rather than a closed circle. End-to-end aggregation, which presumably gives rise to long pieces of nucleocapsid, could join the two ends of a linear nucleocapsid to produce a circle of the type seen here.

The structural similarities between SV5 nucleocapsid and TMV have been discussed previously. The present finding of an RNA content of 4.1% in SV5 nucleocapsid is somewhat less than the 5.1% RNA content of TMV (Knight and Woody, 1958); however, the methods used in the present study are dependent on the content of aromatic amino acids in the nucleocapsid protein, which is presently unknown. It is possible that the exact RNA content of SV5 nucleocapsid resembles that of TMV even more closely.

The 4.1% RNA content of SV5 nucleocapsid differs markedly from the spectrophotometrically estimated value of about 10% in the nucleocapsid of Newcastle disease virus (Rott, 1964). It is closer to the earlier chemical estimate of 5.7% RNA for NDV (Schäfer and Rott, 1959); however, this report also included an estimate of 9.6% for mumps nucleocapsid. Because of the structural similarities of the subgroup II myxoviruses, it seems likely that these discrepancies are due to differences in the purification procedures employed. Since the determinations on NDV and mumps nucleocapsid were performed on material purified by differential centrifugation, it is possible that some cellular ribonucleoprotein may have been present. In addition, repeated pelleting and resuspension might cause partial disruption of the nucleocapsid with loss of some protein subunits. It is possible that light scattering also affected the spectrophotometric estimation of the RNA

content. Any of these possible sources of error would cause the estimate of the RNA content to be higher than the correct value. Recently Kingsbury (personal communication) has purified NDV nucleocapsid by velocity sedimentation on sucrose gradients, and estimated its RNA content to be 4.6%, which is in good agreement with the value obtained for SV5 nucleocapsid in the present study.

IV. ISOLATION AND PROPERTIES OF SV5 RNA

Although intact, infective RNA molecules have been extracted from a variety of animal viruses (Schaffer and Schwerdt, 1965), attempts to extract intact RNA from myxoviruses were not successful until recently. As discussed previously, early estimates of the size of myxovirus RNA's were based on the RNA content of an average virus particle, and values of $2-3 \times 10^6$ daltons were obtained (Ada, 1957; Rott, 1962). These values were uncertain because of the possibility of impurities in virus preparations, and because of the heterogeneity in the size of myxovirus particles. Many attempts have been made to isolate myxovirus RNA in an infectious form (Ada et al., 1959; Portocala et al., 1959; Sokol and Szurman, 1959; Maasaab, 1959; 1963), but the results are contradictory, and the sizes of the extracted RNA's were usually not determined.

Because of the structural similarities between SV5 nucleocapsid and tobacco mosaic virus, and the finding of intact pieces of nucleocapsid $0.9-2 \mu$ in length, it was suggested (Choppin and Stoeckenius, 1964b) that SV5 and structurally similar viruses might contain RNA of molecular weight several times the 2×10^6 daltons that TMV contains in its 0.3μ length. The studies reported here describe the isolation of a rapidly sedimenting RNA from SV5 virions or purified SV5 nucleocapsid, and the determination of its base composition and sedimentation coefficient.

While the present studies of SV5 were in progress, several investigators reported the isolation of RNA with a high sedimentation coefficient from Newcastle disease virus (Adams, 1965; Sokol et al., 1966; Duesberg and Robinson, 1965; Kingsbury, 1966a). The homogeneity and sedimentation behavior of the isolated NDV RNA suggests that it is the intact genome. The RNA obtained from SV5 in the present study has a sedimentation coefficient similar to that reported for NDV RNA.

Materials and Methods

The growth of SV5 in MK cells and purification of SV5 nucleocapsid in cesium chloride gradients were carried out as described above.

Hemagglutination assay. After an initial 100-fold dilution, serial 2-fold dilutions of gradient fractions were made in BS. To 0.5 ml of each dilution was added 0.5 ml of a 0.36% suspension of chicken erythrocytes in BS.

Assays were read after 90 minutes at 4° C, and the endpoint considered to be the dilution showing complete agglutination of erythrocytes.

Chemicals and isotopes. Potassium tartrate was obtained from J. T. Baker Chemical Co., Phillipsburg, N. J.; ^{32}P -phosphoric acid from New England Nuclear Corp., Boston, Mass.; and ^{14}C -amino acid mixture from Nuclear Chicago, Des Plaines, Ill. ^{14}C -thymidine-labelled adenovirus type 12 DNA was kindly supplied by Dr. Walter Doerfler, who has determined its sedimentation coefficient to be 29 S.

Radioactive labelling. ^3H -uridine and ^{32}P -phosphate were added to growth medium at a concentration of 20 $\mu\text{C}/\text{ml}$. ^{14}C -amino acids were added at a concentration of 2 $\mu\text{C}/\text{ml}$.

Results

Purification of SV5 virions. Precipitation with ammonium sulfate, followed by equilibrium zonal centrifugation in a preformed potassium tartrate gradient (McCrea et al., 1961) was found to be a rapid method for concentrating and purifying SV5 virus with good recovery of infective virus (Figure 31). The virus forms a sharp, visible band at a density of 1.22-1.23, which is similar to the buoyant density reported for Newcastle disease virus (Stenback and Durand, 1963). When virus is doubly labelled with ^{14}C -amino acids and ^3H -uridine, the bulk of the radioactivity in the gradient coincides with the peak of virus, and is well separated from the remaining radioactivity. More than 90% of the initial infectivity was recovered in representative experiments. Although the illustrated gradient was centrifuged for 19 hours, a centrifugation time of 3 hours is sufficient for the virus to reach equilibrium, and was routinely used to prepare virus in the experiments which follow.

Isolation of SV5 RNA. The marked reduction in sedimentation velocity of the ^3H -uridine label in SV5 nucleocapsid by SDS was described in the previous section. In view of the ability of this detergent to dissociate NDV nucleic acid from protein (Kingsbury, 1966a) it seemed likely that prolonged centrifugation of SDS-treated virus or nucleocapsid on a sucrose gradient might separate SV5 nucleic acid from viral protein. Such centrifugation of ^3H -uridine-labelled purified SV5 virus is illustrated in Figure 32A. Most of the ^3H -uridine is found in a single, rapidly sedimenting peak. A variable amount

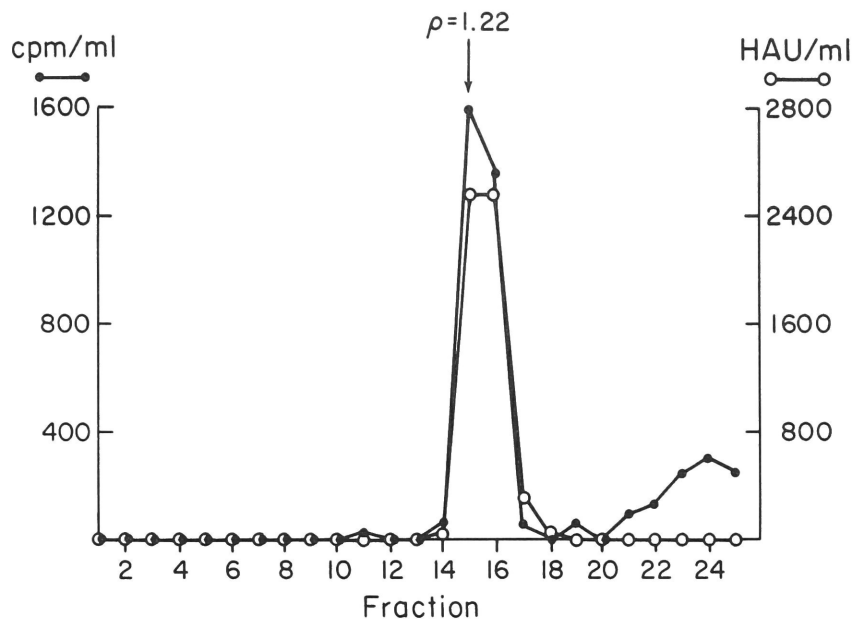


Figure 31. Purification of SV5 in a potassium tartrate gradient. Tissue culture fluid from SV5-infected MK cells, containing ^{14}C -amino acids and ^3H -uridine, was centrifuged at 2000 g for 15 minutes to remove debris, and an equal volume of saturated ammonium sulfate was added with stirring. The mixture was stirred at 4°C for 30 minutes, and the precipitated virus pelleted by centrifugation at 2000 g for 20 minutes. The precipitate was dissolved in TEN, layered over a 24 ml linear gradient of potassium tartrate, 18-40% in TEN, and centrifuged 19 hours at 24,000 rpm, 4°C , in a Spinco SW 25.1 rotor. A heavy white band was visible near the center of the tube, and was collected in fractions 15 and 16. Density was determined by pycnometry.

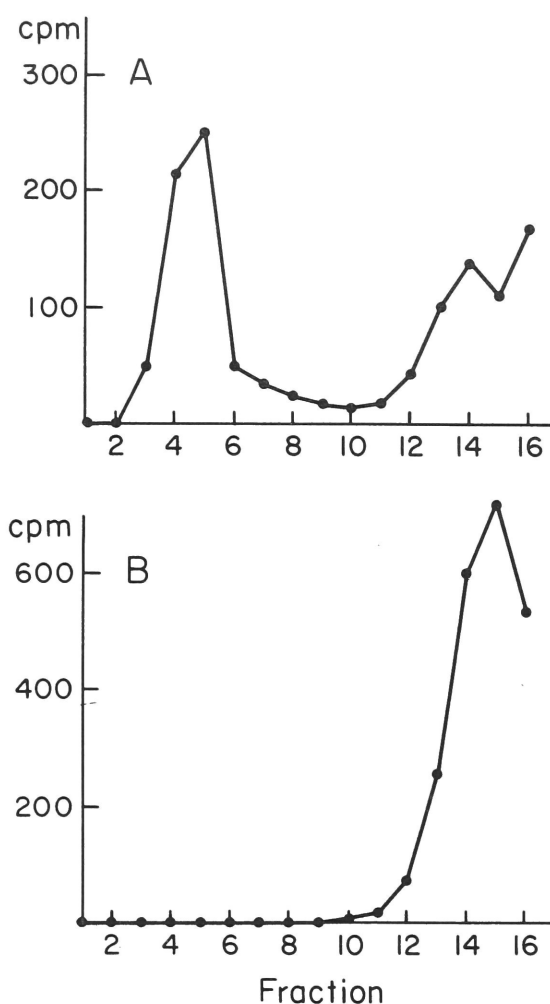


Figure 32. Sedimentation of SDS-treated SV5 virions in sucrose density gradients. After purification in a potassium tartrate gradient, virus was dialyzed vs. Eagle's medium. Samples of 200 μl were mixed with 10% SDS (50 μl), warmed to 60 $^{\circ}$ C for 1 minute, and layered over sucrose gradients. A. ^3H -uridine-labelled RNA. B. ^{14}C -amino acid-labelled protein. Gradients were centrifuged for 150 minutes at 35,000 rpm, 20 $^{\circ}$ C, in a Spinco SW50 rotor, fractions collected, and radioactivity determined as described above.

of RNA label in such gradients remains at the top of the tube, and presumably represents degraded material. In order to determine whether the rapidly sedimenting RNA peak was free of viral protein, a sample of virus labelled with ^{14}C -amino acids was centrifuged on an identical gradient in an adjacent tube (Figure 32B). The protein label remained entirely at the top of the gradient, indicating that the rapidly sedimenting RNA had been separated from protein by the centrifugation procedure.

Additional evidence of the purity of the rapidly sedimenting RNA was obtained by determining its ultraviolet absorption spectrum. Amounts sufficient to determine the spectrum were obtained by SDS treatment of 1-2 mg of purified nucleocapsid, followed by centrifugation on a 30 ml gradient of 5-20% sucrose for $6\frac{1}{2}$ hours at 24,000 rpm in a Spinco SW 25.1 rotor. The ultraviolet absorption profile resembled that shown in Figure 34, with a rapidly sedimenting peak in the lower half of the gradient. The peak fractions were combined and precipitated with 67% alcohol. The ultraviolet absorption spectrum of the redissolved material was characteristic of pure nucleic acid (Figure 33), with ratios of $260/280 = 2.08$ and $260/230 = 2.15$.

Sedimentation coefficient of SV5 RNA. The sedimentation coefficient was estimated by the procedure of Martin and Ames (1961), comparing the optical density profile from SDS-treated nucleocapsid to the radioactivity peak of ^{14}C -labelled adenovirus type 12 DNA used as a marker (Figure 34). The optical density at the top of such a gradient is due largely to nucleocapsid protein. Gradients were run in 0.05 M NaCl, and in five experiments the sedimentation coefficient of SV5 RNA averaged 50 ± 2 S. A similar value was obtained in 0.1 M NaCl. When gradients were prepared in 0.001 M EDTA, a value of approximately 40 S was obtained.

Ribonuclease sensitivity of SV5 RNA. As shown in Figure 35, all of the rapidly sedimenting RNA became acid soluble by treatment with 1 $\mu\text{g}/\text{ml}$ of ribonuclease. The small amount of acid precipitable radioactivity remaining in the top gradient fractions is probably due to inhibition of ribonuclease by the SDS contained in these fractions.

Comparison of RNA's from virions and purified nucleocapsid. In order to demonstrate that purified SV5 nucleocapsid contained the same species of RNA as that contained in virions, nucleocapsid and virus labelled with ^3H -uridine were treated with SDS and sedimented in identical gradients in the same rotor.

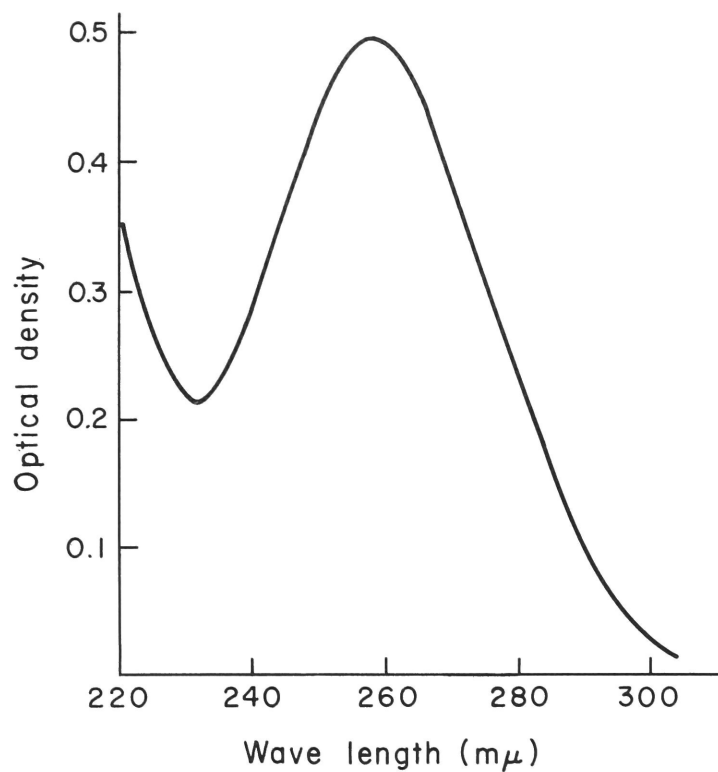


Figure 33. Ultraviolet absorption spectrum of SV5 RNA, determined in a Zeiss PMQ II spectrophotometer.

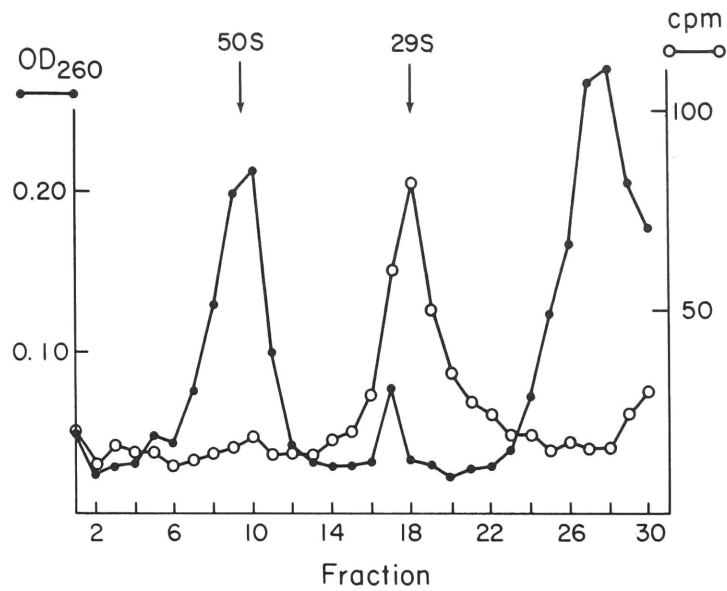


Figure 34. Estimation of the sedimentation coefficient of SV5 RNA.

Approximately 200 μg of purified SV5 nucleocapsid was mixed with 1/10 volume of 10% SDS and 3 μl of ^{14}C -thymidine-labelled adenovirus type 12 DNA. The resulting mixture (250 μl) was layered over a sucrose gradient and centrifuged as described for Figure 32. Fractions of 0.17 ml were collected, and optical densities read in a microcuvette. The sedimentation coefficient of the rapidly sedimenting RNA was estimated by comparing the distance it had sedimented to the distance traveled by the radioactivity peak, assuming sedimentation initiated at the midpoint of the sample layer.

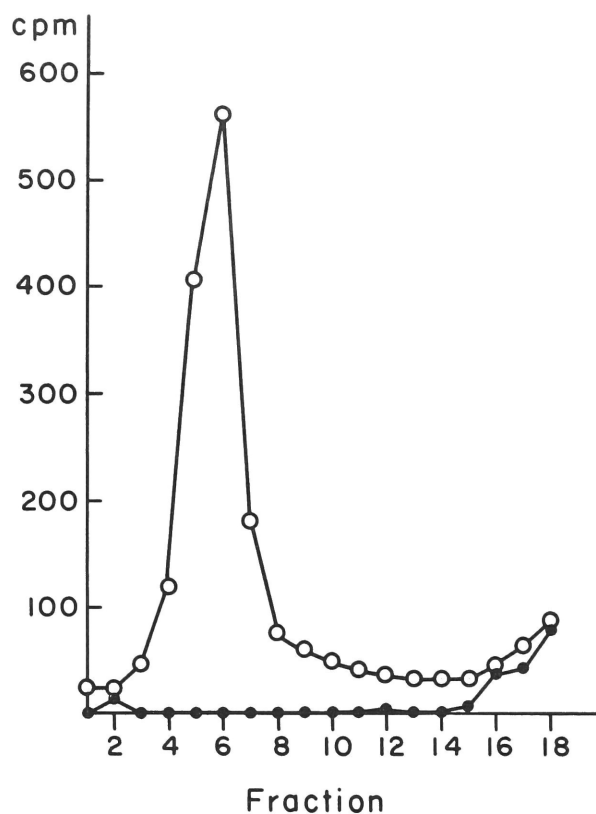


Figure 35. Ribonuclease sensitivity of SV5 RNA. Nucleocapsid labelled with $^{32}\text{PO}_4$ was treated with SDS and centrifuged as described for Figure 32. Fractions were collected, and radioactivity determined directly (o—o) or after 20-minute incubation at room temperature with $1\text{ }\mu\text{g/ml}$ of ribonuclease in PBS, followed by addition of carrier yeast RNA and acid precipitation as described for Figure 25 (●—●).

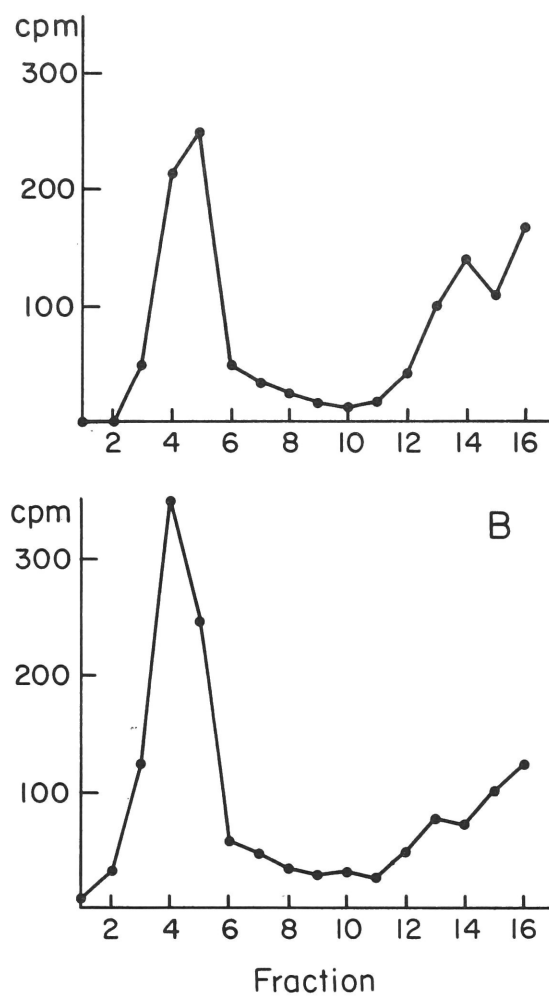


Figure 36. Comparison of RNA from SDS-treated SV5 virus and SV5 nucleocapsid. Samples were treated with SDS and centrifuged in sucrose gradients as described for Figure 32.

A. RNA from ^3H -uridine-labelled virus.

B. RNA from ^3H -uridine-labelled nucleocapsid.

TABLE 6
Base Composition of SV5 RNA*

Source of RNA	Mole %			
	C	A	G	U
Virus	20.1	27.8	21.1	30.8
Nucleocapsid	20.8	27.9	21.4	29.9

* Means of 5 determinations on RNA from virus and 4 on RNA from nucleocapsid.

As shown in Figure 36, most of the RNA label released from SV5 nucleocapsid by SDS treatment sediments as a single peak in the 50 S position, which is indistinguishable in sedimentation velocity from the RNA released from virions.

Base composition of SV5 RNA. The base composition of SV5 RNA was determined using RNA extracted from virus or nucleocapsid grown in the presence of ^{32}P -phosphate. The rapidly sedimenting RNA peak was identified by counting small aliquots of sucrose gradient fractions, and the remainder was precipitated twice with alcohol after the addition of carrier yeast RNA. After hydrolysis in 0.3 N KOH, the nucleotides were separated by high voltage electrophoresis (Ingram and Sjöquist, 1963), and their radioactivity determined. The base composition is listed in Table 6. Samples of RNA were obtained from nucleocapsid and from virus particles, and no significant differences in base composition were detected between the two sources. The base composition of SV5 RNA is similar to that of other myxoviruses (Schaffer and Schwerdt, 1965; Duesberg and Robinson, 1965; Kingsbury, 1966a) in that a high proportion of uracil is present.

Discussion

The present results indicate that a single RNA component with a high sedimentation coefficient is released from SV5 virions or nucleocapsid by treatment with sodium dodecyl sulfate. The ribonuclease sensitivity, nucleotide composition and sedimentation behavior of this RNA indicate that it is single-stranded. An empirical relationship has been proposed by Spirin (1963) for estimating the molecular weights of single-stranded RNA's from their sedimentation coefficients in 0.1 M NaCl:

$$M = 1550 (S_{20,w})^{2.1}$$

Using this relationship, a value of approximately 6×10^6 daltons would be obtained for a 50 S RNA molecule. However, this relationship was derived from data on tobacco mosaic virus RNA, and may not accurately apply to other RNA molecules. Further studies are therefore necessary to determine the exact value for the molecular weight of SV5 RNA.

The above molecular weight estimate is in general agreement with estimates that can be made for the RNA content of a 1 μ length of nucleocapsid,

which is presumed to contain one SV5 genome. If the value 1.3 is used as an approximation of the density of the nucleocapsid, and the RNA content is calculated on the basis of density, volume, and chemical composition, a value of 6.8×10^6 daltons is obtained for the amount in a 1.02μ length. A similar value of 6.7×10^6 daltons is obtained on the basis of the ratio of the 1.02μ length of SV5 nucleocapsid to the 0.3μ length of TMV, which contains RNA with a molecular weight of 2×10^6 . The similarity of these values to the estimated molecular weight of the 50 S RNA extracted from SV5 supports the conclusion that $\sim 1 \mu$ is the unit length of SV5 nucleocapsid. In addition, the fact that RNA's which are indistinguishable in sedimentation behavior can be isolated from virus and from purified nucleocapsid supports the conclusion that purified nucleocapsid contains the intact genome.

The sedimentation coefficient of 50 S obtained for SV5 RNA in the present study is the same as that determined for NDV RNA by Kingsbury (1966a) in the same buffer. Duesberg and Robinson (1965) have obtained a value of 57 S for NDV RNA, and based on this they have estimated its molecular weight to be 7.4×10^6 daltons. The results described in the previous section indicated that a unit length of $\sim 1 \mu$ may apply to the nucleocapsids of all the subgroup II myxoviruses. The results of studies on SV5 and NDV now suggest that a value of $6-7 \times 10^6$ daltons may be the size of the RNA genome of this subgroup of viruses.

Final proof that the 50 S RNA represents the entire SV5 genome must probably await demonstration of the infectivity of this RNA, and preliminary attempts to do this have not been successful. However, all of the viral RNA's which have clearly been demonstrated to be infective have a much lower molecular weight, i.e., $\sim 2 \times 10^6$, than that estimated for SV5 RNA. Therefore, it is not unreasonable that the conditions which have been used to demonstrate infectivity of other viral RNA's may not be successful with these larger RNA's.

V. GENERAL DISCUSSION AND CONCLUSIONS

The Structure of Myxoviruses

The results of the present studies on the structure of SV5 virus (Compans et al., 1966; Compans and Choppin, 1967a), together with other recent studies of subgroup II myxoviruses (Choppin and Stoeckenius, 1964b; Hosaka et al., 1966; Duesberg and Robinson, 1965; Kingsbury, 1966a; Compans and Choppin, 1967b), appear to establish a consistent picture of the structure of these viruses, which is summarized in Figure 37. Their genetic material consists of a single-stranded RNA with a sedimentation coefficient of 50-57 S, which is compatible with a molecular weight in the range of $6-7 \times 10^6$ daltons. This RNA is contained within the single-stranded helical nucleocapsid, and it appears likely that a length of $\sim 1 \mu$ of nucleocapsid contains one viral genome. The nucleocapsid is enclosed within the viral envelope, which consists of a 70 A unit membrane with spikes on its outer surface. The envelope possesses the viral lipid, neuraminidase, hemagglutinin, and the viral component responsible for inducing cell fusion. The virions may be approximately spherical or filamentous particles, the latter probably containing multiple unit lengths of nucleocapsid and therefore multiple genomes.

Among the undetermined features of the structure of subgroup II myxoviruses is the arrangement of proteins in the viral envelope. It has been proposed that influenza virus spikes represent hemagglutinin only, and that neuraminidase lies between the spikes (Noll et al., 1962; Drzenieck, 1966), but there is little evidence to support this hypothesis. Neither the chemical nature of the component responsible for cell fusion nor its location in the virion has been determined. The size of the protein subunits in the nucleocapsid and the arrangement of RNA within them have yet to be clearly established. The most likely arrangement would appear to be one in which the RNA strand is itself wound helically within a series of subunits to form the strand of the nucleocapsid. Such an arrangement has been determined for TMV by X-ray diffraction (Caspar, 1963) and attempts to carry out such studies on SV5 nucleocapsid have now been initiated. Finally, the exact size of the viral RNA remains to be established. Light scattering measurements or electron microscopic determination of its length may be means by which this can be accomplished.

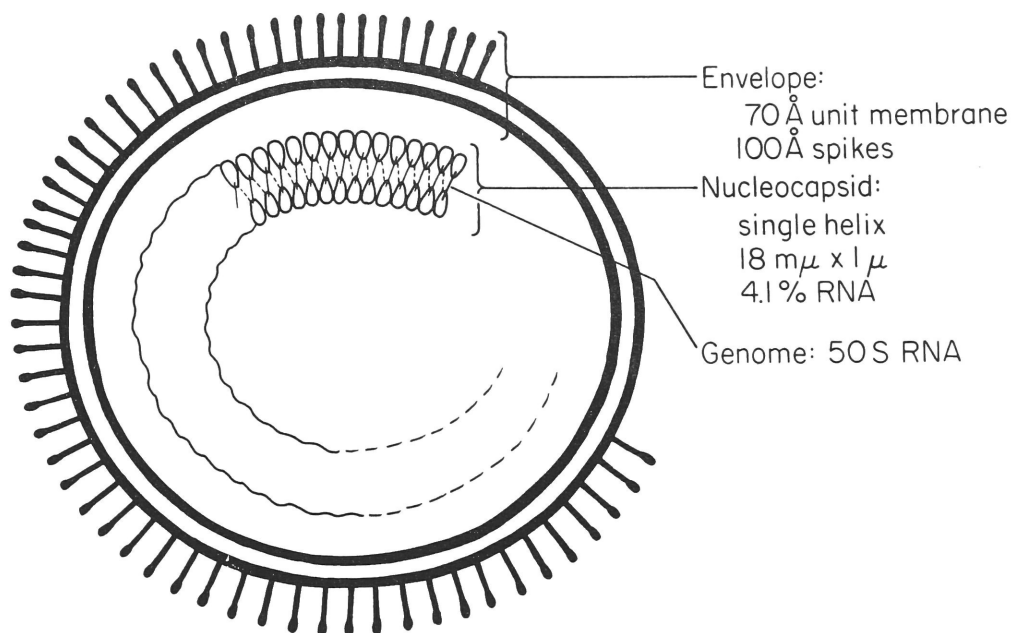


Figure 37. Diagram of the structural components of a parainfluenza virus.

The nucleocapsid of SV5 is a relatively stable structure, whereas infectivity of the virus is extremely labile (Choppin, 1964). The nucleocapsid is able to withstand centrifugation at high gravitational forces, and is resistant to digestion by some proteolytic enzymes. It therefore appears to serve as an efficient protective coat for the viral nucleic acid. It has not been possible to infect cells with purified nucleocapsid under conditions where intact virus is infective, probably because of an inability of the nucleocapsid to adsorb and penetrate into susceptible cells. The viral envelope provides an efficient mechanism of attachment and penetration, and may not add stability to the virion itself. The lability of viral infectivity is probably due to the fragility of the viral envelope, rather than instability of the nucleocapsid or nucleic acid itself.

The studies carried out to date indicate that the subgroup II myxoviruses are very similar in the dimensions of their structural components. Further studies would be of interest to determine the extent to which their nucleic acids possess similar nucleotide sequences, and their proteins, similar sequences of amino acids. The availability of the simple method for purifying the nucleocapsids of these viruses developed in the present studies should facilitate such further investigations, as well as the determination of the exact immunological relationships among these viruses.

The purification of viral nucleocapsid from infected cells in cesium chloride gradients has been of value in studies of the structure and classification of pneumonia virus of mice (Compans et al., 1967), which are described in the Appendix which follows. The diameter of the helical nucleocapsid of PVM is 120-150 Å, which is different from that of either of the established subgroups of myxoviruses.

The methods which were useful in studies of the structure of the subgroup II myxoviruses have been less successful when applied to subgroup I. RNA extracted from influenza virus particles has been isolated as relatively small pieces with sedimentation coefficients of 16-20 S (Davies and Barry, 1966; Pons, 1967; Duesberg and Robinson, 1967), or as a 38 S component (Agrawal and Bruening, 1966) which is thought to be an aggregate of smaller pieces (Pons, 1967; Duesberg and Robinson, 1967). As discussed by the above authors, it is possible that several small pieces of RNA serve as genetic material, which may account for the high rate of genetic recombination

and cross-reactivation observed with influenza virus, as suggested by Burnet (1956) and Hirst (1962). We have made attempts to isolate the nucleocapsid of influenza virus by the procedures developed with SV5, but only amorphous material was recovered. The details of the structure of this component are still unknown.

A summary of the known properties of helical nucleocapsids of animal viruses is shown in Table 7. On the basis of their diameter, the nucleocapsids can be segregated into three classes. Largely because of their relative stability, the properties of nucleocapsids of subgroup II myxoviruses (parainfluenza and NDV) have been determined in greatest detail. Whereas the unknown features of influenza nucleocapsid are due to the inability to isolate well-preserved material, the lack of information about PVM nucleocapsid is a result of inability to obtain sufficient amounts of this material for chemical studies. All of the animal viruses which have thus far clearly been shown to have helical nucleocapsids can be considered members of the myxovirus group on the basis of their structure and morphogenesis.

The Replication of SV5

Determination of the size and nature of the structural components of SV5 is a necessary prerequisite for a study of the detailed mechanisms involved in its replication. The present studies were directed toward characterization of SV5 RNA and nucleocapsid, as well as those aspects of SV5 replication which may be visualized with the electron microscope. These consist of the initial stage as well as the final process of assembly and release; the latter is likely to be the stage at which SV5 differs most strikingly from the structurally simple viruses.

SV5 appears to enter cells by a process resembling phagocytosis, like all other animal viruses which have been studied adequately (Dales, 1965b). Because of the high multiplicity of virus used to facilitate observations in these experiments, it may be argued that the observed particles were not involved in the infectious process. However, alternative proposals for the mechanism of myxovirus uptake, involving fusion of the viral envelope with the cell membrane (Hoyle, 1954; Hoyle et al., 1962) were not supported by the present morphological studies.

TABLE 7

Helical Nucleocapsids of Animal Viruses

	Influenza*	PVM	Parainfluenza, NDV
Diameter	90 A	120-150 A	180 A
Strands in helix	?	1	1
Unit length	?	?	$\sim 1 \mu$
RNA content	$\sim 5\%$	+	4-5%
Molecular weight of RNA	(?) multiple pieces of $5-7 \times 10^5$?	$6-7 \times 10^6$

* RNA content of influenza nucleocapsid from Frisch-Niggemeyer and Hoyle, 1956; molecular weight of influenza RNA from Davies and Barry, 1966, and Pons, 1967.

The replication of SV5 is not inhibited by Actinomycin D, which inhibits DNA-dependent RNA synthesis (Reich et al., 1961), although continued production of the virus is inhibited due to secondary effects of the drug on the host cell (Choppin, 1965). RNA synthesis induced by SV5 has been studied in MK cells which were treated with Actinomycin to inhibit cellular RNA synthesis (Choppin and Holmes, 1967). Virus-induced RNA synthesis is first detected about 3 hours after inoculation, and during the exponential increase phase precedes the appearance of infectious virus by $1\frac{1}{2}$ to 2 hours. The maximum level of SV5-induced RNA synthesis is very low, amounting to less than 1% of normal cellular RNA synthesis, despite the high yield of infectious virus.

The low level of SV5-induced RNA synthesis is in agreement with the electron microscopic observation that the infected cells appear essentially normal. Only small numbers of SV5 nucleocapsids are observed in the cytoplasm, but high titers of SV5 are produced. These observations imply two unusual features in the multiplication of SV5, which may be essential for the moderate virus-cell interaction which results: a) viral macromolecular synthesis is held to a low level by some control mechanism; b) viral components are efficiently removed from the cell by extrusion as mature virus particles. It is possible that a control mechanism which keeps RNA synthesis at a low level is, in fact, the rapid enclosure of newly-synthesized RNA in nucleocapsid protein, thus preventing buildup of a large pool of free RNA available as template for RNA replication. It is also possible that a cellular protein may be involved in the control of SV5 RNA synthesis, since inhibition of cellular protein synthesis by superinfection with poliovirus appears to cause a stimulation of SV5 RNA synthesis (Choppin and Holmes, 1967). Such stimulation is also caused by cycloheximide or puromycin.

An interesting problem in the assembly of SV5 nucleocapsid concerns the mechanism by which nucleocapsid protein seems specifically to enclose viral RNA, rather than some other RNA. This is particularly true in view of recent studies with Newcastle disease virus (Kingsbury, 1966b; 1967; Bratt and Robinson, 1967) indicating that most of the virus-induced RNA in infected cells will hybridize to that found in mature virus particles. This RNA is presumed to be "minus strands" which are complements of the "plus strands" found in virus particles. Such minus strands are presumed to be intermediates in the synthesis of new plus strands, but the reason for

the large amounts in infected cells is not clear. Since the rapidly-sedimenting RNA in NDV virus particles appears to be homogeneous and does not hybridize to itself, a mechanism presumably exists for the preferential incorporation of plus strands into virions. Some possible mechanisms for preferential incorporation of plus strands include: a) formation of a pool of plus strands and capsid protein in a localized region of the cytoplasm; b) immediate attachment of capsid proteins to those plus strands which serve as messenger for their synthesis; c) specific initiation of formation of nucleocapsid by preferential attachment of capsid protein to a certain sequence of bases on the plus strand. Mechanism (c) may be tested experimentally if conditions for dissociation and reconstitution of nucleocapsid can be worked out. Whether the replication of SV5 resembles that of NDV in production of large amounts of complementary RNA has not been determined.

The final stage in the replication of SV5 intimately involves the cell membrane. The present electron microscopic observations are compatible with the following hypothesis for the sequence of events in the maturation process. Virus-specific envelope proteins become incorporated into regions of the cell membrane, and perhaps confer an affinity for SV5 nucleocapsid on these regions. The nucleocapsid aligns closely under these regions, and the proteins incorporated in the membrane may simultaneously rearrange or polymerize to form morphologically identifiable surface projections. The presence of these abnormal, probably somewhat rigid components on both sides of the cell membrane may provide the stimulus which induces the budding process.

The organization of viral components at the cell membrane has been determined more clearly with the subgroup II myxoviruses than with other animal viruses with helical nucleocapsids. Results of investigations with pneumonia virus of mice, described in the Appendix, indicate that the morphogenesis of this virus occurs by a process very similar to that observed for SV5. Cells infected with influenza virus have also been examined by the same techniques. As demonstrated in previous studies, it was observed that the viral envelope is acquired during budding at the cell membrane. The cellular unit membrane appears to be incorporated into the viral envelope, as observed with other myxoviruses. It has not been possible to positively identify the nucleocapsid of influenza virus in

thin sections, and further details of virus assembly were not observed. However, it seems likely that the assembly of influenza virus occurs by a process very similar to that observed with SV5 and PVM. All of these viruses have been observed to mature only at the plasma membrane, and in all cases the result may be a spherical or filamentous particle. In the case of influenza viruses, it has been found (Kilbourne, 1963) that the proportion of filaments or spheres is a genetic trait of the virus.

APPENDIX

THE STRUCTURE AND MORPHOGENESIS OF PNEUMONIA VIRUS OF MICE

Pneumonia virus of mice (PVM) was first isolated as a latent virus from apparently healthy mice, and induced a fatal pneumonia after serial blind passages (Horsfall and Hahn, 1939; 1940). A high incidence of inapparent PVM infection has been observed in laboratory mouse colonies, and immunological evidence has been obtained of latent infection in numerous mammalian species (Horsfall and Hahn, 1940; Tennant, 1966; Parker et al., 1966; Horsfall and Curnen, 1946). The multiplication of PVM is inhibited by bacterial polysaccharides (Horsfall and McCarty, 1947), and infection of mice with PVM has been successfully treated with the capsular polysaccharide from Friedlander bacillus (Ginsberg and Horsfall, 1951). This was the first successful application of chemotherapy to a virus infection in an animal.

PVM has remained an unclassified virus, and its structure has not been described, largely due to lack of a suitable cell culture system. Recently, the virus was successfully propagated in a line of baby hamster kidney cells, and evidence was obtained that it is an RNA virus which replicates in the cytoplasm (Harter and Choppin, 1967). The propagation of PVM in cultured cells has enabled an electron microscopic study of the structure and morphogenesis of the virus. The results of this investigation, described here, indicate that the morphology and development of PVM are typical of the myxovirus group (Compans et al., 1967).

Materials and Methods

Virus and cells. PVM was propagated in BHK21 cells in a modified Eagle's medium (Sturman and Tamm, 1966) with 10% calf serum, as described by Harter and Choppin (1967). BHK21 cells (MacPherson and Stoker, 1962) were grown in modified Eagle's medium with 10% calf serum and 10% tryptose phosphate broth.

Negative staining. PVM grown in BHK21 cells was sedimented by centrifugation for 3 hours at 19,600 g. Pellets were held overnight at 4° C in approximately 0.2 ml of the residual supernatant and then resuspended in that volume. A small drop was spread over a Formvar-coated grid with a heavy carbon film, rinsed with phosphate-buffered saline (PBS), and fixed with a drop of 1% glutaraldehyde in PBS. The grid was then rinsed with distilled water and stained with 2% phosphotungstic acid, pH 6.2.

Thin sections. Monolayers of cells were detached from Petri dishes by scraping or treatment with 0.25% trypsin and 0.05% EDTA. Cells were centrifuged for 4 minutes at 200 g, and the pellet was fixed for 4 minutes in 1% glutaraldehyde in PBS, and postfixed with 1% osmium tetroxide in BS. In some experiments specimens were stained immediately after fixation with 0.5% uranyl acetate in veronal acetate buffer, pH 5, for 2 hours (Farquhar and Palade, 1965). The cell pellets were dehydrated in a series of alcohols and embedded in epoxy resin. Thin sections were stained by a 1 minute application of a saturated solution of uranyl acetate diluted 1:1 with ethanol, followed by a 1-2 minute application of lead citrate solution. Specimens were examined in a Hitachi HS-7S electron microscope.

Results

Structure of PVM virions: negative stain. The morphology of the virus particle was examined in thin sections as well as by the negative staining technique. PVM particles are extremely fragile (Harter and Choppin, 1967), and no virus particles were seen in unfixed, negatively stained preparations. However, if PVM suspensions were fixed with glutaraldehyde prior to negative staining, and grids were scanned extensively at low magnification, a number of long, filamentous particles were observed.

These filaments (Figures 1 and 2) usually have a uniform diameter of 100-120 m μ , and a total length of 2-3 μ . Frequently one end of the filament shows an enlarged, bulbous tip (Figure 1). The outer surface consists of an envelope covered with a layer of short projections or spikes 80-90 A in length. In most instances the particles were not penetrated by the negative stain, and it was not possible to discern the internal structure. An irregular, strandlike internal component occasionally has been seen in some filaments. Much of the grid surface was covered with strandlike material which may represent disrupted internal component from broken virus particles. Failure to detect small, spherical particles in negatively stained preparations probably resulted from inability to recognize such particles when scanning grids at low magnification.

Structure of PVM virions: thin sections. Thin sections of BHK21 cells infected with PVM showed frequent extracellular filamentous particles which correspond in size to those seen with negative staining (Figures 3 and 4). In

addition, circular profiles 80-120 m μ in diameter were seen in thin sections (Figure 3). The frequency with which circular profiles were observed suggests that they are sections of spherical virus particles, rather than cross-sections of filamentous particles.

The sectioned particles are bordered by a membrane with outer projections, corresponding to the envelope seen with negative staining. The internal structure is seen more clearly in sectioned particles than within negatively stained particles. Electron-dense internal strands extend across the circular profile in Figure 3, and a similar component occurs coiled within filamentous particles (Figure 4).

The particles described above were found only in PVM-infected cells and were the only virus-like structures which could be associated with PVM, either in sections or with negative staining. It was therefore concluded that these represented PVM virions. Additional evidence which supports the conclusion that these are PVM particles includes the time course of their appearance and their interaction with murine erythrocytes (see below).

Release of a helical component from cells infected with PVM. The PVM particles described above bear an obvious morphological resemblance to the myxoviruses, having an outer, spike-covered envelope and a strandlike internal component. Since it was not possible to visualize the exact structure of the internal component within virions, isolation of the component was attempted.

Prominent eosinophilic inclusions appear in the cytoplasm of BHK21 cells after infection with PVM (Harter and Choppin, 1967). These inclusions appear to consist of strandlike elements (cf. Figure 9). Similar inclusions in BHK21-F cells infected with the parainfluenza virus SV5 consist of aggregates of the helical SV5 internal component, and large amounts of SV5 internal component have been isolated from such infected cells. The procedure developed for isolation of SV5 internal component from cells was therefore applied to PVM-infected cells.

Cells were inoculated at a multiplicity of 0.5 TCID₅₀ per cell, and after 3-4 days were suspended by treatment with 0.25% trypsin and 0.05% EDTA. The cells were pelleted at 200 g for 5 minutes, and resuspended in distilled water at a concentration of approximately 1.5×10^7 per ml. Many cells were disrupted, and a large number of nuclei free of cytoplasm were observed.

These extracts were clarified by centrifugation at 6500 g for 15 minutes, and the supernatant (4.5 ml) was mixed with cesium chloride (2.0 g). The resulting solution (average density = 1.30) was centrifuged for 7-10 hours at 45,000 rpm in a Spinco SW50 rotor. After centrifugation, fractions were collected from the bottom of the tube, and densities determined by refractive index measurements.

A diffuse band with a density of 1.29 g/ml was observed near the center of tubes that contained extracts of PVM-infected cells; no bands were observed in this position in control tubes containing extracts of uninfected cells. The material in the band was examined in the electron microscope. As illustrated in Figures 5 and 7, the observed structures have the general appearance typical of the helical nucleocapsids of myxoviruses. However, the diameter of the PVM component is 120-150 Å, which differs from the diameters of the nucleocapsids of the two subgroups of myxoviruses. For a direct comparison, the component from PVM-infected cells (Figure 5) and the nucleocapsid of SV5 (Figure 6), were photographed at the same magnification in the microscope, and enlarged by the same factor. It is apparent that the internal component of SV5, which has a diameter of 150-180 Å, is larger than the component from PVM-infected cells.

The helical PVM component is usually seen somewhat stretched or extended; tightly coiled helices, such as the segment of SV5 nucleocapsid shown in Figure 6, were not observed. In selected regions, the turns of the helix of the PVM component are well separated, and their orientation suggests that the structure is a single helix (Figure 7).

Formation of virus particles. Uninfected BHK21 cells are similar in morphology to the BHK21-F cells previously described (Compans et al., 1966). They are fibroblastic, contain an extensive rough-surfaced endoplasmic reticulum and few smooth-surfaced cisternae, and possess the other usual cytoplasmic organelles. The surfaces of BHK21 cells show relatively few microvilli. Bundles of fibers are frequently seen in the cytoplasm, particularly in cells examined several days after monolayers have become confluent. Uninoculated BHK21 cells also contain the virus-like particles which have been previously described (Bernhard and Tournier, 1964; McGee-Russell et al., 1965; Compans et al., 1966).

Figure 1. A filamentous PVM particle, 3 μ in length and 110 m μ in diameter, with a bulbous tip 400-500 m μ in diameter. Much of the background in negatively stained PVM preparations is covered with material which in some areas has an irregular strandlike appearance.

Figure 2. A portion of a PVM filament showing the layer of projections or spikes covering its surface.

Figure 3. A circular profile of a PVM virion which is traversed by well-defined strands approximately 120 A in diameter (arrow). Below is a section of a filamentous particle whose internal structure is not well defined.

Figure 4. Section of a PVM filament in which electron-dense strands (arrow) traverse a portion of the interior.

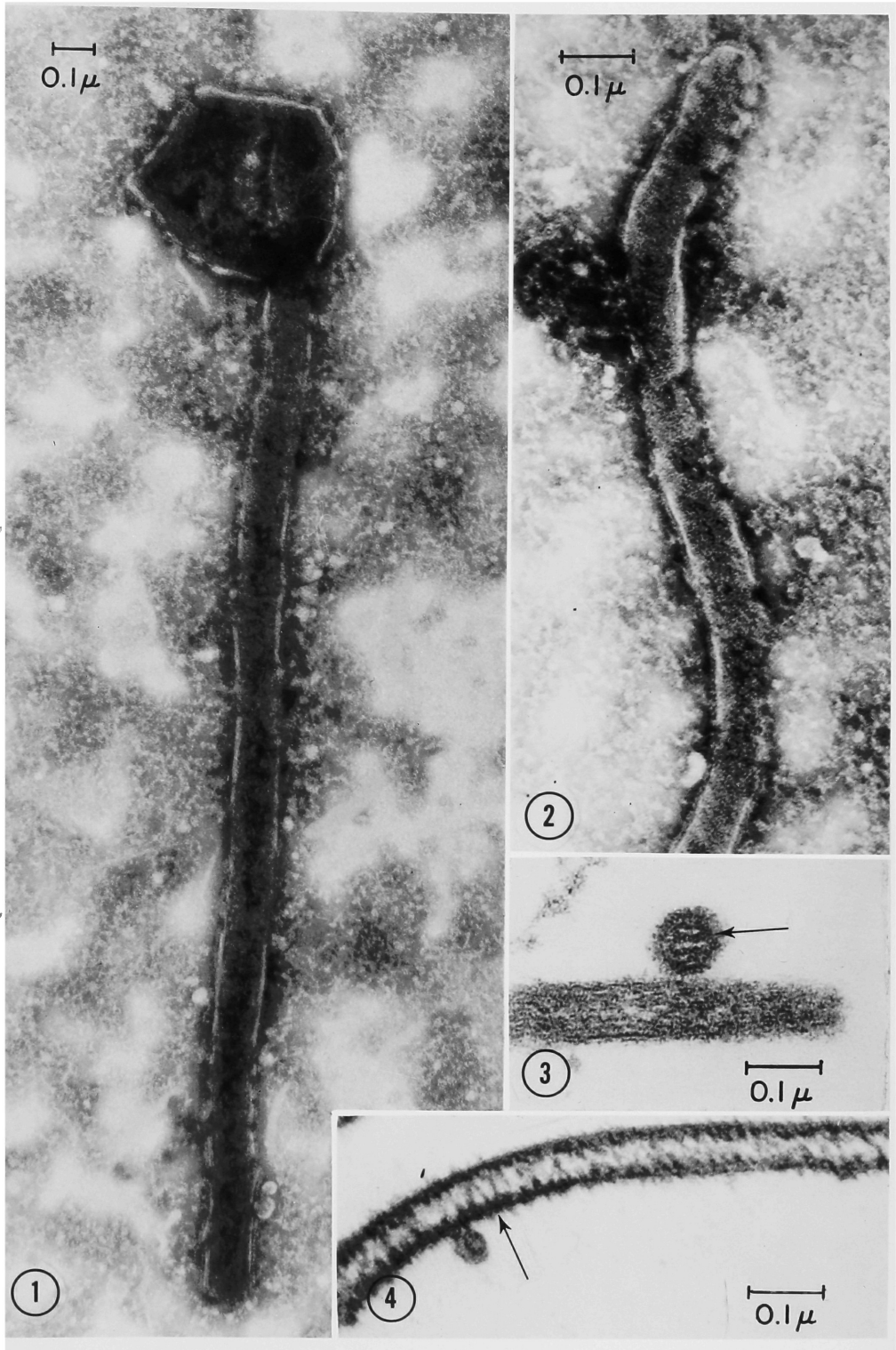
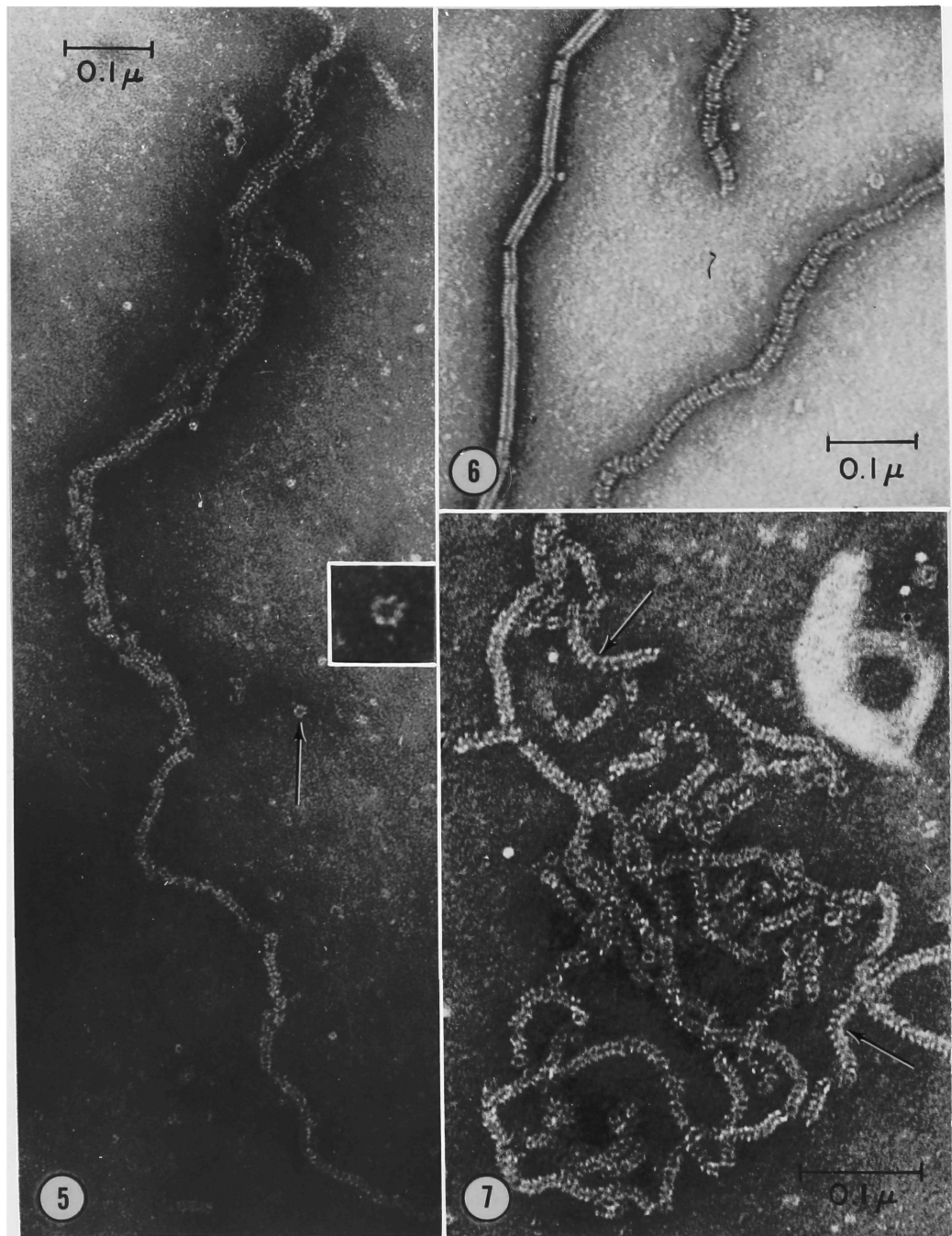


Figure 5. Helical component (nucleocapsid), 120-150 A in diameter, isolated from PVM-infected cells. It appears to be loosely coiled and fragmented. The arrow indicates an end view of a segment of the nucleocapsid suggesting the presence of subunits. This is shown at higher magnification in the insert.

Figure 6. Segments of the helical nucleocapsid of the parainfluenza virus SV5, 160-180 A in diameter, shown for comparison with that of PVM. Both loosely and tightly coiled segments are seen. Figures 5 and 6 were photographed at the same magnification and enlarged by the same factor; the smaller diameter of the PVM nucleocapsid is apparent.

Figure 7. The PVM nucleocapsid at higher magnification. In several regions (arrows), the helix is stretched into a loose coil which suggests that it is a single-stranded structure.



Cells examined 24 hours after inoculation at a multiplicity of 0.5 TCID₅₀ per cell showed no characteristic alterations in structure and extracellular virus particles were seen infrequently. By 48 hours, extracellular PVM particles were numerous, and examples are shown in Figures 3, 4, 11, 13, and 17. In addition, many cells observed at this time contain dense cytoplasmic inclusions (Figures 8-11) which appear to consist of elements with a threadlike appearance (Figure 9). Occasionally, similar dense inclusions are seen extracellularly, apparently resulting from rupture of the cells in which they were formed. These intra- and extracellular inclusions are similar in size, shape, and distribution to the inclusions seen in the light microscope, which stain flame-red with acridine orange (Harter and Choppin, 1967).

Virus particles acquire their envelope by budding at the outer cell membrane (Figures 10-12, 14, 16). The interior of budding virus particles (Figures 10-12) has a dense appearance similar to that of the material in inclusions, and in some areas the inclusion appears to extend into the budding particle (Figure 11). In most regions no well-defined organization is visible in the dense interior of budding virus particles; occasionally, however, a strand is seen (Figure 12) which resembles the internal component seen in some mature, extracellular virions. Filamentous particles are also seen budding at the cell surface (Figures 14 and 16). All of the budding particles are bordered by an electron-dense membrane which is continuous with the outer cell membrane. Increased electron density on the outer surface of the particles corresponds to the spikes seen with negative staining.

The leaflets of the unit membrane were not readily resolved in the BHK21 cell membrane by the usual post-embedding staining procedure. However, in specimens stained with uranyl acetate prior to embedding, the staining of membranes was enhanced. With this procedure it was possible to observe a typical unit membrane in the envelope of mature, extracellular virus particles (Figure 13), and the leaflets in the BHK21 cell membrane were also resolved. The membrane in the envelope of budding virus particles is continuous with, and appears morphologically identical to, the outer cell membrane (Figure 14).

Cells on which budding virus particles are present also exhibit rows of closely spaced vesicles projecting inward from their surfaces (Figure 11). These vesicles have a rather uniform diameter of 60-100 μ , and are seen with

greatest frequency on regions of the cell surface between the regions where virus is budding. Occasionally, similar vesicles are seen closely adjacent to, or just beneath, budding virus particles (Figure 10). Although the relationship of these vesicles to virus formation is not clear, they are numerous only on surfaces of cells which exhibit budding virus, suggesting a possible connection between virus maturation and vesicle formation.

Apart from the cytoplasmic inclusions and surface phenomena involved in virus maturation, no consistent virus-specific structural changes were observed in infected cells. Dense masses were observed in a few nuclei, but these could not be positively identified as virus-related.

Interaction of PVM and infected BHK21 cells with murine erythrocytes. The interaction of PVM particles and PVM-infected cells with murine erythrocytes, which the virus agglutinates (Mills and Dochez, 1944; Harter and Choppin, 1967), was examined in thin sections of cells harvested 48 hours after infection.

Monolayers of cells were rinsed twice with PBS, and overlaid with 2 ml of a 0.8% suspension of murine erythrocytes in buffered saline. After gentle agitation at 10-minute intervals for 30 minutes, the unadsorbed erythrocytes were removed by washing twice with PBS. The erythrocytes adsorb firmly to infected BHK21 cells, but are readily washed from uninfected cells. The cells were then suspended, fixed, and sectioned by the usual methods.

Erythrocytes were seen in direct contact with budding virus particles at the surfaces of infected cells (Figure 15). Frequently, however, erythrocytes were observed attached to areas on the BHK21 cell surface where no virus-specific morphological changes were visible (Figure 16). Attachment of erythrocytes to apparently unmodified cell surfaces may be due to budding virus which is not in the plane of sectioning; however, this seems unlikely because of the frequency of such attachment. In Figure 16 the shape of the erythrocyte is distorted to conform to that of the cell surface, and a space separates the adsorbed erythrocyte from the cell membrane. Such an apparent gap has been observed with hemadsorption to measles virus-infected cells (Baker et al., 1965), and may contain material which is not stained by the procedures employed, or result from separation of the two membranes during processing.

Figures 8-17. Sections of BHK21 cells 48 hours after infection with PVM.
Key to abbreviations: N, nucleus; E, murine erythrocyte;
I, inclusion.

Figure 8. Low magnification view showing a dense, well-circumscribed cytoplasmic inclusion near the periphery of the cell.

Figure 9. Higher magnification of a cytoplasmic inclusion (outlined by arrows). It consists of tangled, electron-dense, threadlike elements.

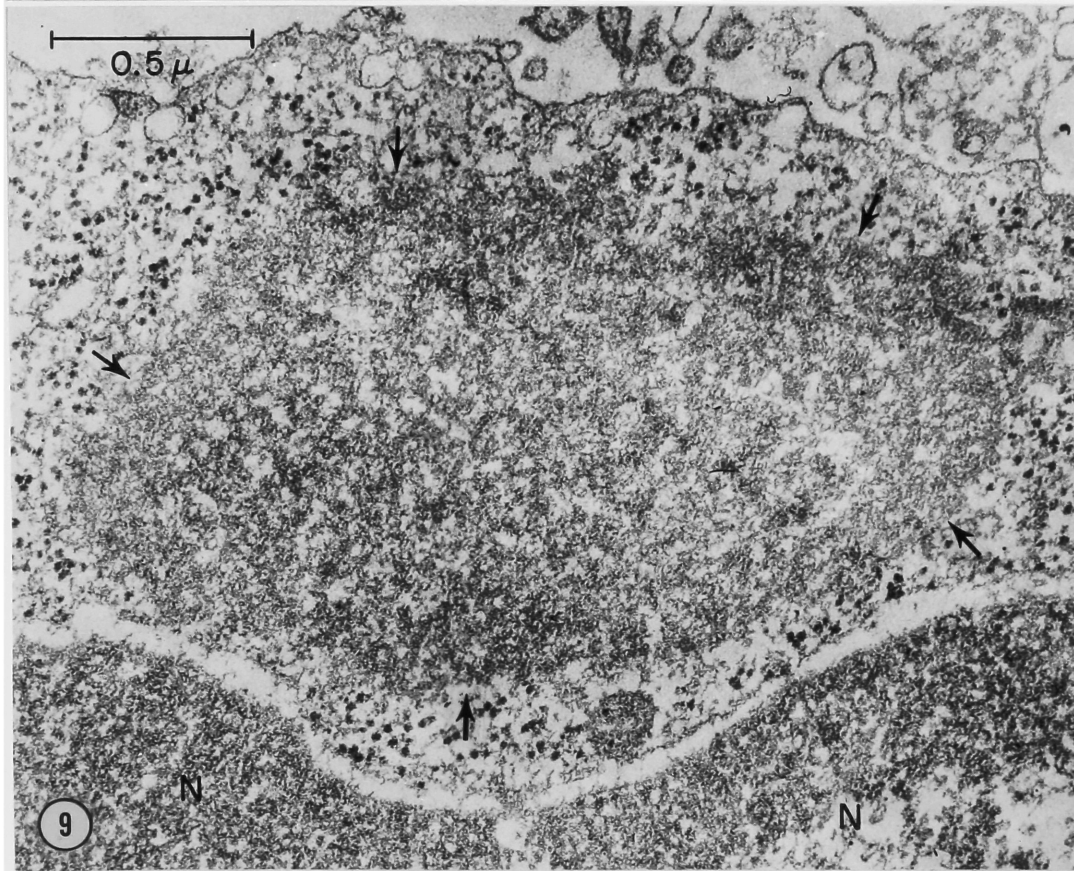
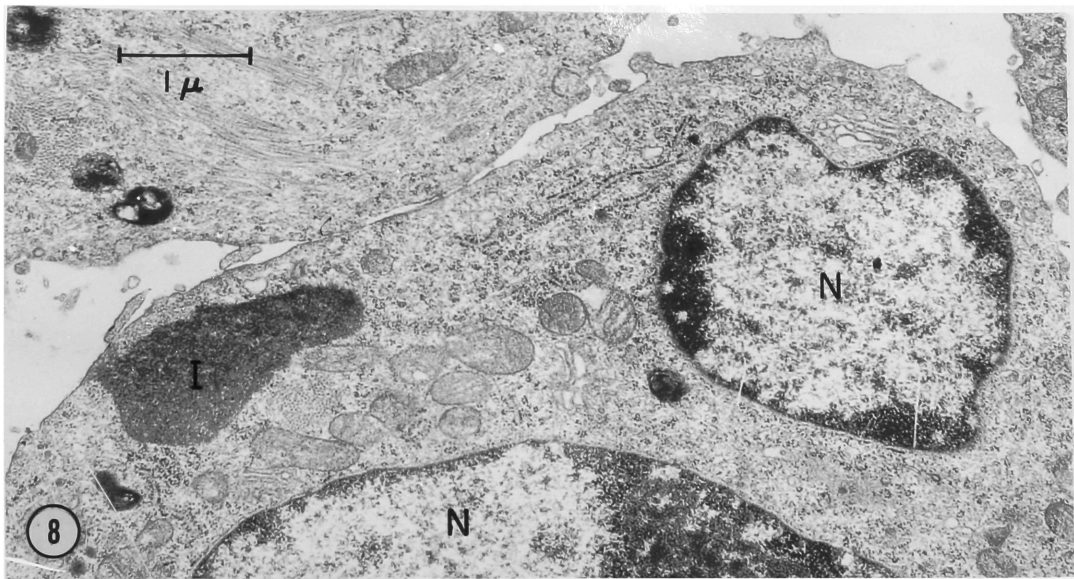
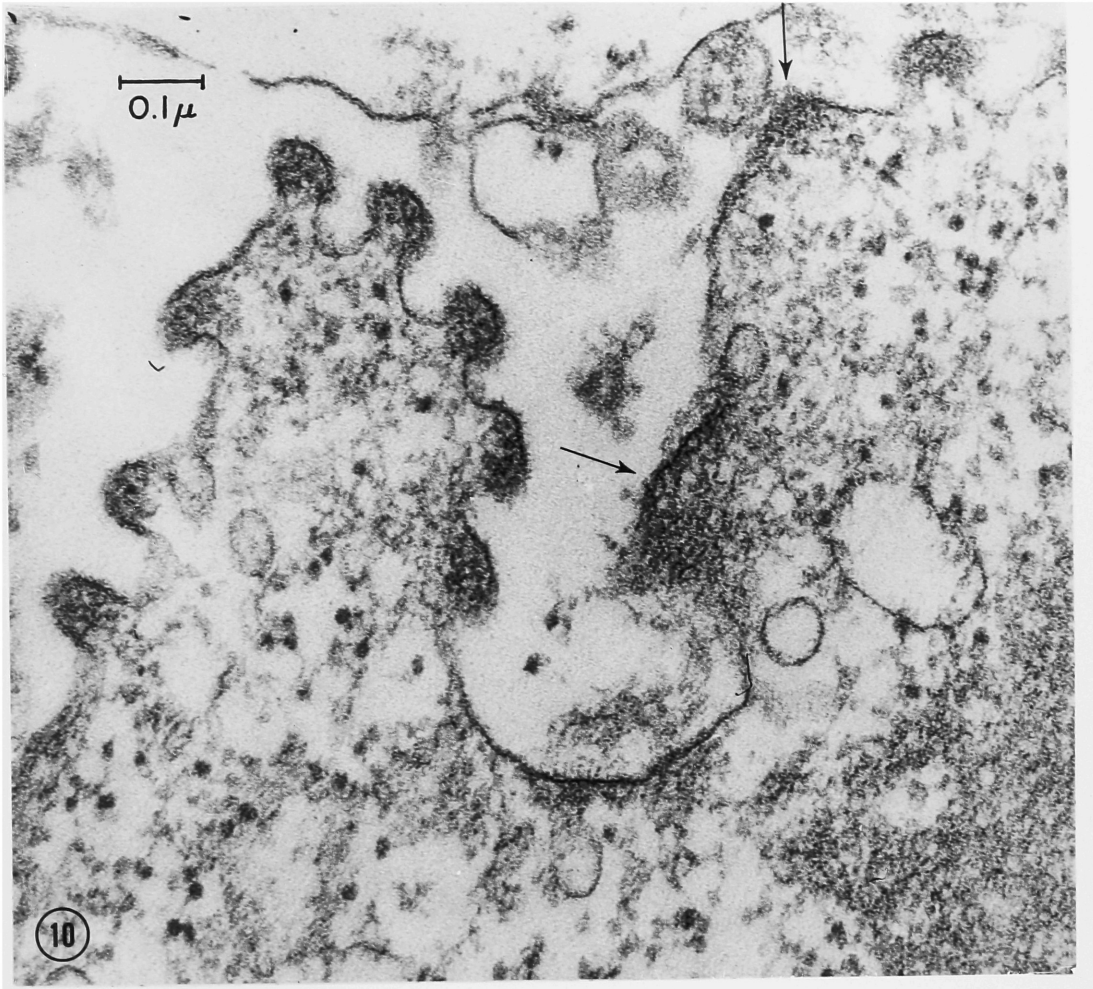


Figure 10. A region of the cell surface on which eight budding PVM particles are arranged in a glovelike configuration. Other regions of the cell surface, indicated by arrows, show underlying dense threadlike material, but do not exhibit outfolding of the cell membrane. These may be regions from which buds will develop.



- Figure 11. Portion of the cell surface studded with budding virus particles, and a PVM filament which appears to have been released. A dense inclusion occupies much of the cell interior. The inclusion consists of dense material similar in appearance to the interior of virus particles, and this material appears to extend into some of the budding particles. Ovoid vesicles or invaginations (arrows), 60-100 m μ in diameter, are frequently observed in regions of the cell surface near budding virus particles.
- Figure 12. Budding virus particles at higher magnification; one particle shows an internal strand (arrow).
- Figure 13. Extracellular virus particles in a specimen stained with uranyl acetate prior to embedding. This procedure is effective for demonstrating the unit membrane, i.e., two electron-dense layers separated by a less dense layer. Such a unit membrane is visible in the envelope of the filament with its bulbous tip as well as in the small circular profile (arrows). The internal structure of virus particles is not well-defined by this staining procedure.
- Figure 14. PVM filaments at the cell surface in a specimen stained with uranyl acetate. The unit membrane structure is resolved in some areas of the cell surface and in the envelope of budding virus particles. The cell membrane appears to be incorporated into the emerging virus.

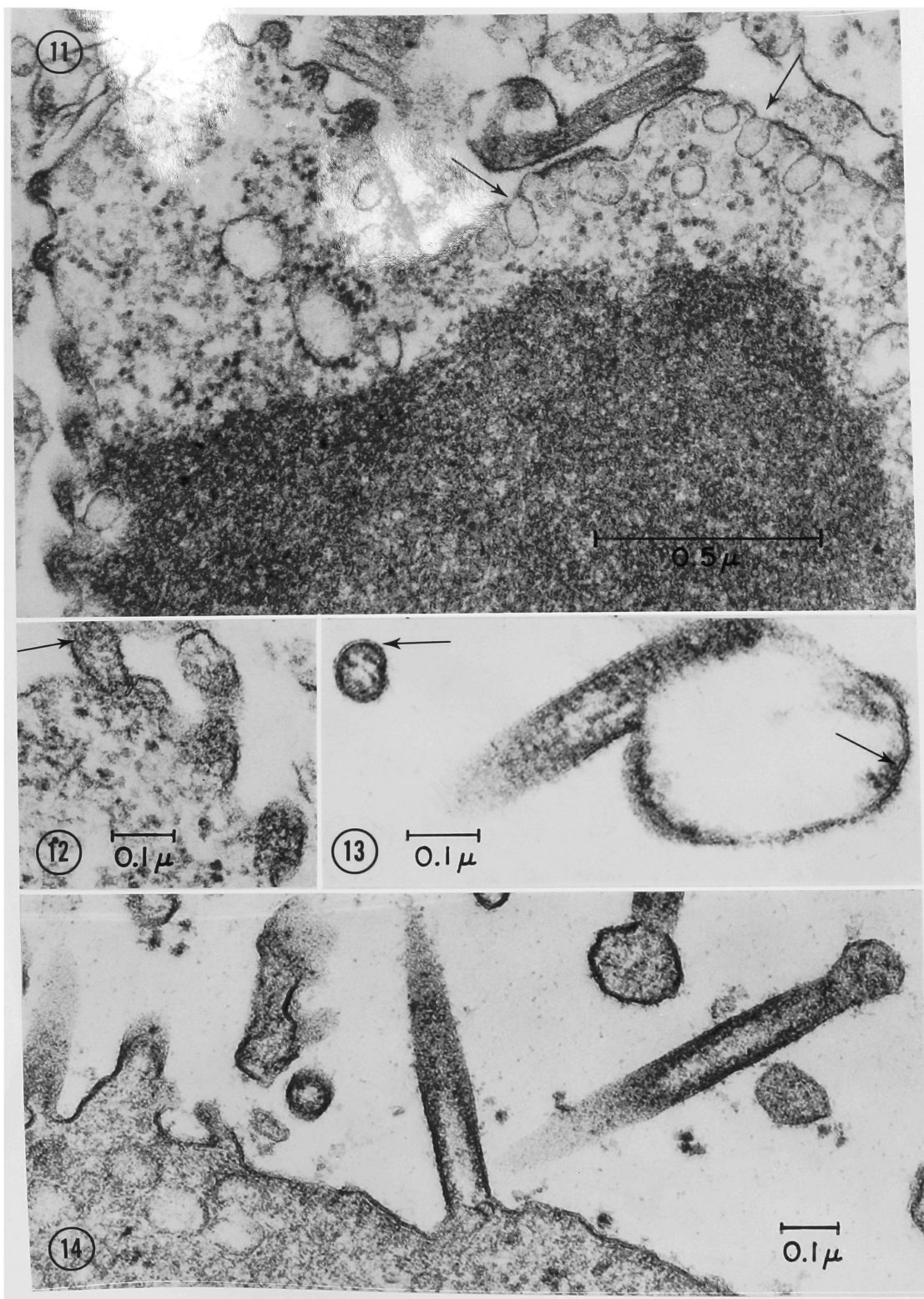
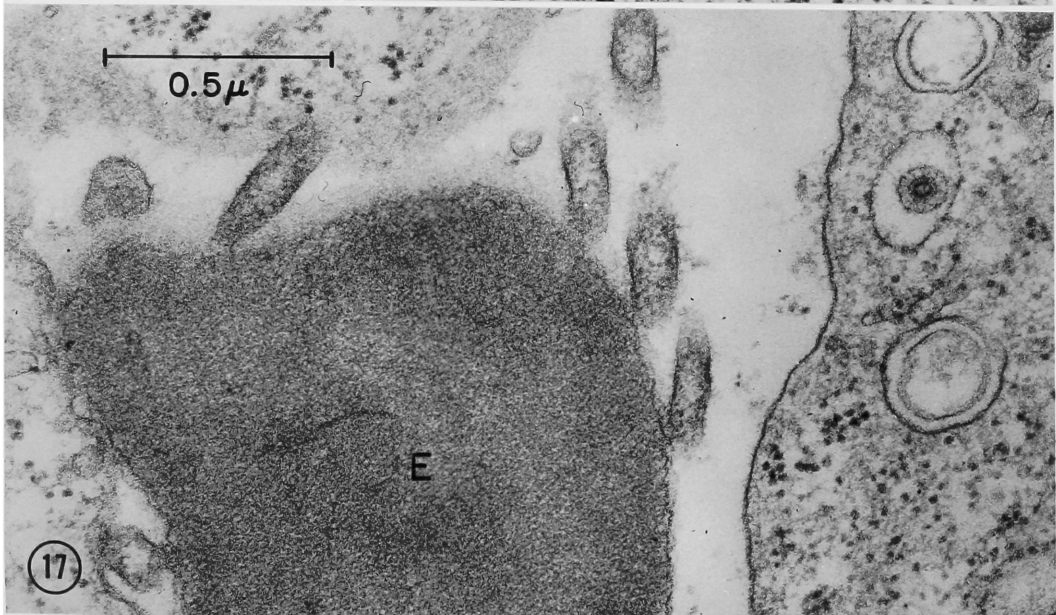
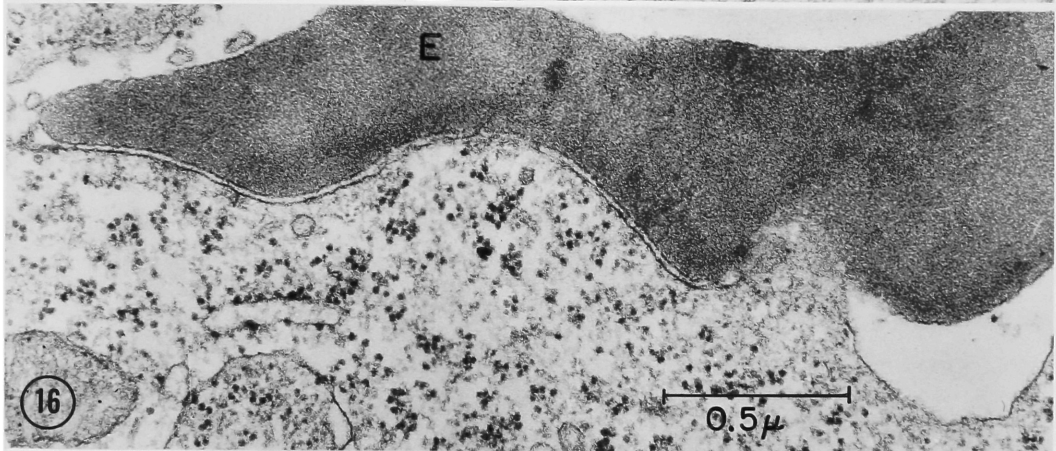
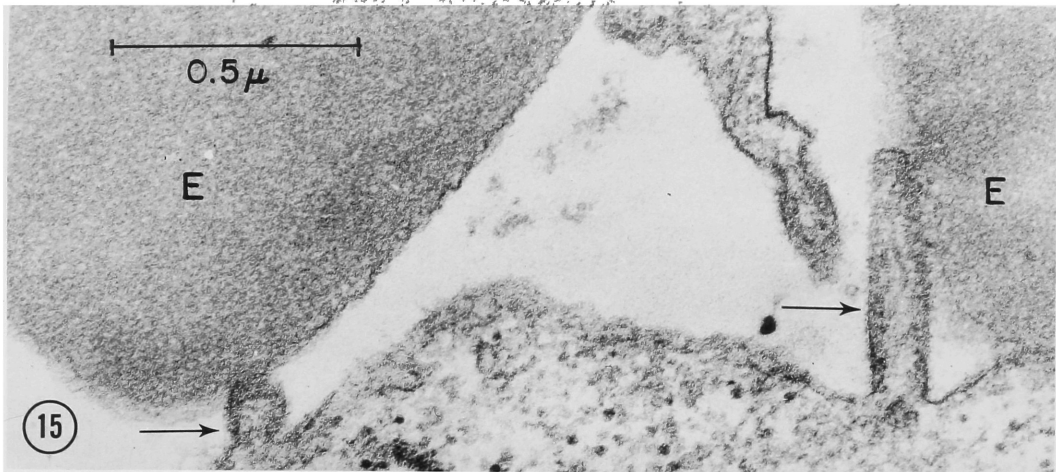


Figure 15. Erythrocytes in contact with PVM particles (arrows) which are budding from the surface of an infected cell.

Figure 16. An adsorbed erythrocyte (E) whose contours closely follow those of the BHK21 cell surface. The erythrocyte membrane and the BHK21 cell membrane are separated by an apparent gap approximately 150 Å in width. No virus-specific structures are seen on the BHK21 cell in the zone of adsorption.

Figure 17. Sections of filamentous PVM particles in contact with the surface of an erythrocyte. A virus-like particle is shown within a vesicle in the cell on the right. Such particles are also found in uninoculated BHK21 cells, and do not resemble PVM virions.



In addition to adsorption of erythrocytes to surfaces of infected cells, adsorption of extracellular virus particles to erythrocytes was also seen (Figure 17). The virus particles observed in these studies thus exhibit the interactions with mouse erythrocytes which would be expected of PVM virions.

Discussion

Evidence has been presented (Harter and Choppin, 1967) that PVM is an RNA virus that replicates in the cytoplasm. The present results indicate that PVM virions are spheres or filaments, 80-120 μ in diameter, which contain a strandlike internal component that is enclosed in an envelope acquired by a budding process at the cell surface. The evidence that the observed particles are PVM virions includes their appearance in infected cells at the time PVM infectivity and hemagglutinin are detected, the absence of such particles in uninfected control cells, and their interaction with murine erythrocytes. In addition, no other virus-like particles have been observed in preparations of PVM, and the structure of these obviously fragile, membrane-bounded particles is compatible with the known ether sensitivity (Franklin and Gomatos, 1961) and extreme fragility (Harter and Choppin, 1967) of PVM. The PVM hemagglutinin with an estimated diameter of 40 μ described by Curnen and co-workers (Curnen et al., 1947) probably represented fragments of 80-120 μ particles such as those observed in the present studies. Evidence for hemagglutination by fragments of PVM virions has been presented previously (Harter and Choppin, 1967).

The internal component of PVM appears to be a single-stranded helix with a diameter of 120-150 A. It was thus smaller than the \sim 180 A helical nucleocapsid of subgroup II myxoviruses, but larger than the \sim 90 A internal component of influenza virus. That the dense inclusions seen in PVM-infected cells represent aggregates of internal component is suggested by their strandlike appearance at high magnification, and by continuity of the inclusion with the dense interior of some budding virus particles. In addition, the inclusions stain red with acridine orange, indicating the presence of RNA (Harter and Choppin, 1967). It has been shown previously that the cytoplasmic inclusions in BHK21-F cells infected with the parainfluenza virus SV5 consist of large aggregates of the helical internal component of this virus.

As with myxoviruses, the outer cell membrane is continuous with the membrane forming the envelope of the budding PVM particle. It thus appears that cellular membrane is incorporated into the virion. The membrane in the viral envelope possesses an outer covering of spikes which are individually visible with negative staining, and appear as a dense outer layer in sections. Some virus-specific proteins may be present on the cell surface before any morphological change can be detected, because virus-specific adsorption of erythrocytes can occur on regions of the cell surface where no budding virus or layer of spikes is apparent. This type of hemadsorption was first demonstrated in influenza-infected cells by Hotchin and co-workers (Hotchin et al., 1958). It is possible that some precursor of the viral spikes may be responsible for the hemadsorption seen in such regions.

The structure and morphogenesis of pneumonia virus of mice suggest that it is a member of the myxovirus group. Although there is no available evidence that PVM adsorbs to a neuraminic acid-containing receptor on erythrocytes, other viruses, such as measles, which are now considered to be members of the myxovirus group, also apparently do not require such a receptor (Hirst, 1965).

The myxoviruses have been segregated into two well-defined subgroups on the basis of structural and biological properties. As summarized in Table 1, PVM does not fit into either of these subgroups, but shares some properties with both. The particle size of PVM is similar to that of the influenza viruses (subgroup I). There is no indication that PVM possesses hemolytic or cell-fusing activity, and in this respect, also, it resembles influenza virus. However, the synthesis of PVM internal component appears to occur in the cytoplasm and eosinophilic cytoplasmic inclusions are prominent; these properties are characteristic of subgroup II myxoviruses. PVM also resembles these viruses in the ease with which it is disrupted, whereas the influenza viruses show greater structural stability. The failure of PVM to fit into either subgroup of myxoviruses, and particularly the 120-150 A diameter of its internal component, suggests that a third subgroup of myxoviruses may exist.

TABLE I

Comparison of Properties of Pneumonia Virus of Mice
with those of the Two Subgroups of Myxoviruses[†]

	PVM	Subgroup I (Influenza)	Subgroup II (Parainfluenza, Mumps, NDV)
Particle size	80-120 mμ	80-120 mμ	120-500 mμ
Diameter of nucleocapsid	12-15 mμ	9 mμ	18 mμ
Filamentous particles	+	+	+
Easily disrupted	+	-	+
Apparent site of synthesis of nucleocapsid antigen	Cytoplasm	Nucleus	Cytoplasm [‡]
Cytoplasmic inclusions	+	Usually absent	+
Hemolytic and cell-fusing activities	-	Weak or absent	+

[†] Summary of properties of the two subgroups adapted from Waterson (1962) and Hirst (1965).

* It was thought that filaments were rare among subgroup II myxoviruses; however, many filamentous virus particles have been observed recently in fixed, sectioned preparations of parainfluenza viruses (Prose et al., 1965; Compans et al., 1966; Howe et al., 1967b).

[‡] Although in most virus-cell systems nucleoprotein synthesis appears to be limited to the cytoplasm, in some instances nuclear synthesis has been reported (Chanock and Parrott, 1965).

BIBLIOGRAPHY

- Ada, G. L. (1957). In Ciba Foundation Symposium on the Nature of Viruses, Churchill, London, p. 104.
- Ada, G. L., P. E. Lind, L. Larkin, and F. M. Burnet (1959). *Nature* 184, 360.
- Ada, G. L., and B. T. Perry (1954). *Aust. J. Exp. Biol. Med. Sci.* 32, 453.
- Adams, W. R. (1965). *Federation Proc.* 24, 159.
- Agrawal, H. O., and G. Bruening (1966). *Proc. Natl. Acad. Sci. U.S.* 55, 818.
- Ananthanarayan, R. (1954). *Brit. J. Exp. Pathol.* 35, 381.
- Andrewes, C. H., F. B. Bang, and F. M. Burnet (1955). *Virology* 1, 176.
- Andrewes, C. H., F. B. Bang, R. M. Chanock, and V. M. Zhdanov (1959). *Virology* 8, 129.
- Ane, C. (1967). *J. Microscopie* 6, 31.
- Avery, O. T., C. M. McCleod, and M. McCarty (1944). *J. Exp. Med.* 79, 137.
- Bablanian, R., H. J. Eggers, and I. Tamm (1965). *Virology* 26, 100.
- Baker, R. F., I. Gordon, and D. Stevenson (1965). *Virology* 27, 441.
- Bang, F. B. (1946a). *Proc. Soc. Exp. Biol. Med.* 63, 5.
- Bang, F. B. (1946b). *Proc. Soc. Exp. Biol. Med.* 64, 135.
- Bang, F. B., and A. Isaacs (1957). In Ciba Foundation Symposium on the Nature of Viruses, Churchill, London, p. 249.
- Behbehani, A. M., J. L. Melnick, and M. E. DeBaakey (1965). *Exp. Mol. Pathol.* 4, 606.
- Berkaloff, A. (1963). *J. Microscopie* 2, 633.
- Bernhard, W., and P. Tournier (1964). *Ann. Inst. Pasteur* 107, 447.
- Bonhoeffer, F., and H. K. Schachman (1960). *Biochem. Biophys. Res. Comm.* 2, 366.
- Bratt, M. A., and W. S. Robinson (1967). *J. Mol. Biol.* 23, 1.
- Breitenfeld, P. M., and W. Schäfer (1957). *Virology* 4, 328.
- Brenner, S., and R. W. Horne (1959). *Biochim. Biophys. Acta* 34, 103.
- Burnet, F. M. (1942). *Aust. J. Exp. Biol. Med. Sci.* 20, 81.
- Burnet, F. M. (1956). *Science* 123, 1101.
- Burton, K. (1956). *Biochem. J.* 62, 315.
- Caspar, D. L. D. (1956). *Nature* 177, 475.
- Caspar, D. L. D. (1963). *Adv. Prot. Chem.* 18, 37.
- Caspar, D. L. D., R. Dulbecco, A. Klug, A. Lwoff, M. S. Stoker, P. Tournier, and P. Wildy (1962). *Cold Spring Harbor Symp. Quant. Biol.* 27, 49.
- Chang, P. W., and G. D. Hsiung (1965). *J. Immunol.* 95, 591.

- Chanock, R. M., K. M. Johnson, M. K. Cook, D. C. Wong, and A. Vargoso (1961).
Amer. Rev. Respirat. Diseases 83, no. 2, pt. 2, 125.
- Chanock, R. M., and R. H. Parrott (1965). In Horsfall, F. L., Jr., and
I. Tamm, eds., Viral and Rickettsial Infections of Man, J. B.
Lippincott, Philadelphia, p. 741.
- Choppin, P. W. (1964). Virology 23, 224.
- Choppin, P. W. (1965). Proc. Soc. Exp. Biol. Med. 120, 699.
- Choppin, P. W., and K. V. Holmes (1967). Virology 33, 442.
- Choppin, P. W., J. S. Murphy, and W. Stoeckenius (1961). Virology 13, 549.
- Choppin, P. W., and L. Philipson (1961). J. Exp. Med. 113, 713.
- Choppin, P. W., and W. Stoeckenius (1964a). Virology 22, 482.
- Choppin, P. W., and W. Stoeckenius (1964b). Virology 23, 195.
- Chu, C. M., I. M. Dawson, and W. J. Elford (1949). Lancet 1, 602.
- Compans, R. W., and P. W. Choppin (1967a). Proc. Natl. Acad. Sci. U.S. 57, 949.
- Compans, R. W., and P. W. Choppin (1967b). Virology 33, 344.
- Compans, R. W., D. H. Harter, and P. W. Choppin (1967). J. Exp. Med. 126, 267.
- Compans, R. W., K. V. Holmes, S. Dales, and P. W. Choppin (1966). Virology
30, 411.
- Crick, F. H. C., and J. D. Watson (1956). Nature 177, 473.
- Crick, F. H. C., and J. D. Watson (1957). In Ciba Foundation Symposium on
the Nature of Viruses, Churchill, London, p. 5.
- Cruickshank, J. G. (1964). In Ciba Foundation Symposium on Cellular Biology
of Myxovirus Infections, Little Brown and Co., Boston, p. 5.
- Cunha, R., M. L. Weil, D. Beard, A. R. Taylor, D. G. Sharp, and J. W. Beard
(1947). J. Immunol. 55, 69.
- Curnen, E. C., E. G. Pickels, and F. L. Horsfall, Jr. (1947). J. Exp. Med.
85, 23.
- Dales, S. (1965a). Am. J. Med. 38, 699.
- Dales, S. (1965b). Progr. Med. Virol. 7, 1.
- Darnell, J. E. (1965). In Horsfall, F. L., Jr. and I. Tamm, eds., Viral
and Rickettsial Infections of Man, J. B. Lippincott, Philadelphia, p. 233.
- Davies, P., and R. D. Barry (1966). Nature 211, 384.
- Drzeniek, R. (1966). Nature 211, 1205.
- Drzeniek, R., M. S. Saber, and R. Rott (1966). Z. Naturforsch. 21b, 254.
- Duc-Nguyen, H., H. M. Rose, and C. Morgan (1966). Virology 28, 404.
- Duc-Nguyen, H., and E. N. Rosenblum (1967). J. Virology 1, 415.

- Duesberg, P. H., and W. S. Robinson (1965). *Proc. Natl. Acad. Sci. U.S.* 54, 794.
- Duesberg, P. H., and W. S. Robinson (1967). *J. Mol. Biol.* 25, 383.
- Dulbecco, R. (1965). *Am. J. Med.* 38, 669.
- Dulbecco, R., and M. Vogt (1954). *J. Exp. Med.* 99, 167.
- Elford, W. J. (1931). *J. Path. Bact.* 34, 505.
- Farquhar, M. G., and G. E. Palade (1963). *J. Cell Biol.* 17, 375.
- Farquhar, M. G., and G. E. Palade (1965). *J. Cell Biol.* 26, 263.
- Folch, J., M. Lees, and G. H. Sloane Stanley (1957). *J. Biol. Chem.* 226, 497.
- Fraenkel-Conrat, H. (1956). *J. Amer. Chem. Soc.* 78, 882.
- Francki, R. I. B. (1966). *Virology* 30, 388.
- Franklin, R. E., A. Klug, and K. C. Holmes (1957). *In Ciba Symposium on the Nature of Viruses*, Churchill, London, p. 39.
- Franklin, R. M., and P. J. Gomatos (1961). *Proc. Soc. Exp. Biol. Med.* 108, 651.
- Frisch-Niggemeyer, W., and L. Hoyle (1956). *J. Hyg.* 54, 201.
- Frommhagen, L. H., C. A. Knight, and N. K. Freeman (1959). *Virology* 8, 176.
- Ginsberg, H. S., and F. L. Horsfall, Jr. (1951). *J. Exp. Med.* 93, 161.
- Gottschalk, A. (1957). *Nature* 181, 377.
- Gottschalk, A. (1966). *In Balazs, E., and R. W. Jeanloz, eds., The Amino Sugars*, Academic Press, New York, p. 225.
- Green, M. (1965). *In Horsfall, F. L., Jr., and I. Tamm, eds., Viral and Rickettsial Infections of Man*, J. B. Lippincott, Philadelphia, p. 11.
- Hall, C. E. (1955). *J. Biophys. Biochem. Cytol.* 1, 1.
- Harris, J. I., and C. A. Knight (1952). *Nature* 170, 613.
- Harris, J. I., and C. A. Knight (1955). *J. Biol. Chem.* 214, 215.
- Harter, D. W., and P. W. Choppin (1967). *J. Exp. Med.* 126, 251.
- Haukenes, G., A. Harboe, and K. Mortensson-Egnund (1965). *Acta Pathol. Microbiol. Scand.* 64, 534.
- Hershey, A. D., and M. Chase (1952). *J. Gen. Physiol.* 36, 39.
- Hirst, G. K. (1941). *Science* 94, 22.
- Hirst, G. K. (1942). *J. Exp. Med.* 76, 195.
- Hirst, G. K. (1962). *Cold Spring Harbor Symp. Quant. Biol.* 27, 303.
- Hirst, G. K. (1965). *In Horsfall, F. L., Jr., and I. Tamm, eds., Viral and Rickettsial Infections of Man*, J. B. Lippincott, Philadelphia, p. 685.
- Holmes, K. V., and P. W. Choppin (1966). *J. Exp. Med.* 124, 501.
- Holmes, K. V. (1968). *Ph.D. Thesis*, The Rockefeller University.
- Horne, R. W., and A. P. Waterson (1960). *J. Mol. Biol.* 2, 75.

- Horne, R. W., A. P. Waterson, P. Wildy, and A. E. Farnham (1960). *Virology* 11, 79.
- Horne, R. W., and P. Wildy (1961). *Virology* 15, 348.
- Horsfall, F. L., Jr., and E. C. Curnen (1946). *J. Exp. Med.* 83, 43.
- Horsfall, F. L., Jr., and R. G. Hahn (1939). *Proc. Soc. Exp. Biol. Med.* 40, 684.
- Horsfall, F. L., Jr., and R. G. Hahn (1940). *J. Exp. Med.* 71, 391.
- Horsfall, F. L., Jr., and M. McCarty (1947). *J. Exp. Med.* 85, 623.
- Hosaka, Y., H. Kitano, and S. Ikeguchi (1966). *Virology* 29, 205.
- Hotchin, J. E., S. M. Cohen, H. Ruska, and C. Ruska (1958). *Virology* 6, 689.
- Howe, C., L. T. Lee, A. Harboe, and G. Haukenes (1967a). *J. Immunol.* 98, 543.
- Howe, C., C. Morgan, C. De Vaux St. Cyr, K. C. Hsu, and H. M. Rose (1967b). *J. Virology* 1, 215.
- Hoyle, L. (1952). *J. Hyg.* 50, 229.
- Hoyle, L. (1954). *J. Hyg.* 52, 180.
- Hoyle, L., R. W. Horne, and A. P. Waterson (1961). *Virology* 13, 448.
- Hoyle, L., R. W. Horne, and A. P. Waterson (1962). *Virology* 17, 533.
- Hsiung, G. D. (1959). *Virology* 9, 717.
- Hsiung, G. D., P. Isacson, and R. W. McCollum (1962). *J. Immunol.* 88, 284.
- Hull, R. N., J. R. Minner, and J. W. Smith (1956). *Am. J. Hyg.* 63, 204.
- Ingram, V. M., and J. A. Sjöquist (1963). *Cold Spring Harbor Symp. Quant. Biol.* 28, 133.
- Isacson, P., and A. E. Koch (1965). *Virology* 27, 129.
- Kates, M., A. C. Allison, D. A. J. Tyrell, and A. T. James (1962). *Cold Spring Harbor Symp. Quant. Biol.* 27, 293.
- Kilbourne, E. D. (1963). *Progr. Med. Virol.* 5, 79.
- Kingsbury, D. W. (1966a). *J. Mol. Biol.* 18, 195.
- Kingsbury, D. W. (1966b). *J. Mol. Biol.* 18, 204.
- Kingsbury, D. W. (1967). *Virology* 33, 227.
- Klenk, E., H. Faillard, and H. Lempfrid (1955). *Z. Physiol. Chem.* 301, 235.
- Klug, A., and D. L. D. Caspar (1960). *Adv. Virus Res.* 7, 225.
- Knight, C. A. (1946). *J. Exp. Med.* 83, 281.
- Knight, C. A. (1963). *Protoplasmologia* 4, 1.
- Knight, C. A., and B. R. Woody (1958). *Arch. Biochem. Biophys.* 78, 460.
- Krim, M., S. C. Wong, and E. D. Kilbourne (1961). *Federation Proc.* 20, 442.
- Kroeger, A. V. (1962). *J. Immunol.* 89, 136.
- Laver, W. G. (1964). *J. Mol. Biol.* 9, 109.
- Laver, W. G., and R. G. Webster (1966). *Virology* 30, 104.

- Levens, J. H., and J. F. Enders (1945). *Science* 102, 117.
- Liebhaber, H., S. Krugman, D. McGregor, and J. P. Giles (1965). *J. Exp. Med.* 122, 1135.
- Liu, C. (1955). *J. Exp. Med.* 101, 677.
- Lowry, O. H., N. J. Rosebrough, A. L. Farr, and R. J. Randall (1951). *J. Biol. Chem.* 193, 265.
- Luft, J. H. (1961). *J. Biophys. Biochem. Cytol.* 9, 409.
- Lush, D. (1943). *J. Comp. Path.* 53, 157.
- Lwoff, A., R. Horne, and P. Tournier (1962). *Cold Spring Harbor Symp. Quant. Biol.* 27, 51.
- Maasaab, H. F. (1959). *Proc. Natl. Acad. Sci. U.S.* 45, 877.
- Maasaab, H. F. (1963). *J. Immunol.* 90, 265.
- Macpherson, I., and M. Stoker (1962). *Virology* 16, 147.
- Martin, R. G., and B. N. Ames (1961). *J. Biol. Chem.* 236, 1372.
- Mayron, L. W., B. Robert, R. J. Winzler, and M. E. Rafelson (1961). *Arch. Biochem. Biophys.* 92, 475.
- McClelland, L., and R. Hare (1941). *Canad. Pub. Health J.* 32, 530.
- McCrea, J. F., R. S. Epstein, and W. H. Barry (1961). *Nature* 189, 220.
- McGee-Russell, S. M., A. D. Visozo, and F. K. Sanders (1965). *In Proc. 3rd European Reg. Conf. Electron Microscopy*, Publishing House of the Czechoslovak Academy of Sciences, Prague, Vol. B., p. 367.
- Mejbaum, W. (1939). *Z. Physiol. Chem.* 258, 117.
- Mills, K. C., and A. R. Dochez (1944). *Proc. Soc. Exp. Biol. Med.* 57, 140.
- Morgan, C., K. C. Hsu, R. A. Rifkind, A. W. Knox, and H. M. Rose (1961a). *J. Exp. Med.* 114, 825.
- Morgan, C., K. C. Hsu, R. A. Rifkind, A. W. Knox, and H. M. Rose (1961b). *J. Exp. Med.* 114, 833.
- Mosley, V. M., and R. W. G. Wyckoff (1946). *Nature* 157, 263.
- Murphy, J. S., and F. B. Bang (1952). *J. Exp. Med.* 95, 259.
- Noll, H., T. Aoyagi, and J. Orlando (1962). *Virology* 18, 154.
- Palade, G. E. (1952). *J. Exp. Med.* 95, 285.
- Parker, J. C., R. W. Tennant, and T. C. Ward (1966). *In Viruses of Laboratory Rodents*, National Cancer Institute Monograph No. 20, p. 25.
- Portocala, R., V. Boeru, and I. Samuel (1959). *Acta Virol.* 3, 172.
- Pons, M. W. (1967). *Virology* 31, 523.
- Prose, P. H., S. D. Balk, H. Liebhaber, and S. Krugman (1965). *J. Expl Med.* 122, 1151.

- Reich, E., R. M. Franklin, A. J. Shatkin, and E. L. Tatum (1961). *Science* 134, 556.
- Reynolds, E. S. (1963). *J. Cell Biol.* 17, 208.
- Robertson, J. D. (1961). *In* Boyd, J. D., F. R. Johnson, and J. D. Lever, eds., *Electron Microscopy in Anatomy*, Williams and Wilkins Co., Baltimore, p. 74.
- Rott, R. (1962). Habilitation thesis, Giessen University.
- Rott, R. (1964). *In* Hanson, R. P., ed., *Newcastle Disease Virus: An Evolving Pathogen*, University of Wisconsin Press, Madison, p. 133.
- Sabatini, D. D., K. G. Bensch, and R. J. Barnett (1962). *Anat. Record* 142, 274.
- Schäfer, W. (1957). *In* Ciba Foundation Symposium on the Nature of Viruses, Churchill, London, p. 91.
- Schäfer, W. (1959). *In* Burnet, F. M., and W. M. Stanley, eds., *The Viruses*, Acad. Press, New York 1, 475.
- Schäfer, W., and R. Rott (1959). *Z. Naturforsch* 14b, 629.
- Schaffer, F. L., and C. E. Schwerdt (1965). *In* Horsfall, F. L., Jr., and I. Tamm, eds., *Viral and Rickettsial Infections of Man*, J. B. Lippincott, Philadelphia, p. 94.
- Schultz, E. W., and K. Habel (1959). *J. Immunol.* 82, 274.
- Scott, T. A., Jr., and E. H. Melvin (1953). *Anal. Chem.* 25, 1656.
- Smith, W., G. Belyavin, and F. W. Sheffield (1953). *Nature* 172, 669.
- Sokol, F., E. Skacianska, and L. Pivec (1966). *Acta Virol.* 10, 291.
- Sokol, F., and J. Szurman (1959). *Acta Virol.* 3, 175.
- Spirin, A. S. (1963). *In* Davidson, J. N., and W. E. Cohn, eds., *Progress in Nucleic Acid Research*, Academic Press, New York, Vol. 1, p. 301.
- Stanley, W. M. (1935). *Science* 81, 644.
- Stenback, W. A., and D. P. Durand (1963). *Virology* 20, 545.
- Sturman, L. S., and I. Tamm (1966). *J. Immunol.* 97, 885.
- Taylor, A. R., D. G. Sharp, D. Beard, J. W. Beard, J. H. Dingle, and A. E. Feller (1943). *J. Immunol.* 47, 261.
- Tennant, R. W. (1966). *In* *Viruses of Laboratory Rodents*, National Cancer Institute Monograph No. 20, p. 47.
- Vogel, J., and A. Shelokov (1957). *Science* 126, 358.
- Von Euler, L., F. S. Kantor, and G. D. Hsiung (1963). *Yale J. Biol. Med.* 35, 523.
- Warburg, O., and W. Christian (1941). *Biochem. Z.* 310, 384.

Waterson, A. P. (1962). Nature 193, 1163.

Waterson, A. P., and J. M. W. Hurrell (1963). Arch. ges. Virusforsch 12, 138.

Waterson, A. P., K. E. Jensen, D. A. J. Tyrrell, and R. W. Horne (1961).
Virology 14, 374.

Wecker, E. (1957). Z. Naturforsch. 126, 208.

Williams, R. C., and K. M. Smith (1958). Biochem. Biophys. Acta 28, 464.

End